UCLouvain

École polytechnique de Louvain

Deep eutectic solvents as green extractant for supported liquid membranes separation of amino acids

Authors : Laure **NGUYEN**
Supervisors : **Patricia LUIS ALCONERO**
Readers : **Juray DE WILDE**, **Denis MIGNON**, **Gilles VAN EYGEN**
Academic year 2023–2024
Master [120] in Chemical and Materials Engineering

Abstract

Essential for many biological processes, amino acids are extensively used among various industries such as in food, pharmaceutics, and cosmetics. However their significance, separation, and purification account for a considerable amount of the total production cost and raise environmental issues. Common industrial techniques, such as ion-exchange chromatography, suffer from high costs and negative environmental effects. Innovative technologies such as extraction through supported liquid membranes (SLMs), which have the potential to cut energy use, have received attention as potential solutions to these problems. Furthermore, there are encouraging developments in the creation of membranes that use deep eutectic solvents (DES). These emerging solvents address waste management, solvent toxicity and aim to improve yield, purity, selectivity, and product recovery. The purpose of this work is to use an SLM to specifically extract a subset of amino acids. Understanding each of the constituent parts of the membrane system, is necessary to comprehend the system as a whole. Trioctylphosphine oxide-thymol (TOPO-thymol) is a previously chosen deep eutectic solvent that will be thoroughly examined to learn more about how it functions and interacts with its environment. Among the experiments, the Polytetrafluoroethylene (PTFE) membrane with 100 nm pores has shown promising results with the highest selectivity towards alanine in an aqueous mixture with acceptable arginine levels. PTFE 100 nm, enabled around 60% recovery of alanine with 20 % of arginine. PVDF 100 nm showed very high selectivity results in a much shorter time period, with almost pure 10 % recovery of alanine in three hours, selectivity then decreased with time.

Aknowledgements

I would like to extend my gratitude to Prof. Patricia Luis Alconero for providing me the opportunity to complete this master's thesis and for her valuable feedback.

I am very grateful for the help that Gilles Van Eygen has offered me throughout the semester. Despite being close to completing his doctoral work, he has been a constant support. His availability and willingness to answer all my questions, no matter how numerous, have been really beneficial.

With special thanks to researchers Sabine Bebelman and Pascal Van Velthem, who helped me with solvent calibration and provided me with instructions on different analyses and their equipment. I am very grateful to them for spending hours assisting me with the interpretation and analysis of the data.

Additionally, I would like to thank Ysaline Toussaint who was working in the lab at the same time. I spent a significant amount of time with her this semester, and her explanations about various lab techniques and instrument operations were incredibly beneficial. Her friendship and support have been greatly helpful.

I would like to thank Denis Mignon and Juray de Wilde, my readers, for taking time to review and evaluate this thesis.

Lastly, I want to state the use of Quillbot and ChatGPT . These AI tools have been really helpful, especially when it comes to the writing process. Both were used as writing and grammatical tools.

Summary

List of Figures

Introduction

Omnipresent across diverse sectors, amino acids serve as building blocks of polypeptides, proteins, and enzymes, essentials for the functions of living organisms [1]. These molecules play a central role in numerous biological processes and hold a considerable significance in various industries. Notably, amino acids find relevance in food additives, pharmaceuticals, and cosmetic production.

Nevertheless, challenges emerge in current production methods. The separation and purification of amino acids currently represent a major portion of the overall production cost, contributing significantly to environmental concerns. The ion-exchange process is a widely employed industrial separation method, but challenges remain, such as high cost, waste management and environmental impact [2]. The urge for innovative technology is, therefore, evident. An extraction process established on liquid membranes has garnered attention and research interest. This approach allows extraction thanks to supported liquid membranes (SLMs), offering the potential to extensively reduce waste and energy consumption. In response to challenges related to solvent toxicity and environmental impact, the development of membranes involving deep eutectic solvents (DES) has emerged as a promising advancement for the extraction industry [3]. Their unique properties display an opportunity to address issues such as product recovery, yield optimisation, and the imperative for purity and selectivity while minimizing energy consumption. The pursuit of higher efficiency and yield is crucial for cost-effectiveness and optimal resource utilisation.

The primary goal of this study is to achieve specific extraction of selected amino acids using an SLM. This work will begin with a comprehensive review of existing literature to understand the current advancements and challenges in the field. Following, the study will proceed with the calibration of the system to optimise conditions for selective extraction. Subsequent experiments will focus on a previously selected deep eutectic solvent; Trioctylphosphine oxide-thymol (TOPO-thymol) and its ability to extract targeted amino acids. Furthermore, specificity and efficiency of the process will be evaluated. Finally, a conclusion and some future prospects are given.

Chapter 1

Literature Study

1.1 Amino Acids

Amino acids form the complex molecular backbone that shapes biological processes. These compounds serve as the building blocks of proteins, playing a vital role in gene expression. In this extensive set, distinctions arise among essential, non-essential, and semi-essential amino acids, depending on whether the human body synthesises them or not. Essential amino acids must be acquired through diet, as the body does not synthesise them, highlighting their irreplaceable role. Conversely, non-essential amino acids are produced within the body. In a nuanced manner, semi-essential amino acids are synthesised within the body, yet their production may be insufficient, necessitating dietary supplementation. Among this vast array of over 300 naturally occurring building blocks, a select group of 20 stands as the monomer units of proteins **amino acid2**. These monomers are linked by peptide bonds in genetically predefined sequences, to form the backbone of every known protein **amino aciddescrp**.

1.1.1 Structure

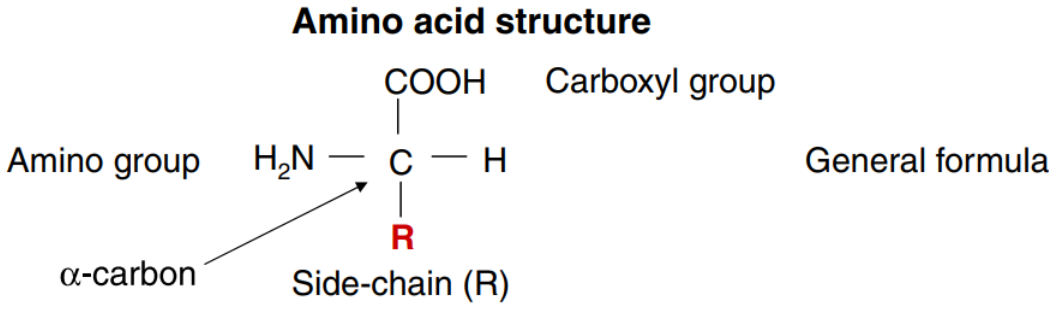

Figure 1.1: Molecular structure, Bischoff and Schlüter [4]

The amino group (H_2N) confers amino acids basic properties, facilitating its role as a proton acceptor in biochemical reactions (H_3N^+). Meanwhile, the carboxyl group ($COOH$) provides acidic characteristics, allowing amino acids to release protons in solution (COO^-). The sidechain (R) varies among different amino acids, dictating their distinct chemical properties such as acid/base behaviour,

thus influencing the overall structure and function of proteins. Finally, the central carbon (C_α) which is the first carbon atom directly attached to a functional group in an organic compound, commonly used for identifying specific carbon atoms within molecules, particularly in organic chemistry and biochemistry contexts.

Amino acids are classified into acidic, basic and neutral categories, exhibiting diverse roles beyond their involvement in protein synthesis. Their sensitivity to pH variations arises from the presence of these two distinct functional groups within their molecular structure (shown in **Figure 1.2**). These functional groups readily undergo ionisation reactions in response to changes in pH levels. The amino group tends to accept protons (H) under acidic conditions, becoming positively charged, while the carboxyl group tends to release protons in basic environments, resulting in a negative charge.

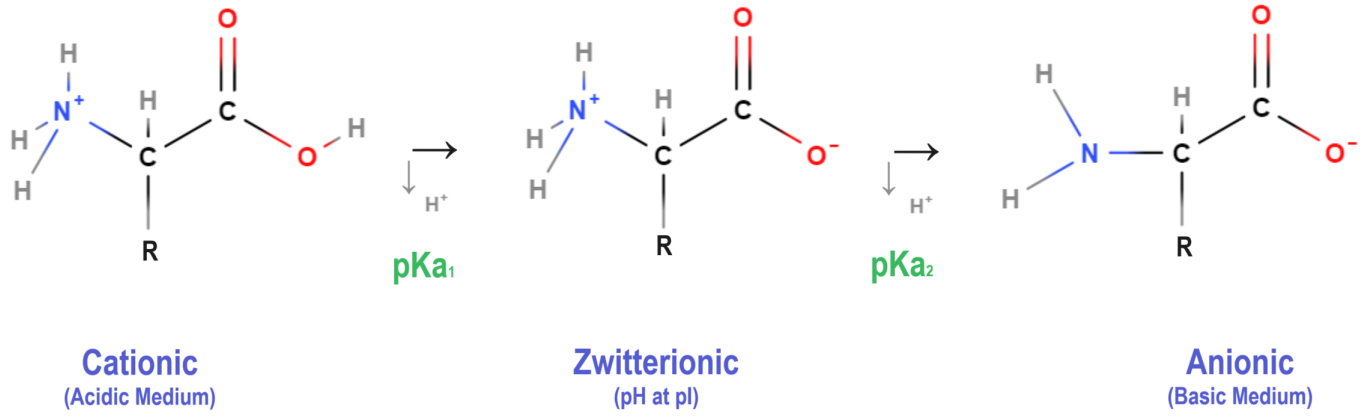

Figure 1.2: Different ionic forms of amino acids, generated via *MolView* [5]

The *Cationic or Acidic* from of amino acids is observable when environment pH value is under the commonly called "pKa_1", which corresponds to the pKa of the carboxyl functional group. pKa is the acid dissociation constant specific to each chemical species, representing its acidic strength. It quantifies the ability of the species to donate a proton in a solution. This pKa_1 is usually around pH of 2. Both carboxyl and amino groups are protonated **amino aciddescrp**. The *Zwitterionic* form is exhibited between pKa_1 and pKa_2 (pKa associated to the amino group), in other words at moderate pH. Both carboxyl and amino groups are deprotonated and protonated, respectively. The amino acid exists as a zwitterion, with no net charge. The Isoelectric point (PI) is the pH at which an amino acid exists in its zwitterionic form. For amino acids with one acidic group and one basic group, the pI is the average of their respective pKa values [6]. The *Anionic or Basic* form of an amino acid is therefore observed when pH level is over pKa_2. The amino and carboxyl groups are mostly deprotonated, resulting in a net negative charge **amino aciddescrp**.

A clear comprehension of the different ionisation states of amino acids is essential for their effective manipulation. Their form can significantly influence the structure of proteins, consequently their function directly impacting enzymatic activity and cellular processes they are involved in. Moreover, these ionisation states have distinct behaviours and interactions towards surrounding species, which is very important for extraction.

1.1.2 Function

As previously mentioned, amino acids serve as essential components for all organisms, acting as the fundamental building blocks of proteins. On the behalf of proteins, amino acids play a vital role in numerous biological processes, with enzymes being a prime example. Enzymes, composed of proteins, regulate various aspects of metabolisms, including energy production. Additionally, proteins influence crucial functions such as immune response, cell signalling, and a countless amount of other biological processes essential for the proper functioning of living organisms.

Protein synthesis is a complex process which relies on the assembly of peptides, where amino acids are linked together through the reaction furtherly illustrated in **Figure 1.3**. The formation of polypeptides is not arbitrary; it follows a genetically predefined sequence, ensuring the specific arrangement of amino acids in the growing protein chain. The specificity of the genetic code ensures that the peptide sequence in the synthesised protein is precisely determined, contributing to the diversity and functionality of the vast array of proteins in living organisms.

This reaction is catalysed by ribosomes, which are cellular structures present within the producing cell. They guide and facilitate the linkage of amino acids.

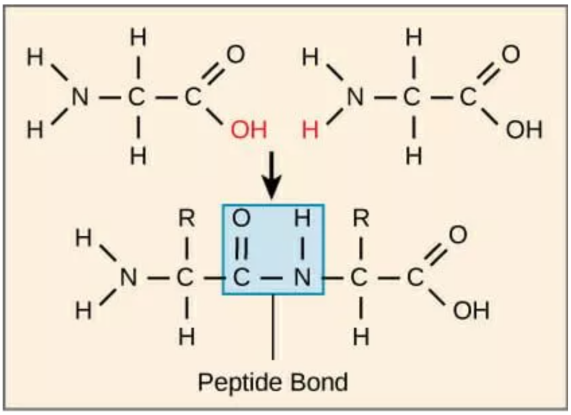

Figure 1.3: Peptide bond formation issued from BD Editors [7]

1.1.3 Conventional extraction

The conventional extraction of amino acid frequently involves an ion-exchange process. Ion exchange separation is a chromatographic technique which is a method to separate components in a mixture based on their respective interactions with a stationary phase and a mobile phase. This is used to separate and purify ions based on their interaction with charged resins. Ions with the same charge as the resin are selectively retained, while the oppositely charged eluent, which contains ions with the opposite charge, competes with the species held by the resin for binding sites. This causes an exchange of ions between the sample and the eluent [8].

In extraction from plant-based feed solutions, a common challenge arises from co-extraction. Substances such as sugars, lipids, salts, and pigments are co-extracted along with the targeted amino acids. This phenomenon may interfere with the interpretation of results and compromise the pu-

rity of solutions **ionexamino acid**. To address these challenges, an additional purification step is required. A common purification method involves adsorbing amino acids onto a short column of cation-exchange resin. It allows the washing out of negatively charged and neutral substances (salts, sugars...) using water or a diluted acid solution. Subsequently, the amino acids can be eluted from the column with a dilute base solution **ionexamino acid**.

Despite these efforts, incomplete recovery of basic amino acids during purification has been observed. This highlights the need for continued optimisation or innovation of extraction methods to achieve higher yields and reliable quantification of amino acids from complex plant matrices. Additionally, ion exchange methods, often involves solvents and chemicals that may have environmental implications. The energy requirements for these processes, particularly in the purification steps, can contribute to their overall inefficiency and environmental footprint.

In addition to ion-exchange chromatography, various other conventional processes are employed for the extraction of amino acids. These methods often involve a combination of chemical treatments. Solvent extractions, and chromatographic techniques are known for amino acids isolation and purification from complex mixtures. Common approaches also include acid precipitation and dialysis. Each method targets specific properties of amino acids, such as their charge, solubility, or reactivity, to achieve efficient separation and concentration while aiming for sustainability.

1.1.4 Liquid Membrane Extraction

In addressing the environmental concerns and cost issues associates with previous conventional methods, liquid membranes have emerged as alternative solutions for amino acids extraction. In a broader sense, they offer a versatile approach to conventional separation methods along with associated advantages. A membrane acts as a permeable barrier, separating two phases and limiting selectively the transport of various chemicals. A liquid membrane, therefore, consists of an organic liquid phase positioned between two restricted phases. The solute is transferred from one phase to another through the liquid membrane, driven by a concentration gradient [9]. Liquid membranes may be classified in three categories based on their structure and operational characteristics.

These categories include *Bulk Liquid Membranes (BLMs)*, which consists of homogeneous liquid phases without any supporting structure or carrier material. The solute migrates from one phase to another through the bulk liquid membrane, and the transport mechanism may include diffusion, complexation, or other relevant processes [9]. BLMs are usually applied to separation processes such as extraction [10] in various industrial fields (pharmaceutical, environmental). These are the simplest type of non-supported liquid membranes, and compared to others, have a relatively low contact area. Although having easy operation and equipment conditions, they are not widely used in industry due to their low rate of mass transfer and as mentioned, contact area between phases.

Emulsion Liquid Membranes (ELMs) are composed of small liquid droplets dispersed in a carrier liquid phase, forming an emulsion. The liquid droplets typically contain the extracting phase, allowing the targeted species to permeate them. Extraction then takes place, leaving only the solute retained while the rest exists the droplets [9]. ELMs, therefore, provide a high contact area per unit of volume between the phases and a minimal thickness, both of which contribute to a relatively rapid separation process. Because of their emulsion structure, which enhances the contact, they are

mainly found in metallurgical applications, such has metal ions extraction and recovery from aqueous solutions [11]. Primary drawbacks of ELMs are their stability issues, specifically emulsion swelling. Emulsion swelling refers to the increase in volume or size of emulsion droplets within an emulsion liquid membrane. As solute molecules enter the emulsion droplets, its concentration inside the droplets increases. This results in an osmotic pressure causing the droplets to swell or expand, leading to changes in the emulsion structure [9].

Finally, the main focus of this study, *Supported Liquid Membranes (SLMs)*, involve a liquid phase immobilised on a support material, which can be a porous solid or a microporous membrane. The solute is transported through the supported liquid layer, often by diffusion or facilitated transport [12]. Their advantage lies in their facilitated selective transport, making them very appealing for different applications such as wastewater treatment in various industries (petrochemistry [13], environment). The characteristics and operations of SLMs will be discussed in greater detail in the upcoming section.

1.1.5 Supported Liquid Membrane (SLM)

In SLM, an organic liquid is embedded in a porous polymer matrix support, and its retention is facilitated by capillary forces. This organic liquid must be immiscible with both the source and receiving phases, to allow the separation of two aqueous phases (as illustrated in **Figure 1.4** [14]). Common configurations of SLMs include flat sheet supported liquid membranes (FSSLM) and hollow fibre supported liquid membranes (HFSLM) [12]. Solute extraction from the aqueous phase occurs through the organic solvent held within the pores and is subsequently reextracted via the stripping solution (purification). Typically, the feed and stripping solutions flow along the outer surface of the membrane allowing exchanges with the solvent held in the lumen. A lumen designates a canal, duct, or cavity of a tubular structure.

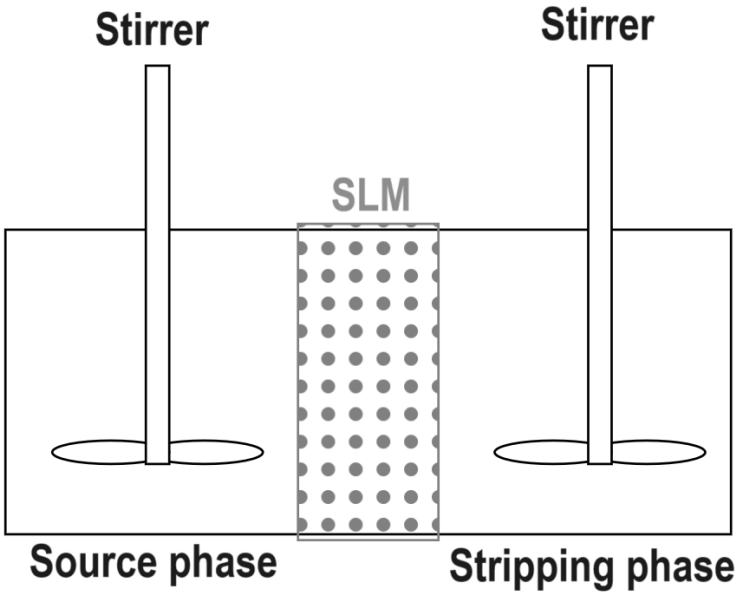

Figure 1.4: SLM components generated via Microsoft Corporation [15]

SLMs propose a low energy consumption alternative, making them attractive for various separation processes. Traditional separation processes are commonly characterised by high energy requirements and the use of toxic solvents [3]. Operating under moderate conditions, SLMs can replace processes for recovery of toxic metal ions, weak acids and bases, hydrocarbons, biologically important compounds, gases, and gaseous mixtures [9].

These membranes, formed from a thin porous polymer or ceramic material, offer a compromise between BLMs and ELMs. Their key advantage lies in their minimal solvent requirement, combining extraction and stripping into a single stage. Other advantages such as selectivity, low energy consumption, and operational simplicity are notable [9]. Overall, the unique characteristics of SLMs position them as a versatile and efficient solution to conventional and potentially harmful separation processes.

Among polymer matrices are typically found in various applications Polytetrafluoroethylene (PTFE) and Polyvinylidene Fluoride (PVDF) (**Figure 1.5**). Each of these polymers possesses unique properties that make them suitable for different purposes. PTFE is known for its exceptional resistance to high temperatures and harsh chemicals [16] conferred by its Carbon-fluor links, making it an ideal material for applications requiring exposure to extreme conditions without degrading. Additionally, PTFE has a very low coefficients of friction which makes it an excellent choice for membrane technology [17]. On the other hand, PVDF is known for its outstanding mechanical properties, including high tensile strength, toughness, and abrasion resistance, due to its methyl groups enabling compact stacking (where PTFE is planar) [18]. Like PTFE, PVDF exhibits excellent resistance to a wide range of chemicals, including acids, bases, and organic solvents which will be required for the SLM process. While thermal stability of PVDF is not as high as PTFE's, it still offers good thermal stability for applications involving moderate to high temperatures.

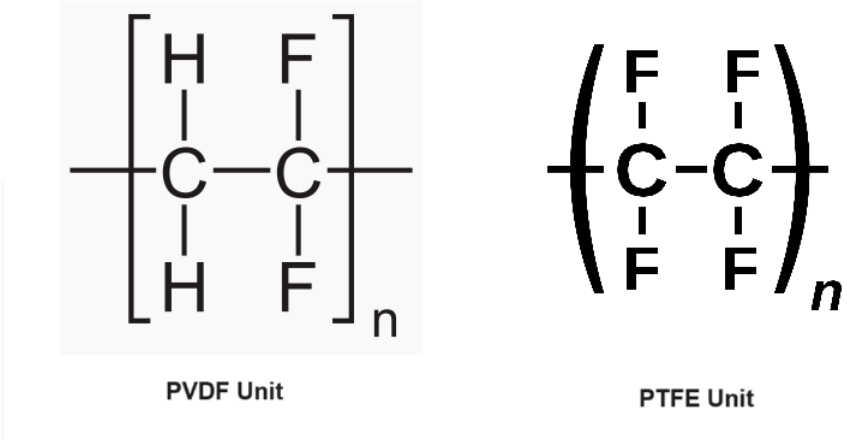

Figure 1.5: Membrane polymers repeating units structure [19], [20]

1.1.6 SLM issues and solutions

However, concerns regarding stability and long-term performance have limited their industrial applications. Solvent leakage from supporting media can be observed over time. Indeed, Volatile Organic Compounds (VOCs), which are the conventional solvents used in SLM, are very volatile and tend to form very unstable membranes [12]. Unfortunately, the adoption of SLM technology for large

scale applications, has been limited by their insufficient stability. The leakage of solvent from the membrane poses a significant challenge on both flux and selectivity. This issue restricts the effectiveness and reliability of SLMs in industrial applications.

Membrane degradation can be linked to various mechanisms. One such mechanism is the progressive wetting of the pores in the membrane support induced by the aqueous phase. Additionally, differential pressure between the inside and outside of the membrane, often caused by the pumping of solution, contributes to degradation. The loss of extractant due to its aqueous solubility further exacerbates this issue. Emulsion formation within the liquid membrane phase is another contributing factor, along with the blockage of membrane pores. Each of these mechanisms plays a role in the overall deterioration of membrane integrity [21][22].

Additionally, the stability of SLMs can be influenced by other factors. Among these are: the type of polymeric support and its pore radius, the organic solvent used in the liquid membrane, the interfacial tension between the aqueous and membrane phase, the flow velocity of the aqueous phases, and the method of preparation [12]. Engineers are actively exploring strategies to improve the membrane stability and address these issues. As part of this research, specialists have delved into the exploration of solvents, specifically the application of ionic liquids to overcome the issues associated with the solvent leakage [9].

1.1.7 Solvent Choice

The replacement of organic solvents is imperative to address the stability concerns, solvent leakage and associated toxicity. The preference of *Ionic Liquids* (ILs) in SLM is motivated by their minimal environmental impact, low toxicity, and operational stability. Their liquid state combined with appealing solvent properties, high ionic conductivity, and thermal stability, positions them as excellent choices for safer processes. Their relatively high viscosity can serve resolving the stability issues of SLMs. ILs are tuneable by nature, known as "designer solvents," which allows the customisation of their chemical and physical properties. In SLM-based processes, ILs exhibit a dual nature, selectively separating both polar and non-polar compounds, making them potentially valuable in chromatographic separation. This shift towards ILs aligns with the global pursuit of greener and more sustainable extraction and separation methodologies [9].

Comparable to ILs, *Deep Eutectic Solvents* (DESs) emerge as a novel class of solvents with significant potential in environment-friendly applications. The interaction between these components through hydrogen bond formation defines their unique characteristics. DESs by accepting or donating electrons or protons, exhibit excellent dissolution capabilities for various substances, making them promising candidates for applications in separation processes. Despite being in the early stages of research compared to ILs, DESs also manifest advantages like high chemical stability and low vapor pressure but offer additional benefits, including cost-effectiveness, accessibility of raw materials, and ease for synthesis [3].

1.2 Extractant : Ionic Liquids

Ionic liquids (ILs) have emerged as a novel class of solvents, seen as environmentally friendly alternatives for toxic substances and VOCs. The wide range of ILs results in an almost limitless variety of compounds, with, each exhibiting diverse physical and chemical properties. This unique feature allows for the careful selection of an IL that best suits a specific application, providing a tailored solution to address challenges [23].

1.2.1 Structure

ILs consist primarily of an asymmetric and diffusely charged organic cations coupled with a polyatomic inorganic or organic anion (as illustrated in **Figure 1.6**). Diffusely charged organic cation refers to a molecule that contains a positively charged group and is distributed across the molecular structure rather than being localised at a specific site. This assembly results in disorganised molecular packing and reduced melting points. This characteristic is also associated with their elevated cohesive energy density, attributed to the bare Coulombic interactions between the constituents [9].

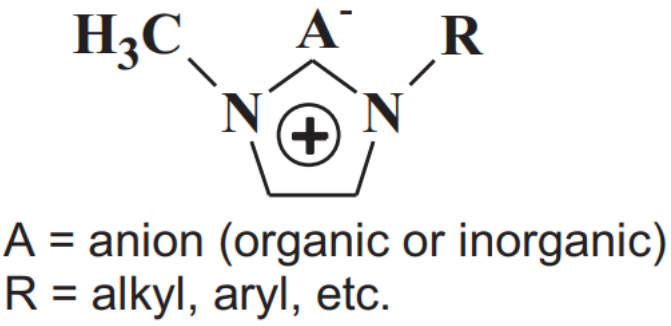

Figure 1.6: Ionic Liquid Structure, Malik, Hashim, and Nabi [9]

1.2.2 Physicochemical Properties

Known for their renowned characteristics of extremely low vapor pressure, minimal volatility, and non-flammability, ILs showcase fascinating physicochemical properties, positioning them as a preferred option for various applications. ILs present different *phase transition* behaviours, with the presence of both glass transition and melting temperatures. Some ILs, particularly those with long-chain salts, display lower melting point, and high clearing point. Clearing point is the temperature at which liquid crystals lose their colour. Their phase transition temperatures are influenced by van der Wamino acidls (VdW) and electrostatic interaction forces. The impact of these two forces depends on the IL type. Furthermore, the effect of anion variation on phase transition temperature is not as pronounced as with cations. ILs featuring symmetric cations tend to have the highest melting points, while melting points decrease steadily with increasing alkyl chain length. Additionally, the melting temperatures generally decrease as the anion radius increases, revealing the complex effect of forces and molecular structures in governing the phase transitions of ILs [24].

The *density* of ILs is higher than water in most cases, with only a few varying from 0.9 to 0.97 $g.cm^{-3}$ [24]. It is worth noting that ILs density decreases with increasing number of carbon atoms in

the alkyl group and the cumulative carbon number for quaternary ammonium. An intriguing observation is the linear decrease in the density of 1-methylimidazolium ionic liquids with rising temperature, at a rate lower than that for typical molecular organic solvents. [24]. VdW forces and hydrogen bonding are the primary influence of ILs *viscosity*. Length, fluorination and ramification of alkyl chains result in an increased viscosity owing to VdW interactions. The temperature dependence of dynamic viscosity in IL systems can be described by an Arrhenius form empirical equation, highlighting the role of temperature. Temperature and additives can alter ILs viscosity. Notably, the addition of small amounts of organic solvent can decrease the viscosity [24]. Data concerning their *surface tension* are very rare, and this feature has not yet been investigated a lot. Nevertheless, available information suggests that liquid/air surface tension values are generally higher than those of conventional solvents, but smaller than those of water. The results indicated that surface tension decreases with an increase in the carbon number. This highlights the potential for tuning surface tension in ILs based on the molecular structure [24].

Finally, ILs possess remarkable *electrochemical characteristics*, displaying a very wide electrochemical window. This wide window signifies their ability to endure an extensive range of voltage without undergoing undesired reactions. Additionally, ILs exhibit notable *electrical conductivity*, allowing for efficient charge transport, making them very appealing for selective transport [24]. Their inherent *polarity* enables their miscibility not only in organic solvents but also in water [9]. This distinctive combination of a wide electrochemical window, high conductivity, and polarity positions ILS as very attractive solvents typically in electrochemical processes and green chemistry initiatives.

1.2.3 Applications

ILs are present in various industrial sectors, including *Industrial Polymerisation*. While there has been extensive research of using ILs in organic synthesis, their application in polymer synthesis has been somewhat limited. However, recent years have witnessed a shift, highlighting the advantageous use of ILs in polymerisation processes. Their application as solvents in Atom Transfer Radical Polymerization (ATRP) proves beneficial by facilitating the separation of the polymer from residual catalyst and diminishing the occurrence of side-reactions [25]. Due to their wide electrochemical range and high conductivity, they can be found in *Energy storage* industry. They function as valuable electrolytes in batteries, supercapacitors, and fuel cells, driving progress said technologies. Their stability under elevated voltage conditions and compatibility with a range of electrode materials make them a promising components for next-generation energy storage devices [26]. ILs find numerous additional applications in various domains, encompassing synthesis, *catalysis* [27], and beyond. Their versatile nature allows for customisation to meet specific requirements, making them highly adaptable in diverse scientific and industrial contexts.

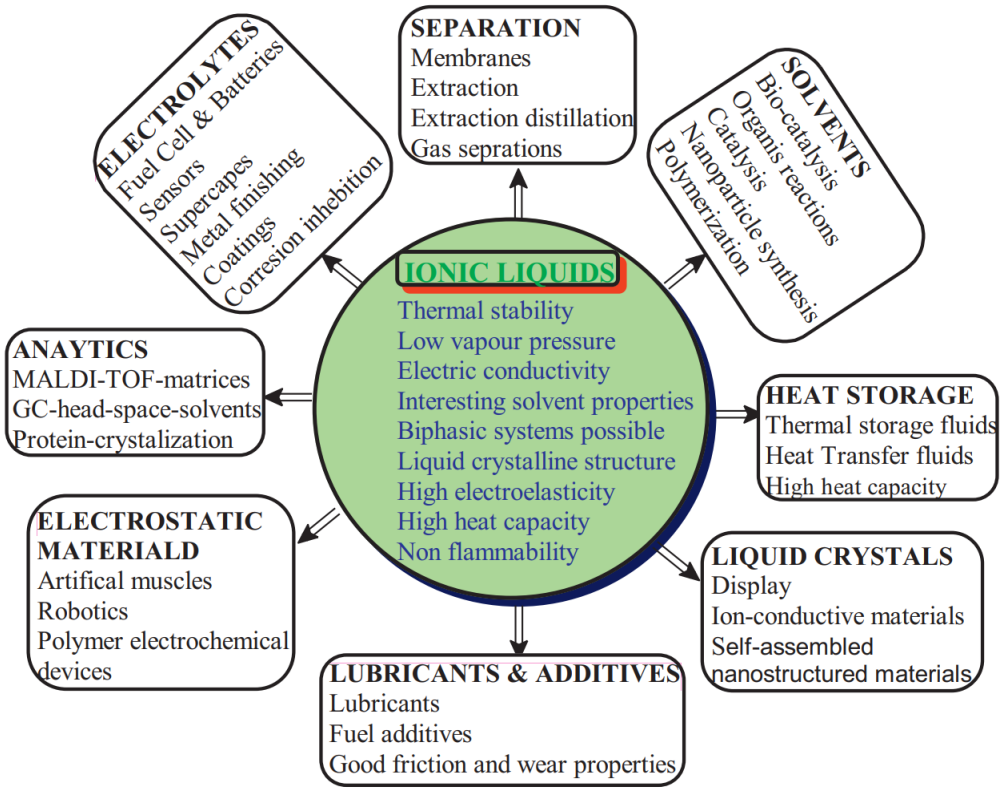

Figure 1.7: Ionic Liquids Applications, Malik, Hashim, and Nabi [9]

1.2.4 Issues

ILs have gained significant interest and resulting in extensive research. Partly because of this investigation, it has become clear that these solvents may not be as advantageous as initially portrayed. While some still claim their unique properties, others have start to emphasise the potential issues and challenges associated with their use [28]. Depicted as green solvents, the main issue of ILs is their *toxicity* [27]. Many neglected potential hazards. The initial expert studies on the toxic hazards indicated that the risk of air pollution is minimal given their non-volatile nature. However, if large-scale industrial use become widespread, the entry into aquatic environments through spills or effluents cannot be overlooked. ILs have been shown to be toxic, as evidenced by various toxicological data collections across diverse organisms, including cytotoxicity and toxicity to microorganisms [29]. ILs also pose challenges related to cost-effectiveness, as their production currently involves considerable expenses. Scaling up their application would require a robust cost-effectiveness strategy. Additionally, they face sustainability concerns due to the limited availability of sustainable feedstocks. Questions regarding sustainability become relevant, especially for ILs synthesised from non-renewable sources.

1.3 Extractant : Deep Eutectic Solvents

Deep Eutectic Solvents (DESs) are eutectic mixtures, which are composed of one or more components with close to the eutectic composition molar ratios. DESs give lowest melting point formed from Lewis and Brønsted acids and bases. Acknowledged as an analogous class of Ionic solvents, DESs have gained significant attention, particularly within metal processing and synthesis industries.

In fact, DESs provide a viable substitute for other solvents in hazardous processes, presenting a more environmentally friendly solution.

DESs exhibit attractive properties for manufacturers, starting with their ease of preparation, relatively inexpensive components, and scalability. The overall production process involves mixing the components at eutectic composition. As represented in **Figure 1.8**, it is evident that the eutectic point has a distinct freezing point compared to the ideal mixture, characterized by ΔT_f. The variation of this temperature difference depends on the specific components of DESs. Based on this, we can categorise them into four classes, which we will elaborate on later.
Other interesting properties are their low vapor pressure, relatively wide liquid-range, and non-flammability. However, they exhibit a great chemical reactivity which is not always desired.

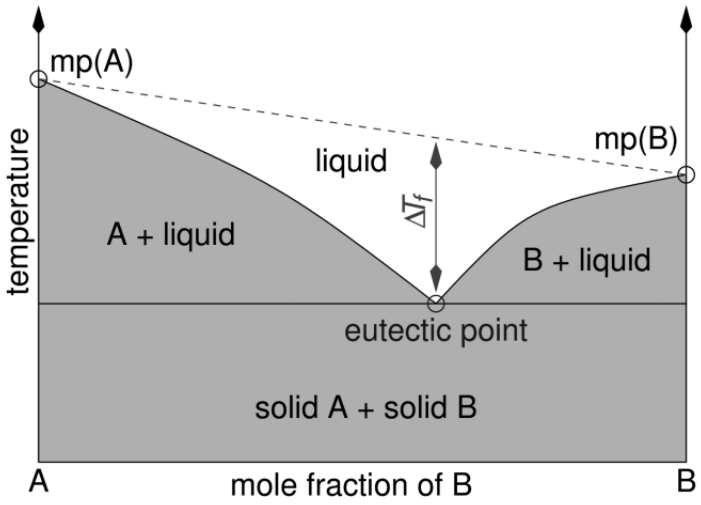

Figure 1.8: Representation of eutectic point within a binary mixture of component A and B, Smith, Abbott, and Ryder [30]

Often compared to ILs due to their similar physical properties, their chemical composition remains significantly different. It is essential to distinguish one another.

1.3.1 Structure

DESs are a eutectic mixture of ions. These solvents typically contain a large asymmetric ion, obtained through the complexation of a quaternary ammonium salt with a metal salt or a hydrogen bond donor (HBD). The electron delocalisation (cf. **Figure 1.9**) within the hydrogen bond allows the cation to possess a low lattice energy, thus resulting in a low melting point.
The general formula is given by :

$$Cat^+X^-zY \tag{1.1}$$

Where : Cat^+ is usually an ammonium, phosphonium, or sulfonium cation. X^- is a Lewis base (electron pair donnor), usually a halide ion. z refers to the number of Y molecules. Y a Brønsted acid (proton donor). Typically, X^- and Y form an ionic complex which enables to classify the DESs depending on its nature.

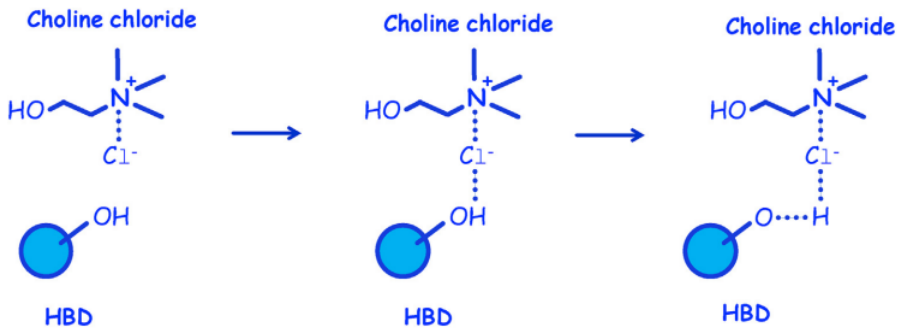

Figure 1.9: Representation of intermolecular interactions during DES synthesis, choline based DES from Santos, Assis, Barreto, *et al.* [31]

Types of DESs

type	general formula	terms
type I	$Cat^+X^-zMCl_x$	M = Zn,[1,5,6] Sn,[7] Fe, Al,[8] Ga,[9] In[10]
type II	$Cat^+X^-zMCl_x{\cdot}yH_2O$	M = Cr,[11] Co, Cu, Ni, Fe
type III	Cat^+X^-zRZ	Z = $CONH_2$,[12] COOH,[13] OH[14]
type IV	$MCl_x + RZ = MCl_{x-1}^+{\cdot}RZ + MCl_{x+1}^-$	M = Al, Zn and Z = $CONH_2$, OH

Figure 1.10: General formulas of different types of DESs according to Smith, Abbott, and Ryder [30]

As shown in **Figure 1.10**, the classification of DESs relies on their composition and properties differences. This classification results into four types with their distinct characteristics [30]:

1. Type I DESs are composed of non-hydrated metal halides, their availability is limited due to their scarcity.

2. Type II DESs involve hydrated metal halides along with choline chloride expanding the range of available formulations.They aim to include other metals, exploiting the lower melting points of metal halide hydrates compared to anhydrous salts.

3. Type III DESs comprise choline chloride and hydrogen bond donor (HBD) which enables a complete natural and eco-friendly formulation [31]. They express an ability of solvate diverse transition metals including chlorides and oxides. When HBDs are multifunctional, the eutectic point tends to converge toward a 1:1 molar ratio of salt and HBD.

4. Type IV DESs incorporates a variety of transition metals into ambient temperature eutectics, expanding DESs applications.

5. Type V: which is not stated in **Figure 1.10** and the last emerging type, contains only non-ionic molecular HBAs and HBDs [32].

Quaternary Ammonium Cation (Choline) are commonly found in DESs formulation. Choline is known for its relatively low cost and non-toxic nature. Its production is realised through an only one step gas-phase reaction producing minimal ancillary waste.

1.3.2 Synthesis

One of the reasons DESs have gained attention, particularly among industrial, is their straightforward preparation process and their relatively affordable cost of constituents. In addition to the conventional and simple approach, alternative methods have been developed to enhance production efficiency and speed of preparation [33].

The simplest approach consists of *Controlled heating and stirring* [34]. The HDB and salt species are directly weighted. It is crucial to highlight their significantly high hygroscopic nature, necessitating precautions to prevent moisture absorption, which could distort measurements. The components are then mixed and stirred in beakers for a few hours until a clear liquid is formed (not excessive temperatures, 50-60°C).

The synthesis process can be assisted by two alternative techniques. *Ultrasound-assisted synthesis (UAS)* utilises ultrasonic bath to expedite the process. The mixture undergoes two rounds of homogenisation and ultrasonic treatment lasting a few minutes [33]. On the other hand, *Microwave-assisted synthesis (MAS)* consists of only two steps: homogenisation followed by a treatment within a microwave reactor lasting less than an hour. This technique allows strict control of the synthesis through regulated temperature, pressure and air flows [33]. Other methods can be found based on thermodynamic reactions such as evaporation and freeze-drying [35].

1.3.3 Physicochemical Properties

The "Deep eutectic solvent" appellation is exclusively granted to mixtures demonstrating lower *melting temperature* than ideal eutectic temperature (c.f **Figure 1.11**). Furthermore, these mixtures must remain in liquid state at room temperature, even if this necessitates deviating from their eutectic composition. Analysing properties of DESs provides a comprehensive overview of their expected behaviour. DESs exhibit greater inertness compared to the ionic liquids [30] and relatively do not interact with other species, making them a very attracting candidate for extraction. In addition to displaying low volatility, non-flammability, and thermal stability, DESs can be chemically tuned for specific applications, thereby influencing properties like phase behaviour, density, viscosity, ionic conductivity, surface tension, and polarity.

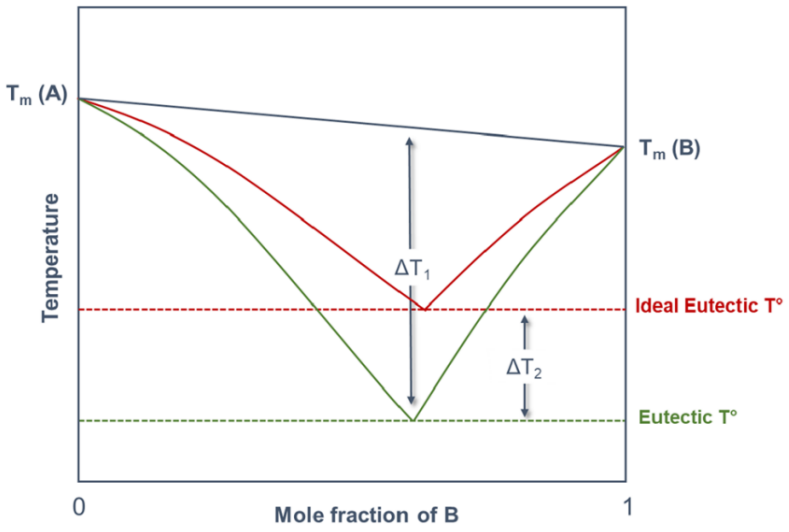

Figure 1.11: Solid-liquid phase diagram of a simple DES, El Achkar, H., and S. [35]

Most documented DESs exhibit a higher density than water, 1.0 to 1.6 g.cm^{-3} [36], derived from metal salts typically demonstrating higher densities. Contrarily, hydrophobic DESs present a lower density than water. It is worth noting that density is a temperature-dependent property, decreasing linearly with increasing temperature. Finally, density is subject to the choice of the HBD and molar ratio [35]. DESs exhibit a broad range of *viscosity*, with some being highly viscous at room temperature [30], primarily due to the extensive hydrogen bond network. Metal salt based DESs generally exhibit higher viscosities. Indeed, viscosity can be chemically tuned varying molar ratio, temperature, and water content. High viscosity tends to show a poor *ionic conductivity*, with very low values [37]. Conductivity can be tuned using the same features as viscosity.

In liquid extraction cases, a fine understanding of fluid behaviours is imperative. *Surface tension* characterises the interaction between two fluids. In the case of DESs, it is greatly dependent on the intermolecular forces between the HBD and the corresponding salt. Typically, surface tension varies between 35 and 75 mN.m^{-1} at room temperature [38], linearly decreasing with increasing temperature. Remarkable values were recorded for sugar based DESs emphasising its extensive hydrogen bond network. As repetitively mentioned, *water uptake* can significantly impact the previously cited physicochemical properties. Despite, typically being considered as impurities due to the pronounced hygroscopic nature of DESs, leading to inevitable water absorption, water is often used to fine-tune these solvents. The water uptake alters the properties for specific applications. However, its presence can compromise the integrity of the solvent and causes inconsistencies. When reviewing literature, deviating values of physicochemical properties can be observed, likely, due to water absorption [39].

1.3.4 "Green Solvent"

Over the last century, and particularly the past few decades, there has been a swift surge in industrial and economic growth. This rapid expansion has led to considerable environment degradation, manifested by climate change, ozone holes development and organic pollutants in all parts of the biosphere. To balance these phenomena, a solution for the protection of the environment and human

health was deemed necessary. The principles of "Green Chemistry" were then introduced to provide guidelines addressing this matter [40]. The concept of "Green Chemistry" proposes twelve principles [41] which aim to reduce or even eliminate hazardous materials from synthesis, production and application of chemicals, taking into account the chemicals safety, toxicity and biodegradability. These will help chemist to achieve this goal of sustainability while preserving environmental and human health.

To be qualified as "green", every reaction must employ clean components, reagents and energy consumption. The development of "green" solvents is, therefore, crucial from the "Green Chemistry" point of view. DESs not only are "green" but they also tick off a few other guidelines, such as principle 3: "Chemical synthesis for less hazardous", principle 4: "Safe solvents", principle 5: "Designing safer chemicals", principle 9: "Biodegradation" and principle 12: "Use of renewable feedstocks". The requirement for "green" solvents driven by their environmental, health and safety attributes, leads to consider the DESs and ionic liquids as prime candidates to replace conventional solvents [31]. Considering their constituent minimal footprint and cost-effectiveness, ease of preparation and properties tunability, DESs are progressively substituting hazardous and volatile compounds in various specific fields [32].

DESs are binary or tertiary mixtures containing at least a hydrogen donor specie and an acceptor. The constituents are strongly linked by hydrogen interaction lowering the lattice energy and thus, the melting point [32]. Another consequence of this hydrogen bonding present in the mixture is its hydrophilic nature. Combined with its low vapor pressure, this characteristic enhances the mixture's ability to dissolve into water [31]. Even though DESs offer more environment-friendly alternatives, they are not inherently "green".

Primarily, only type III DESs can be regarded as such, as type I, II and IV contain metal salts with their own toxicity [30]. Due to their miscibility, they can easily end up into aqueous environment. To achieve true "green" status, DESs must be properly recycled after any application in order to reclaim harmful compounds. Promising candidates in the regard, are Natural Deep Eutectic Solvents (NADES) which consist of primary metabolites constituent compounds. NADES are mainly constituted of: amino acids, organic acids, sugars, or choline derivatives. These solvents almost entirely meet the "Green Chemistry" principles and can be found in nature, most often in plants [31]. NADES offer solute stabilisation, negligible volatility, adjustable viscosity, sustainability, biodegradability combined with acceptable toxicity profiles, high solubilisation power of polar and non-polar compounds, low cost, and simple preparation.

1.3.5 Applications

Due to their remarkable and adjustable characteristics, DESs have gained significant interest from various industrial sectors. The versatile nature of DESs, allowing for fine-tuning of their properties, has made them appealing in diverse applications.

Among these industrial domains, *Metal industry* is worth being point out. Traditional processes rely on water, but show several drawbacks such as toxicity issues. Replacement of water by DESs in this sector provides improved solubility of metal salts and wider windows of operation. The cost-effectiveness and up-scaling possibility make them well-suited for applications such as metal electrodeposition, metal electropolishing, and metal extraction and the processing of metal oxides

[30].

Considering the increasing demand for solutions to address global warming, DESs emerge as viable option for CO_2 *adsorption* and flue gas treatment. Their exceptionally low vapor pressures provide significant potential for such application. Furthermore, their high thermal and chemical stability, nonflammable characteristics, high solvation capacity, and promising gas solubility features make DESs particularly appealing for application in carbon dioxide reduction [38].

Numerous applications are available such as biodiesel purification [34], biotransformation [30] but more interestingly, *biocatalysed reactions* [32]. Surprisingly, isolated enzymes and whole-cell microorganisms are active in DESs, which facilitates the conversion of basic materials into high-value pharmaceutical products under mild conditions of pH, temperature, and pressure. This environmentally and economically advantageous approach replaces the water-based approach in biochemical processes, mimicking cellular metabolites and lipids while preserving protein structures and enabling cofactor recycling. These processes show higher reaction rates, enhanced selectivity and stability of biocatalysts.

1.3.6 Comparision with ionic liquids

Initially, the DESs investigation aims to replace ILs and overcome their associated drawbacks. When comparing the two solvents families, a significant distinctions despite certain similarities is revealed. While ILs were originally considered nonvolatile and nonflammable, recent insights expose, that many exhibit volatility, flammability, instability, and potential toxicity, attributed to the extensive combinations of cations and anions within the IL definition. In contrast, DESs offer a more favorable profile, presenting generally nontoxic, readily accessible, cost-effective, and sustainable compounds. Notably, DES components, derived from natural sources, propose minimal hazards when released into the environment [42].

One key difference lies in their composition: ILs consist of organic heterocyclic cations and organic or inorganic anions, while DESs are composed of hydrogen bond acceptors and hydrogen bond donors. DESs therefore, show a distinct advantage in terms of safety and sustainability due to the properties of their components [42]. Synthesis methods further distinguish ILs and DESs. IL synthesis involves multiple steps, various reagents, and the generation of by-products and waste. On the other hand, DESs can be easily prepared through heating or grinding methods (as mentioned earlier), offering a more straightforward, cost-effective, and environmentally friendly process [33]. Intermolecular interactions control the structure and properties of both ILs and DESs. IL behaviour is dominated by ionic interactions (Coulomb forces), while DESs, as eutectic mixtures, heavily rely on hydrogen bonding. Despite these differences, both exhibit similarities in their properties such as low melting points, density and viscosity, and high polarity, making them versatile solvents for various applications [42]. From an environmental perspective, DESs surpass ILs in terms of higher biodegradability and lower toxicity associated with their natural constituents. ILs, often derived from onium salts, which exhibit higher toxicity. Green chemistry assessments further favour DESs due to factors like shorter reaction times, the use of renewable solvents, reduced chemical quantities, and lower stability in water.

1.4 DES based Membrane

1.4.1 Principle

In order to be operational, the DES based SLM requires to be compressed between the two solutions cells. The feed cell consists of an aqueous solution containing amino acids to extract, while the receiving cell contains an aqueous solution. This configuration allows for the efficient transport of amino acids through the SLM for separation and extraction purposes. Indeed, amino acid will diffuse from one cell to another through the interface by mass transfer [9].

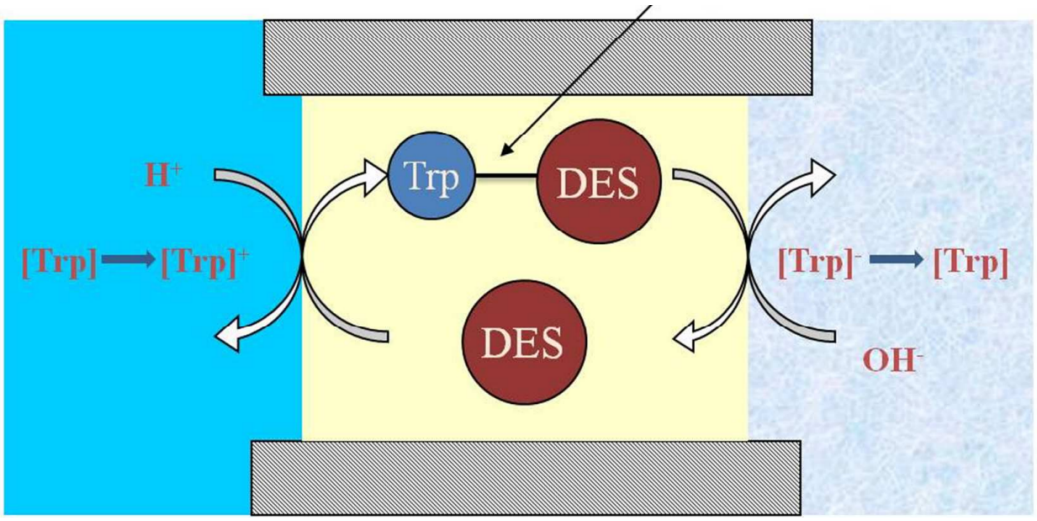

Figure 1.12: amino acid transfer through a DES SLM, Li, Cui, Shen, *et al.* [3]

As illustrated in **Figure 1.12**, the feed cell (depicted on the left) comprises Tryptophan (Trp) an essential amino acid for the human body. Trp is transferred to the receiving phase (located on the right of the figure).

It is crucial to highlight the pH distinction between the two cells. As previously mentioned, amino acid manifest different forms depending on the pH of their surroundings. In this case, it is observable that the feed cell has an acidic pH, associated to HCl addition, while the receiving cell has a basic pH due to NaOH addition. The pH difference is deliberately manipulated to favour the amino acid extraction, allowing control of their solubility. Within an acidic environment, amino acids predominantly exist in their protonated forms, making them more soluble in the extraction phase of the SLM (here DES). As the amino acids migrate to the receiving cell with a basic pH, they undergo deprotonation, leading to their extraction into the aqueous phase of the receiving cell [3].

1.4.2 Optimisation and condition adjustements

The mechanism illustrates that several factors can be optimised to enhance the extraction process. On one hand, we can distinguish chemical factors such as the nature of the feed and extractant solutions; on the other hand, we can consider mechanical properties for optimisation such as membrane structure or the addition of turbulence. Firstly, it is evident that the *choice of the DES* significantly affects the extraction outcome. DESs, as tailored solvents, possess diverse properties, indicating that

some are better suited for this application than others. A critical feature of the DES is its viscosity. Solvents with high viscosity are prone to adhere to the membrane material, resulting in a more stable SLM. Conversely, a too low viscosity leads to instabilities and membrane leaks. Moreover, the extraction behaviour is determined by the species involved. The role of the selected DES is to provide an active site for the amino acid to bind with. As previously discussed, amino acids exhibit two distinct functional groups: an amine (NH_2) and a carboxylic (COOH). These groups are the fundamental basis of the extraction mechanism; thus, the choice of an appropriate DES should consider compatible active sites.

The nature of the binding between the functional group and the DES's active site leads us to consider the operational conditions necessary to optimise extraction, one of which is the *pH of the solutions*. As well understood, the functional groups of amino acids vary with pH, assuming different forms (cationic, anionic, zwitterionic) that are crucial for effective extraction. Depending on whether the DES's active site acts is an HBA or an HBD, the amino acid can be adjusted through pH variations to present complementary functional groups [3]. Furthermore, once the amino acid is extracted, it must be recovered using a stripping solution. The pH of this stripping solution also necessitates to be carefully adjusted to ensure that it has the right affinity for the amino acids. Additionally, pH is a significant condition that can be manipulated to achieve varying levels of extraction efficiency. Given that amino acids are considered weak acids with distinct pKa values, intelligently manipulating the pH by considering the pH ranges between these known pKas can enable selective extraction of different amino acids. Another interesting operational condition is the *feed concentration*. In fact, the driving force behind the SLM is the mass transfer, an increase in concentration can provide a concentration gradient which can enhance the mass transfer. However it is crucial to keep in mind that these amino acids have solubility limits, the concentration should be chosen with care.

Finally, some attention must also be given to the configuration of the system, particularly to the *choice of membrane*. The properties of the membrane, such as its porosity and pore size, can significantly influence the diffusion of species across it. If the goal is to selectively extract specific solutes, selecting an appropriate pore size is crucial. This can enable the membrane to differentiate between molecules based on size, ensuring that only targeted solute pass through while others are retained. Thus, carefully optimizing the membrane characteristics is essential for achieving efficient and selective extraction. In this case, the pore size might not have a great influence because of the very little molecule volumes ($10^{-10}m^3$) [43]. A major characteristic of the membrane is that they vary not only in their physical properties but also in their mechanical and chemical stabilities. These variations can significantly affect the overall efficiency and longevity of the extraction process. A membrane that is mechanically robust can withstand higher pressures and more rigorous operational conditions, while chemical stability is crucial for ensuring that the membrane does not degrade or react adversely with the solutes or solvents used in the process. Therefore, selecting a membrane that aligns well with the specific environmental conditions and chemical nature of the extraction system is vital for maintaining operational effectiveness and durability. To improve the efficiency of the system, incorporating *agitators* can be beneficial as they induce turbulence within the feed and stirring phases. The presence of turbulence significantly alters fluid behaviours, with a direct impact on transfer processes. Turbulence effectively disrupts the boundary layer that typically forms at the interface between the membrane and the feed phase. By diminishing this limiting layer, turbulence facilitates a more rapid and efficient mass transfer across the interface. This enhancement not only speeds up the overall process but can also contribute to increased yield of the separation and extraction efficiencies within the system [44].

1.5 System Components

1.5.1 Amino Acids

Initially, it is capital that the amino acid chosen for this study is pertinent to real-world applications. This ensures that the findings are applicable and beneficial outside of laboratory settings. The choice of amino acid was influenced not only by its relevance to practical applications but also by considerations of analytical ease. The concentration of amino acids within aqueous samples is analysed using an HPLC analyser. This instrument serves effectively as a separator, identifier, and quantifier of compounds within a mixture. The operational principle relies on a mobile phase that transports the sample through a packed column (stationary phase). Compounds demonstrate varying degrees of retention based on their affinity for the column material. Eventually, a detector identifies the presence of these compounds in the mobile phase, each represented by a distinct absorbance peak given in mAU (milli-absorbance-unity). The arrival time of compounds at the detector varies according to their affinity, and each peak is associated to a specific retention time, which can be related with a particular species [45]. In some cases, species may not interact with the column material, resulting in no observed peaks. To enhance certain characteristics of the species, derivatisation agents are often necessary. In this instance, Mercaptopropionic Acid (MPA), Ortho-Phthaldialdehyde (OPA), ultrapure water, and a phosphate buffer were employed. MPA is known to form metal complexes, OPA enhances the detection of amino acids, and the combination of ultrapure water and phosphate buffers maintains stability [46] (HPLC solutions preparation can be retrieved from Appendix A).

After examining aqueous solutions of various amino acids (1g/l), two were selected. The first one being Alanine:

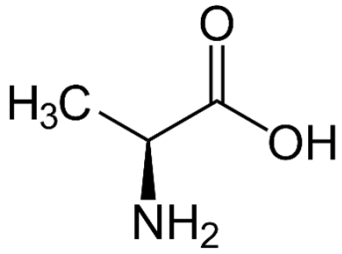

Figure 1.13: Molecular structure of Alanine retrieved from Carl Roth [47]

Alanine is classified as a non-essential amino acid, the human body is capable of synthesising it. It is involved in the glucose metabolism, contributing significantly to energy provision [48]. Among amino acids, alanine is noted for its simple structure [49], represented by the formula $C_3H_7NO_2$, its radical chain being a methyl group. The molar mass of alanine is approximately 89.093 grams per mole. At room temperature, its solubility in water is relatively high, at 164 grams per litre, which enables the use of high concentrations for this application. Additionally, it has pKa values of 2.33 and 9.71 and an isoelectric point of 6, features that are important in understanding its behaviour in biological and chemical systems. These characteristics make alanine particularly suited for studies and applications that require a substance with both stability and effective performance in aqueous solutions.

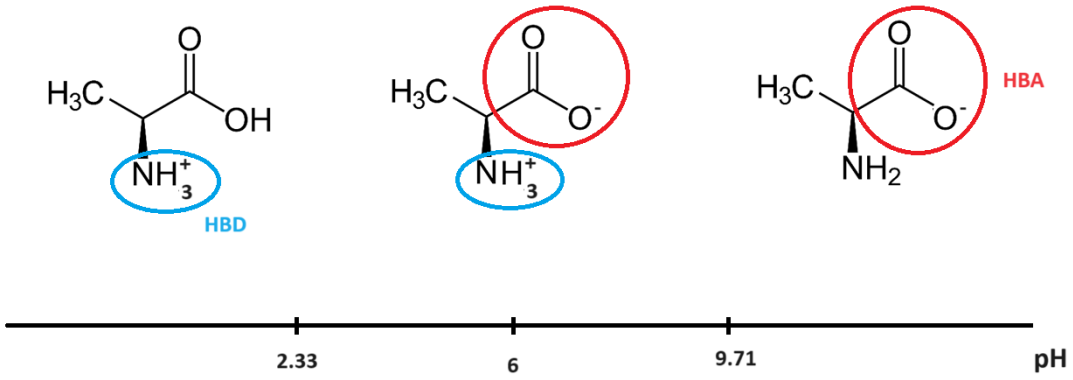

Figure 1.14: Alanine forms depending on the pH environment, based on Carl Roth [47], modified via Microsoft Corporation [15]

Depending on the pH, alanine, like all amino acids, displays both HBD and HBA characteristics. Adjusting the pH to tailor the type of interaction can prove to be highly efficient. On the other hand, its uncomplicated structure and modest size make alanine an outstanding candidate for subsequent extraction process [49]. Moreover, it is well-established that alanine participates in various metabolic and transport mechanisms, features that comforts the idea of its suitability for extraction.

The selection of the second amino acid for this extraction was strategically based on the need to achieve a distinctly separate peak in HPLC analysis compared to alanine. This criterion led to the choice of arginine, an amino acid with significantly different retention characteristics towards the HPLC column, exhibiting a much shorter retention time. Furthermore, arginine and alanine are frequently found naturally together, they are retrieved in diverse animal or vegetal proteins sources e.g. in fish hydrolysate with varying proportions depending on the fish species [50]. Arginine is classified as a semi-essential amino acid, while the body can synthesise arginine under normal conditions, in extreme situations such as periods of rapid growth or severe stress, the body's demand for arginine exceeds its production capacity, necessitating nutritional intake to meet physiological needs [51]. This amino acid plays crucial roles in wound healing and detoxification, highlighting its importance in biological processes [52].

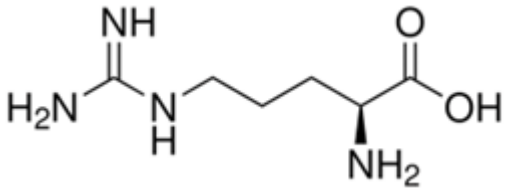

Figure 1.15: Molecular structure of Arginine, retrieved from Carl Roth [53]

Chemically, arginine is considered to be a basic amino acid, primarily due to its guanidium ion group (CH_5N_3). This structural feature considerably differentiates it from alanine, offering an advantage for the extraction process by exploiting these differences in chemical behaviour. Arginine's pKa values are 2.03, 9, and 12.10, with an isoelectric point (PI) of 10.76, which further distinguishes

it in terms of ionisation and solubility profiles under various pH conditions. Arginine's molar mass is 174.201 g/mol, and it is relatively soluble in water, with a solubility of 182 g/L at 25°C. As for alanine, these physical and chemical properties not only facilitate its identification and quantification in analytical processes but also predict a possible selective extraction.

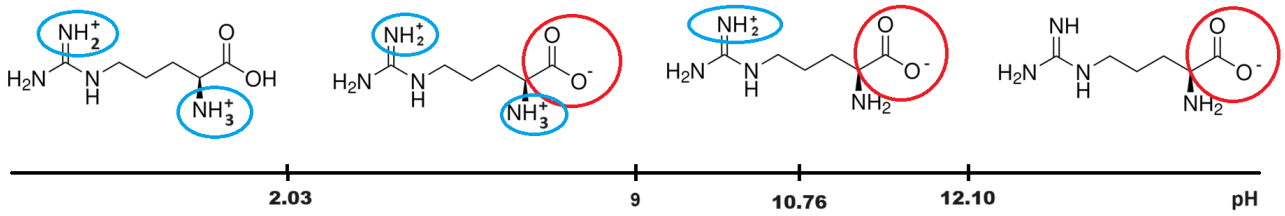

Figure 1.16: Arginine forms depending on the pH environment,based on Carl Roth [53], modified via Microsoft Corporation [15]

From the **Figures 1.14** and **1.16**, it is already clear that there is a particularly interesting operational window based on pH levels. Specifically, the range between pKa values 9 (arginine) and 9.71 (alanine) emerges as a significant zone.

1.5.2 DES

The solvent used in this extraction process comprises a mixture of Trioctylphosphine Oxide (TOPO) and thymol, which plays a crucial role in the selective and efficient extraction of target amino acid. Each component of this solvent mixture brings specific properties that enhance the overall effectiveness of the extraction process.

Focusing on the chemical and physical properties of **TOPO**, it is important to highlight the feature that makes it suitable for this application. TOPO is mainly known for its use as a separating agent in the metal industry [54]. TOPO is an organophosphorus compound with the molecular formula $C_{24}H_{51}OP$. This complex structure consists of a phosphine oxide group (P=O) linked to three octyl chains.

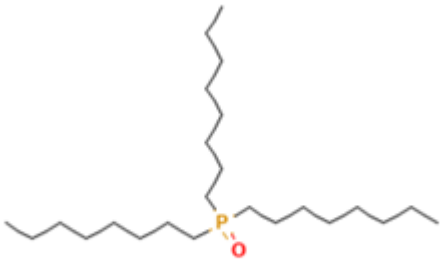

Figure 1.17: Molecular structure of TOPO, retrieved from NIH National Library of Medicine NCBI [55]

As illustrated in **Figure 1.17**, the phosphine oxide group in TOPO, which acts as a HBA, is crucial for enabling strong interactions with surrounding species. The presence of the three long alkyl chains significantly enhances van der Waals interactions within the molecule itself. These interactions contribute to its high viscosity and hydrophobic nature, making TOPO soluble in hydrocarbons and certain alcohols but not in water. This solubility profile is essential for its use in non-aqueous extraction processes. Furthermore, TOPO has a melting temperature of 55°C [56], which influences how it is handled and utilized in various applications. TOPO is a solid whitish compound at room temperature. Regarding chemical safety, TOPO is generally considered to have low toxicity, which is advantageous for handling and environmental considerations. However, it is somewhat corrosive and can be an irritant [55], necessitating proper safety measures during handling to avoid potential harm to skin or eyes.

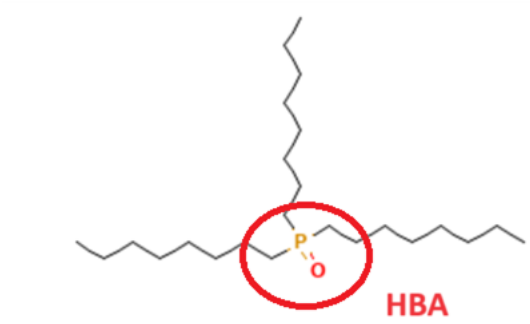

Figure 1.18: Molecular Structure of TOPO highlighting its hydrogen bond donor group, based on NIH National Library of Medicine NCBI [55], modified via Microsoft Corporation [15]

Thymol, the second principal component, is widely known for its antiseptic and antibacterial properties, making it an effective disinfectant [57]. Derived from thyme oil, thymol is a monoterpenoid phenol, chemically identified as 2-Isopropyl-5-methylphenol, with chemical formula $C_{10}H_{14}O$.

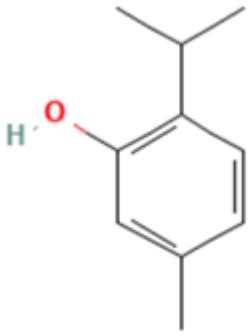

Figure 1.19: Molecular structure of thymol, retrieved from NIH National Library of Medicine NCBI [58]

The structure of thymol includes a benzoic ring (**Figure 1.19**), which is capable of stabilisation through resonance, enhancing its chemical stability and reactivity. Attached to the ring is a hydroxyl

group, which further contributes to its chemical activity. These groups are significant because they enable thymol to engage in various chemical reactions and interactions, particularly useful in the formation of DES where strong interactions with other substances are necessary. Despite its light solubility in water, thymol dissolves well in alcohols and ethers. This solubility pattern is particularly beneficial in pharmaceutical and cosmetic industries where thymol is used in formulations without high water content [59].

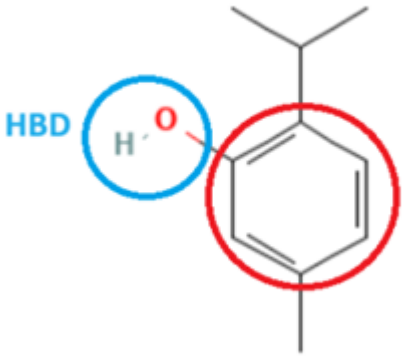

Figure 1.20: Molecular structure of thymol highlighting both hydrogen bond donor and acceptor groups, based on NIH National Library of Medicine NCBI [58], modified via Microsoft Corporation [15]

Additionally, thymol has a melting temperature of around 50°C, making it solid crystal at room temperature but easily melted for use in various applications. However, its strong odour and potential environmental hazards require careful handling. It is dangerous for mucous membranes, displaying corrosive and irritant characteristics. It is necessary to handle it under controlled conditions, typically in a fume hood, to minimize exposure and prevent environmental contamination [60].

As depicted in **Figures 1.18** and **1.20**, both substances feature groups capable of hydrogen bonding. The formation of the DES occurs through the interaction between TOPO's HBA phosphine oxide group and thymol's HBD hydroxyl. This configuration leaves thymol's HBA benzoic ring available for external interactions. It is noteworthy that thymol can also interact with itself via hydroxyl-benzoic ring interactions. When the molar ratio of thymol is increased, thymol tends to link to itself. Consequently, this free benzoic ring becomes the only reactive group remaining, thus becoming the principal component in the extraction process [60].

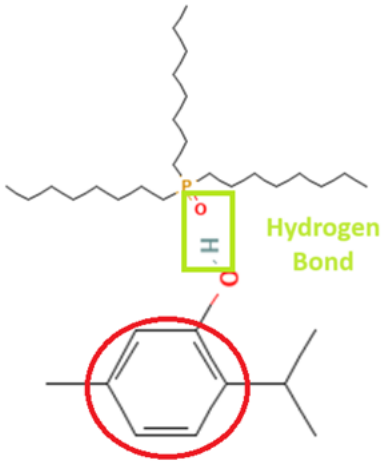

Figure 1.21: TOPO-thymol bond, higlighting in red the thymol HBA group, Figures 1.17 and 1.19 modified via Microsoft Corporation [15]

Provoking the HBD groups on the target amino acid will thus improve the extraction process. As discussed in **section 1.5.1**, the amino acid can be protonated in an acidic environment. In their cationic forms, both alanine and arginine will exhibit HBD groups that are capable of interacting with the thymol benzoic ring.

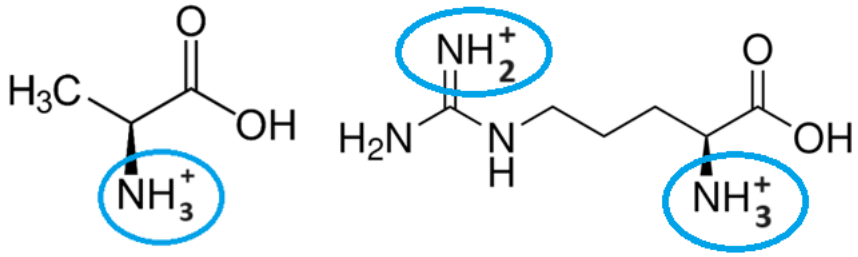

Figure 1.22: Cationic forms of Alanine and Arginine highlighting their HBD groups, based on Figures 1.13 and 1.15 modified via Microsoft Corporation [15]

Chapter 2

Materials and Methods

The experiment methodology involves the preparation of a supported liquid membrane impregnated with a Trioctylphosphine oxide (TOPO) and thymol mixture. The TOPO-thymol based DES was chosen specifically for its high hydrophobicity. This characteristic is crucial as it prevents the DES from mixing with the aqueous solution, thereby facilitating an efficient liquid-liquid extraction process. The selection of TOPO-thymol was also influenced by previous research conducted within the department, which highlighted its efficiency in the extraction of chiral amines. It showed an ability to form a stable membrane that is resilient to leaks. This stability is vital in ensuring that the membrane maintains its integrity throughout the extraction process.

Once the membrane setup is complete, an aqueous solution containing the target amino acids is introduced and brought into contact with the impregnated membrane. The TOPO-thymol DES selectively captures the amino acids due to its tailored chemical affinity. Following the extraction, the isolated amino acids are quantified using high-performance liquid chromatography (HPLC). This technique provides measurements of the amino acids' concentration, validating the efficiency of the TOPO-thymol DES system and its suitability for selective extraction.

2.1 System Characterisation

2.1.1 Amino acids

To accurately characterise the amino acids involved in the study, the computation of a calibration line is indispensable. This analytical tool is essential for the correct interpretation of the results obtained from the extraction process. To construct this calibration line, aqueous solutions of both alanine and arginine are prepared at varying concentrations, specifically at 0.5, 1, 2, 2.5, 5, 10, and 20 g/L. These solutions are then analysed using the HPLC device twice for accurate results. The motive behind this approach is that the area under the peak in the HPLC chromatogram can be correlated to the concentration of the amino acid in the sample. By establishing a series of known concentrations and measuring their respective peak areas, a calibration line can be plotted. This curve serves as a reference for determining the concentrations of amino acids in unknown samples, thereby providing a quantitative measure of the amino acids extracted. However, the HPLC has a saturation limit, which leads to a linear region and a saturated region. The extraction will only be conducted at concentrations within the linear region for the sake of analysis. Once all the peak areas from the HPLC analysis are identified, a calibration line is computed using linear regression. This

statistical method minimizes the distances between the observed values (the peak areas) and the values predicted by the linear model.

2.1.2 DES

To explore the properties of our DES, a series of TOPO-thymol mixtures were prepared, each with a different molar ratio. These formulations, totaling 20g each, were prepared. For a molar ratio of 1:x, where x represents the proportion of thymol, it requires to solve the following system:

$$\begin{cases} x\ n_{TOPO} = n_{thymol} \\ m_{TOPO} + m_{thymol} = 20g \end{cases}$$

Given the molar mass of TOPO at 386.6 g/mol and thymol at 150.22 g/mol, we can perform calculations to determine the appropriate masses for each component needed to achieve a desired molar ratio in a mixture:

$$n_{TOPO}M_{TOPO} + x\ n_{TOPO}M_{thymol} = 20 \tag{2.2}$$

$$n_{TOPO} = \frac{20}{M_{TOPO} + xM_{thymol}} \tag{2.3}$$

$$\begin{cases} m_{TOPO} = n_{TOPO} \times 386.6 \\ m_{thymol} = x\ n_{TOPO} \times 150.22 \end{cases}$$

The prepared DES are reported (mass in grams):

Table 2.1: TOPO-thymol, molar ratio proportions

Molar Ratio	**Theoritical** m_{TOPO}	**Theoritical** m_{thymol}
1:1	14.403	5.597
1:2	11.254	8.746
1:3	9.235	10.765
1:4	7.830	12.170
1:5	6.797	13.203
1:6	6.003	15.997
2:1	16.746	3.254
3:1	17.707	2.293
4:1	18.229	1.771

The primary property being explored was their **melting point**, it is now well-understood that the components of the DES engage in strong hydrogen bonding interactions, which can significantly alter their phase transition behaviour. The melting temperatures of both thymol and TOPO are quite similar, around 50°C, yet their combined behaviour in a mixture exhibits considerable differences. To highlight this distinct characteristic of DES, the melting points of the mixtures were measured using a Differential Scanning Calorimeter (DSC) [61]. This analysis measures the heat flow of a sample as it is heated, cooled, or maintained at a constant temperature. The results are readily interpretable since

phase transitions are manifested as peaks in the heat released or absorbed, depending on whether the transition is endothermic or exothermic. This technique not only helps to identify the mixture that most closely approximates the eutectic point but also allows for the assessment of the thermal stability of the solvents. For this experiment, solvent samples, whether in liquid or solid form, were sealed into a DSC sample holder, which contains approximately five milligrams of material. The samples were subjected to multiple heating cycles: initially, they were heated at a rate of 10°C/min from room temperature up to 80°C, followed by maintaining this temperature for one minute. Subsequently, they were cooled at the same rate down to -80°C, held for another minute, and then reheated back to 80°C. Peaks observed in the heat flow per unit mass during these cycles indicate phase transitions.

Since the DES will be used in a liquid-liquid extraction involving an aqueous phase, it is essential to assess the **water content** of this solvent. Although typically hydrophobic, the presence of a minor amount of water is still possible. Therefore, it is imperative to accurately measure this water content. This analysis is carried out using a thermogravimetric analysis (TGA) [62], which allows for the observation of variations in a sample's mass. It is placed on a weighing scale within a chamber that is regulated by a flow of nitrogen. The temperature of the chamber varies according to the programmed cycle, the sample is perforated to facilitate the release of vapours, enabling to measure and record weight variations. Therefore, assessing the water content involves closely monitoring mass fluctuations around 100°C. It is important to note that while this method may not provide absolute precision due to the potential evaporation of other volatiles around 100°C, it nonetheless offers a sufficiently accurate estimation of water content [63].

Subsequently, the preparations were subjected to Fourier Transform Infrared (FTIR) spectroscopy analysis. This technique serves as an identification and **structure comprehension** of organic compounds. FTIR analysis works on the principle of infrared (IR) light interaction with the compound. Each type of bond within the molecules absorbs or transmits light at different frequencies [64]. These frequencies are dependent on the energy required to induce vibrations in the bonds, corresponding to various functional groups within the molecule. By measuring which frequencies of IR light are absorbed and which are transmitted, we can determine the composition and structure of the compound. The absorption spectrum that is obtained through this analysis provides an insight to identify and study in depth the component. For the analysis of DES, FTIR spectroscopy is particularly useful. It allows to observe how interactions within the solvent change with variations in molar ratio. Especially focusing on hydrogen bonds which can significantly influence the properties of DES, such as viscosity, melting points, and chemical reactivity. To do so, a close evaluation of the range 3500 to 3000 cm^{-1} is necessary [65]. Understanding these interactions and how they vary with changes in composition can provide valuable insights into designing DES with tailored properties for specific applications.

The analysis of the solvent's **viscosity** using a rheometer was deemed impractical due to the solvent's odorous and irritant characteristics, necessitating the test be conducted under a fume hood, which made the procedure unfeasible. However, understanding the viscosity is crucial as it helps determine the most effective molar ratio for the solvent when used in applications such as membrane technologies. Overall, the combination of DSC, TGA, and FTIR analyses provided a robust scheme for understanding and manipulating the properties of DES to enhance their application. This strategic approach to solvent characterisation ensures that despite practical challenges, the performance and application potential of DES can be fully realised, leading to more effective and efficient industrial processes.

2.2 Preliminary tests: Liquid-Liquid Extraction

Prior to proceeding with the membrane setup, it is necessary to conduct preliminary tests to optimise the system. These tests will reduce the number of experiments needed with the actual membrane equipment. These preliminary evaluations are carried out through a liquid-liquid extraction process, which serves multiple fundamental purposes. Firstly, these tests assess the feasibility of the extraction process itself, determining whether components are successfully transferred from one phase to another. This step enables to verify the basic operational viability of the system. Secondly, the choice of solvent is determined during this stage by testing the various molar ratios of the DES prepared. This ensures that the most effective solvent composition is selected for the specific application. Furthermore, the tests are designed to establish the optimal operational conditions. This includes experimenting with different pH levels and concentrations to observe their effects on the extraction process. By cautiously adjusting these parameters, the most efficient conditions for the membrane operation can be identified [66], ultimately leading to a more controlled and effective separation process in subsequent stage.

The liquid-liquid extraction (LLE)[67] procedure is performed within tubes, each containing 3 ml of the aqueous mixture with the amino acid and 3 ml of the DES extractant. To ensure the integrity of the samples during the extraction process, the tubes are securely sealed with parafilm strips. The procedure includes an agitation phase lasting 24 hours to facilitate thorough mixing, followed by a rest period of an additional 24 hours, resulting in a total experimental duration of 48 hours. This step is notably the most time-consuming part of the process. For every liquid-liquid extraction, two tubes with the same experiment were prepared, this is a precaution in order to have accurate results by comparing them.

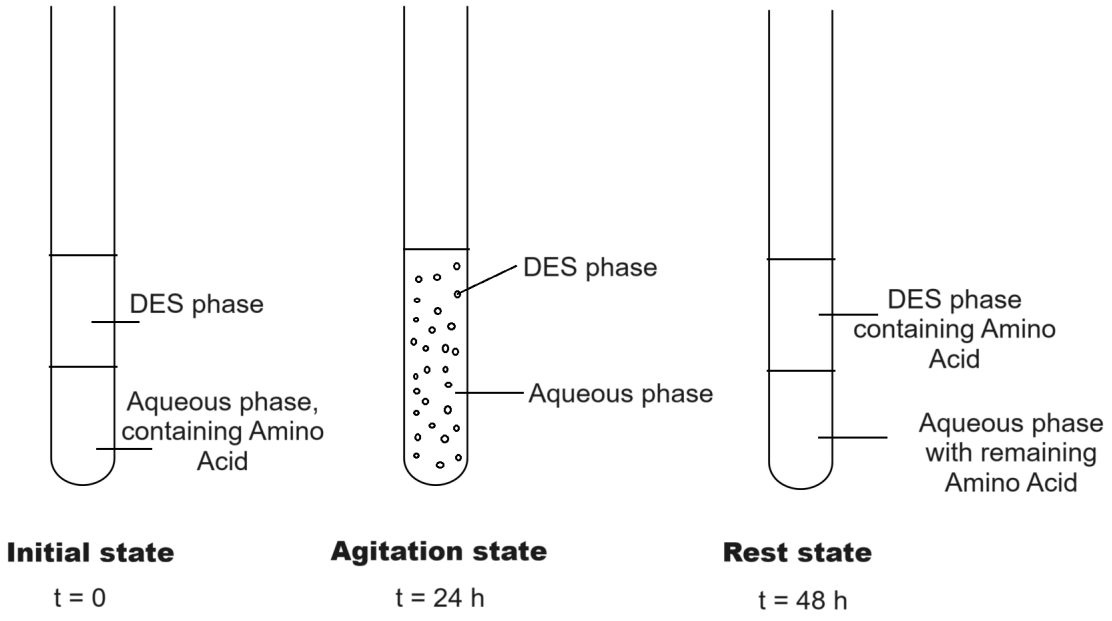

Figure 2.1: Liquid-Liquid Extraction schematic scenario, generated via Microsoft Corporation [15]

Given that the HPLC device is equipped solely for analysing aqueous solutions, only the aqueous

phase is subjected to analysis post-extraction. This analysis enables the quantification of the amino acids that have been transferred from the aqueous phase to the DES phase. Through this approach, the efficiency of amino acid extraction by the DES can be assessed, providing crucial insights into the solvent's effectiveness and the optimal conditions for amino acid recovery.

Referring to section 2.1.1, as illustrated by **Figures 1.14 and 1.16**, it is clear that pH is an essential parameter in the behaviour of amino acids during extraction processes. pH levels influence whether amino acids display HBD groups, which leads to interactions with the DES, hence the extraction. To comprehensively understand the influence of pH, various levels are tested to evaluate their effects on the solvation and extraction behaviours of amino acids. Initially, an acidic environment at pH 1 is examined to induce HBD groups on amino acids. Subsequently, a neutral pH is tested to establish a baseline for amino acid behaviour without the extreme influences of either acidic or basic conditions. Furthermore, a highly basic pH of 10 is investigated to assess the impact of reduced proton availability on amino acid interactions. Additionally, pH 9.3 is specifically targeted because it lies between the second pKa values of arginine and alanine, potentially highlighting unique interactions at this midpoint. Finally, the testing includes pH 3 and 6 to identify any variations in extraction efficiency under moderately acidic and mildly acidic conditions. These tests are vital for identifying the most effective pH for maximizing extraction efficiency.

2.2.1 pH selection

To ensure precise control over the experimental conditions, the use of buffer solutions is imperative. This necessity arises because amino acids can interact with water, potentially leading to significant alterations in the solution's pH. Utilising buffers that can resist minor pH variations is particularly advantageous, as it helps maintain stable conditions throughout the experiment. To select the most appropriate buffer, one must consider the pKa values of the available buffer pairs. Ideally, these pKa values should be close to the target pH for the experiments. This alignment ensures that the buffer can effectively stabilise the pH, thereby minimizing fluctuations that could influence the behaviour of the amino acids and the overall outcome of the extraction process.

For this specific experiment, three buffer pairs have been chosen based on their pKa values to accommodate a range of pH conditions. The first pair, H_3PO_4/NaH_2PO_4, is used for acidic preparations and has a pKa of 2.148. The second pair, NaH_2PO_4/Na_2HPO_4, arises from the combination of NaH_2PO_4 and NaOH and is suitable for conditions that are neutral to moderately acidic or basic, with a pKa of 7.198. Lastly, the $NaHCO_3/Na_2CO_3$ pair, with a pKa of 10.33, is selected for basic conditions.

Buffers were prepared following these calculations (e.g for pH = 1, for 100 ml at 1 mol/l):

$$\begin{cases} [AH] + [A^-] = 1mol/l \\ pKa + log\left(\dfrac{[A^-]}{[AH]}\right) = pH \end{cases}$$

With AH/A^- the given Acidic/Basic buffer couple. The pair chosen for acidic buffers is as follows:

$$H_3PO_{4aq} + OH^-_{aq} \leftrightarrow H_2PO_{4aq}^- \tag{2.6}$$

Table 2.2: Properties of Phosphoric Acid and Sodium Dihydrogenophosphate

Phosphoric acid	Form	Liquid
Phosphoric acid	Concentration	85%
Phosphoric acid	Molar mass (M)	98 g/mol
Phosphoric acid	Volumic mass (ρ)	1.695 g/ml
Sodium dihydrogenophosphate	Molar mass (M)	119.98 g/mol
$H_3PO_4/H_2PO_4^-$	pKa	2.148

$$\begin{cases} [H_3PO_4] + [H_2PO_4] = 1 \\ 2.148 + log\left(\dfrac{[H_2PO_4]}{[H_3PO_4]}\right) = 1 \end{cases}$$

$$\begin{cases} [H_3PO_4] = 9.336 \times 10^{-1} mol/l \rightarrow n = 9.336 \times 10^{-2} mol \\ [H_2PO_4] = 6.640 \times 10^{-2} mol/l \rightarrow n = 6.640 \times 10^{-3} mol \end{cases}$$

$$m_{H_3PO_4} = [H_3PO_4] \times M_{H_3PO_4} = 9.336 \times 10^{-2} \times 98 \approx 9.149\ g \quad \rightarrow m_{tot} = \frac{9.149g}{0.85} \approx 10.764\ g \quad (2.9)$$

$$V_{H_3PO_4} = \frac{m}{\rho} = \frac{10.764}{1.695} \approx 6.35\ mL \quad (2.10)$$

$$m_{NaH_2PO_4} = n_{H_2PO_4} \times M_{NaH_2PO_4} = 6.640 \times 10^{-3} \times 119.98 \approx 0.797\ g \quad (2.11)$$

pH 3 buffer has been computed the same way:

Table 2.3: Phosphoric Acid Buffers, pairs' proportions

pH	$V_{H_3PO_4}$ (ml)	$m_{Na_{H2}PO_4}$ (g)
1	6.35	0.797
3	0.84	10.52

For the more **moderate solutions**, the addition of NaOH to NaH_2PO_4 should be considered:

$$H_2PO_{4_{aq}}^- + OH_{aq}^- \leftrightarrow HPO_4^{2-}{}_{aq} \quad (2.12)$$

Table 2.4: Phosphoric buffer, components properties

Sodium hydroxyde	Molar mass (M)	39.997 g/mol
Disodium phosphate	Molar mass (M)	141.96 g/mol

Table 2.5: Phosphoric Buffers, moderate pH pairs' proportions

pH	$m_{NaH_2PO_4}$ (g)	m_{NaOH} (g)
6	12.0	0.237
7	11.998	1.55

For **basic solutions** a sodium carbonate buffers is considered :

$$HCO_{3_{aq}}^{-} + OH_{aq}^{-} \leftrightarrow HCO_{3}^{2-}{}_{aq} \tag{2.13}$$

Table 2.6: Sodium carbonate buffer, component properties

Sodium hydrogen carbonate	Molar mass (M)	84.007 g/mol
Sodium carbonate	Molar mass (M)	105.989 g/mol

Table 2.7: Sodium Carbonate Buffers pairs' proportions

pH	m_{NaHCO_3} (g)	$m_{Na_2CO_3}$ (g)
9.3	6.19	2.788
10	5.723	3.378

2.2.2 Solvent selection

Once the optimal pH level has been established, the appropriate solvent selection can proceed. In this experiment, various molar ratios of TOPO-thymol, including 1:1, 1:2, 1:3, and 1:4, were evaluated. Higher molar ratios of TOPO mixtures were excluded. It was observed that increasing the proportion of TOPO leads to the formation of solid mixtures at ambient temperature, making extraction unfeasible under these conditions. Additionally, higher ratios of thymol were not further examined (1:5 and 1:6). This decision was based on the fact that if any significant differences in behaviour were to manifest, they would already be evident at the tested ratios. Thus, exploring these initial configurations provides sufficient insight into the solvent's characteristics without the need for additional, potentially redundant testing. If significant variations were to be observed, higher molar ratios of thymol will be tested.

Furthermore, a reduced concentration of 3g/L was tested to verify the presence of concentration effects. This approach aims to explore whether varying the concentration influences the outcome of the experiments. By examining the effects at a lower concentration, it is possible to better understand the dynamics of the extraction process and optimise conditions for efficiency and effectiveness.

Finally, a feasibility test was conducted using a mixture of alanine and arginine at a concentration of 5 g/L, combined with DES at molar ratios of 1:1 and 1:2. These experiments were performed at pH levels of 7 and 9. This approach aimed to evaluate the interaction between the amino acids and the solvent under varying pH conditions. Having previously tested amino acids separately, this subsequent test, involving a mixture of alanine and arginine, will allow for the observation of potential interactions between the amino acids themselves. This investigation will determine whether the amino acids influence each other's behaviour in a mixed environment, thereby affecting the overall feasibility of the extraction process. This final experiment will determine the viability of the process, and serves as a checkpoint before proceeding on the membrane set up.

The process can be illustrated as follows. LLE is based on the principle that the target compounds exhibit different solubilities in the two immiscible phases. This difference in solubility drives the solute from one phase to the other, facilitated by a concentration gradient.

Diffusion behaviours are governed by the Fick laws, particularly the first [68]:

$$J_{A_Z} = -D\frac{dC_A}{dz} \tag{2.14}$$

This law describes how the flux of solute A in the z-direction (J_{A_z}) is influenced by two main factors: the concentration gradient and the diffusion coefficient (D) of A within the phase, which is dependent on the intrinsic properties of both the solvent and solute. In this specific scenario, amino acids migrate from the aqueous phase to the DES phase. For example the flux of alanine migrating between the two phases can be written conventionally as:

$$N_{AL} = k_{AL}(C_{aq_{AL}} - C_{DES_{AL}}) \tag{2.15}$$

However, it's important to consider the reverse process, known as back extraction, which influences overall diffusion behavior. The interplay between forward extraction and back extraction significantly impacts the efficiency and dynamics of mass transport. The total flux can be written as:

$$N_{AL} = k_{AL}(C_{aq_{AL}} - C_{DES_{AL}}) - k_{-AL}(C_{DES_{AL}} - C_{aq_{AL}}) \tag{2.16}$$

Moreover, both arginine and alanine are extracted. With simplified flux calculation (K = k + k$_-$), the total movement can thus be expressed as:

$$N = N_{AL} + N_{AG} = K_{AL}(C_{aq_{AL}} - C_{DES_{AL}}) + K_{AG}(C_{aq_{AG}} - C_{DES_{AG}}) \tag{2.17}$$

To accuratly compare separation processes, a set of analytical tools has been developed, which includes split fraction, split ratio, and split power. Each of these metrics serves a specific function in measuring the effectiveness and efficiency of a separation process, enabling detailed evaluation and comparison. The split fraction quantifies the proportion of a particular component that is separated from a mixture in a specific process stream. This measure is crucial for assessing how effectively a separation system can isolate desired elements from other substances within a mixture. The split fraction is defined as (e.g alanine in a LLE with a DES and an aqueous phase) [69]:

$$SF_{AL} = \frac{n_{out}}{n_{in}} = \frac{n_{AL_{DES}}}{n_{AL_{aq}}} \tag{2.18}$$

The split ratio extends this analysis by examining the distribution of a component between two distinct phases a separation system. It is calculated by comparing the concentration of a component in one phase to its concentration in another, providing insight into the balance and distribution efficiency of the system. It is defined as:

$$SR_{AL} = \frac{SF_{AL}}{1 - SF_{AL}} \tag{2.19}$$

Lastly, split power evaluates the overall effectiveness of a separation process. It compares the behaviours of two species towards the extraction process, which quantifies the selectivity. A process is considered highly selective when $SP_{i,j} >> 1$. For a separation of Alanine and Arginine, split power is defined as:

$$SP_{AL,AG} = \frac{SR_{AL}}{SR_{AG}} \tag{2.20}$$

2.2.3 Membrane Experiments

In the progression of the study, the focus shifts to the experiments utilising the membrane setup. Prior to this stage, operational conditions were meticulously determined through liquid-liquid extraction experiments. These initial tests identified the optimal conditions for effective and efficient results. This section will detail the execution of the membrane setup tests.

Equipment Description

The membrane setup used for this experiment, as provided by the department, differs from the schematic representation shown in **Figure 1.4**:

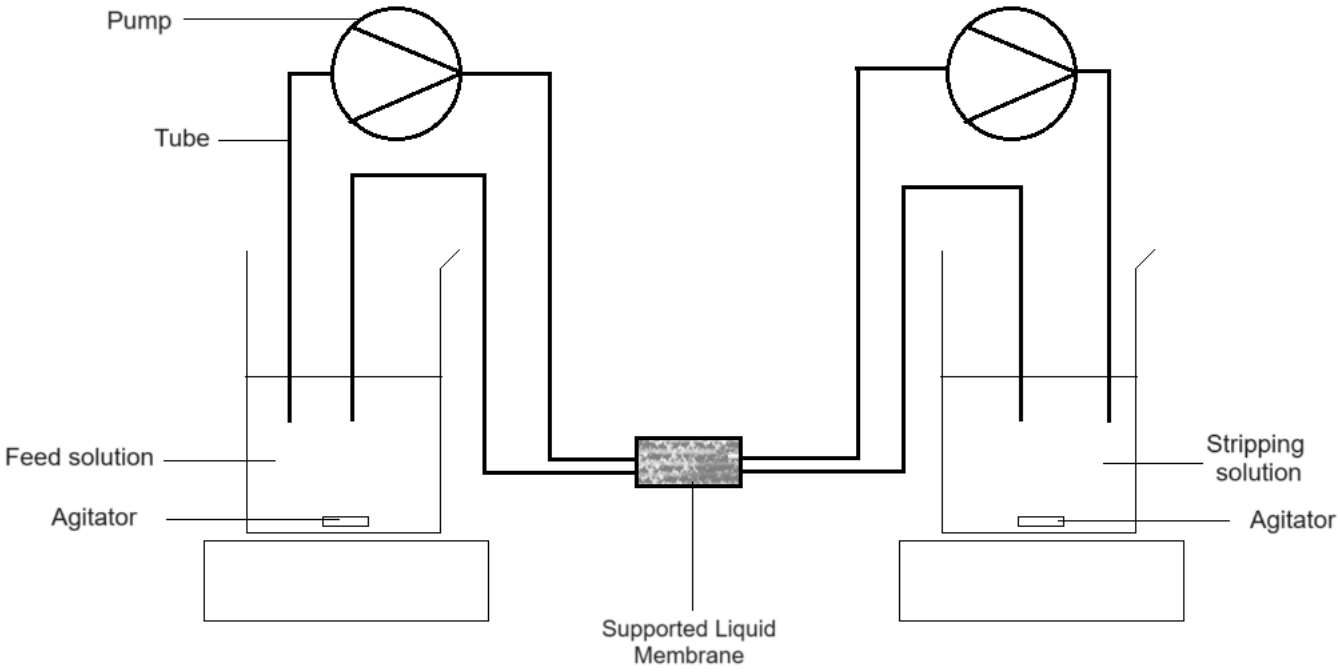

Figure 2.2: Membrane setup, schematic representation

The system comprises :

1. A beaker holding the feed solution (mixture of amino acids).
2. A beaker holding the stripping solution (basic solution).
3. Two agitators (one located in each beaker), that are in movement thanks to a pressurised air system.
4. Two pumps ensuring the contact of both phases with the membrane, providing a flow rate of 10 l/h.
5. A supported liquid membrane screwed into a holder.

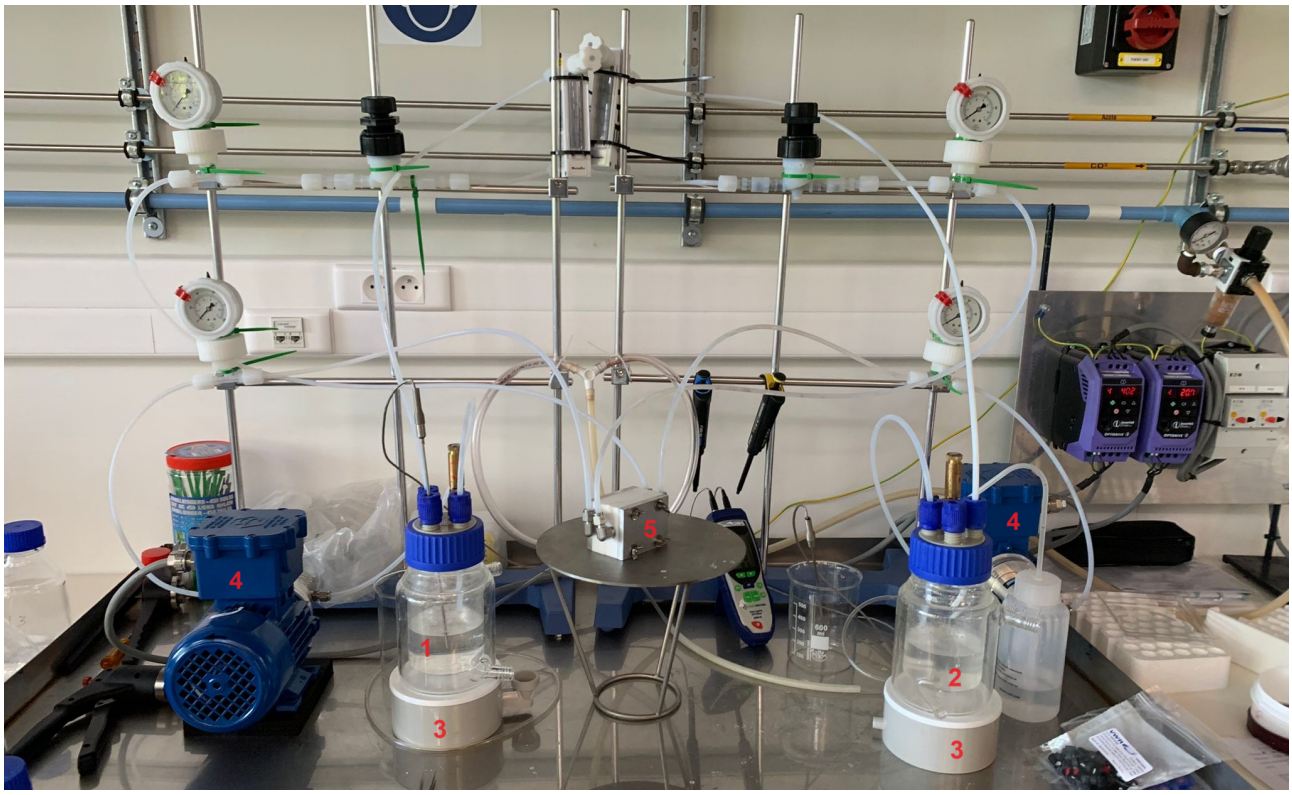

Figure 2.3: True membrane set up in the lab, numbers previously enumerated

As illustrated in **Firgure 2.2**, the experimental configuration incorporates a pumping system, an adaptation necessitated by the physical separation of the membrane from the two phases. In this setup, the membrane is securely sealed within a holder that is connected to a system of tubes. This arrangement facilitates the circulation of the solution while providing the membrane integrity. The pumping system ensures the pumping into both beakers and then cycling back. Such design ensures continuous fluid movement across the membrane, which is critical for maintaining consistent contact between the phases and the membrane surfaces.

A notable feature of the system is that the agitators are powered by pressurised air, chosen specifically for its consistent flow and reliability as an energy source [70]. The use of pressurised air avoids the need for electrical power, offering a safer alternative particularly suitable for applications in sensitive environments where safety is essential. Additionally, this method helps to prevent thermal overloads, which could interfere with the system, more precisely with the solubility of components into aqueous phases. Thus ensuring the operational integrity and longevity of the equipment.

The pH of the stripping solution must be carefully selected, just as the feed solution is for selective separation. Given that the amino acids interact with the DES via their amine groups, the objective of the stripping process is to deprotonate these groups. Consequently, a basic solution would be effective in extracting the amino acid from the DES. Membrane extraction can be understood as two sequential liquid-liquid extractions, both of which operational conditions can be optimised. Employing a pH that specifically deprotonates the amine group of Alanine may be intresting, thereby necessitating a pH range between 9.7 (the pKa of Alanine's amine group) and 12.10 (the pKa of Arginine's guanidine

group). However, it should be noted that some Arginine may also be extracted, given that its amine pKa is 9.

Experiments

Based on the experiments detailed in previous sections, the process of SLM separation is now ready to take up. As the operational conditions, which were previously evaluated and optimised through liquid-liquid extraction experiments, the focus now shifts to testing aspects specifically related to the membrane's nature. This involves examining the membrane's properties and performance under the established conditions to ensure it functions effectively within the system, aligning with the overall objectives of the separation process.

This investigation explores various types of membranes, each of which will be impregnated with the DES, identified as the most effective from prior experiments. The impregnation process, which takes approximately one hour, involves repeatedly pouring DES onto the membrane using a vacuum pump to ensure thorough saturation. The amount of DES (2 ml) needed to cover the entire membrane surface was added three times, first at 20, then at 40 minutes. The membrane is then cleared from the excess solvent and weighed to compare to its initial weight, enabling to determine the mass of solvent impregnated.

The study will examine several specific aspects of membrane performance to understand how different variables impact the separation process, every experiment will be conducted twice. A Polyvinylidene fluoride (PVDF) membrane with 100 nm pores will be tested initially to establish a baseline for performance, setting a standard against which other membranes can be compared. Additionally, another PVDF membrane, this one with 200 nm pores, will be used to evaluate how an increase in pore size affects the efficiency of the separation process. Furthermore, a Polytetrafluoroethylene (PTFE) membrane with 100 nm pores will be included to explore any differences that may be attributed to the material nature of the membrane itself, providing insights into how material properties influence overall performance. These examinations are integral in determining the most effective membrane characteristics for specific separation tasks.

SLM modelling

For SLM of thickness L, concentrations profiles can be understood as follows:

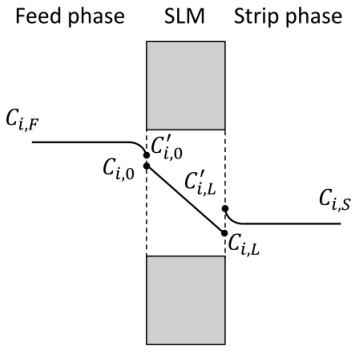

Figure 2.4: Concentration profiles through SLM Van Eygen, Van der Bruggen, Buekenhoudt, *et al.* [71]

Where $C_{i,F}$ and $C_{i,S}$ are the bulk feed and strip concentration of solute i, $C_{i,0}$ and $C_{i,L}$ concentrations at the membrane surface in both feed and strip. Finally $C'_{i,0}$ and $C'_{i,L}$ are the membrane inner concentration at feed and strip surfaces. The fluxes throughout the membrane can be defined as [71]:

$$J_i = K_t(K_{d_F}C_{i,F} - K_{d_S}C_{i,S}) = K_t\left(\frac{C_{i,0}}{C'_{i,0}}C_{i,F} - \frac{C_{i,L}}{C'_{i,L}}C_{i,S}\right) \tag{2.21}$$

With partitions coefficients $K_{d,f}$ and $K_{d,s}$ at the feed and strip interfaces, and K_t the mass transfert resistance coefficient. This overall resistance coefficient is combination of different phenomenons. Among these are the transfer between the aqueous phases and the membrane solvent inside the pores, and the diffusion of the solute-carrier complex through the liquid membrane.

To effectively compare the experiments with each other, an approximation of each transfer coefficient will be calculated. First of all the fluxes will be defined as :

$$J_i(t) = \frac{C_i(t_1) - C_i(t_2)}{t_2 - t_1} \times \frac{V}{A_{eff}} \tag{2.22}$$

With J the flux, C concentrations, t times, V volume of phase and A_{eff} the membrane effective area. Considering that the partition coefficient is the same for both feed and strip (because they are both aqueous phases), this equation 2.21 can be simplified as:

$$J_i = K_t \times K_d \times \Delta C_i \tag{2.23}$$

Where ΔC_i represents the concentration difference between the feed and the strip.
The objective of this study is to selectively separate alanine from arginine, which results in maximising selectivity. Selectivity is derived from both alanine and arginine flux ratios. It is assumed that selectivity is based on feed fluxes, indeed, selective extraction occurs on the feed side, where the recovery on the strip side does not depend on the intrinsic properties of the DES. Selectivity is calculated as follows:

$$S_{i,j}(t) = \frac{J_i(t)}{J_j(t)} \tag{2.24}$$

Chapter 3

Results and Discussion

3.1 System Characterisation

3.1.1 Amino acids

Every amino acid were dissolved at a concentration of 1 g/L and analysed using HPLC. Following this procedure, it was determined that alanine and arginine exhibited sufficiently distinct retention times in the HPLC analysis :

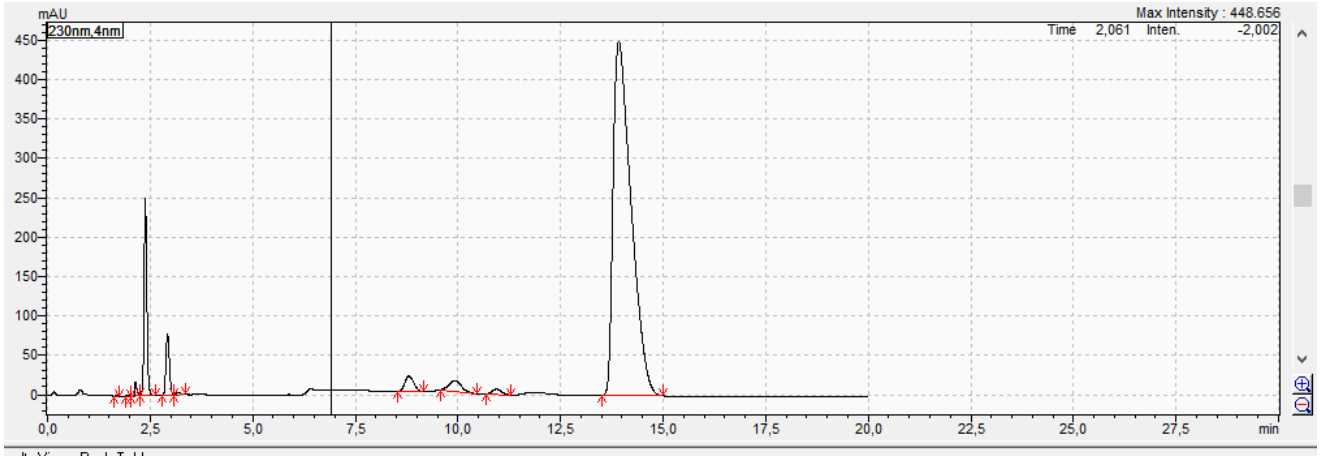

Figure 3.1: Alanine's spectrum provided by the HPLC

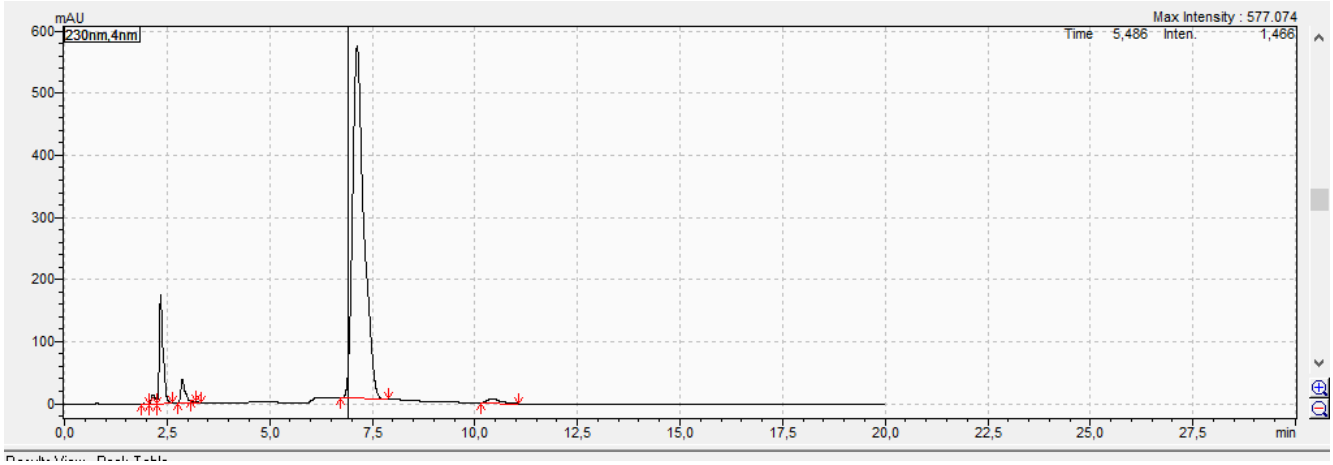

Figure 3.2: Arginine's spectrum provided by the HPLC

Noise observed around 2.5 minutes in the HPLC analysis was identified as water noise and can be deducted from each spectrum for clarity. Peaks in the HPLC can be directly associated with the specific components introduced into the system, where both the height and area of each peak are indicative of the concentration present in the sample. It is expected that these measurements will increase linearly until the column reaches saturation. A series of samples with varying concentrations were analysed (Appendix B):

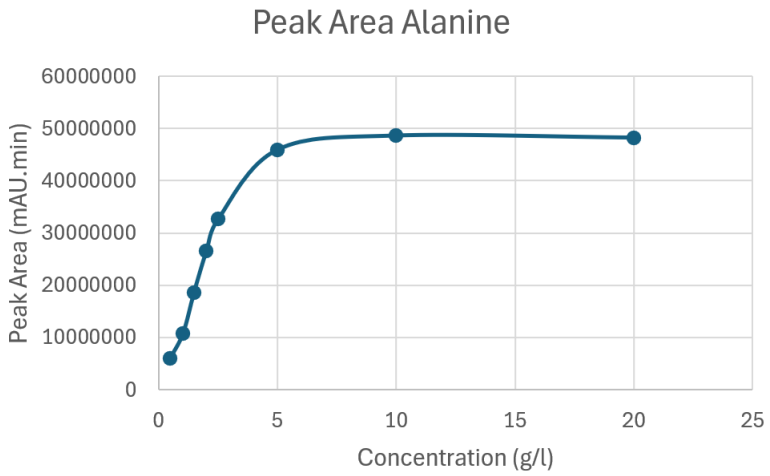

Figure 3.3: HPLC peak area of varying concentrations of alanine

The linear part is clearly observable until 5g/l and saturation occurs afterwards. The calibration line was therefore calculated between 0.5 and 2.5 g/L using a finite difference.

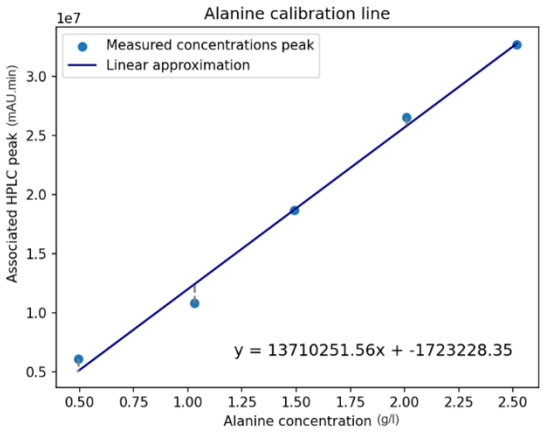

Figure 3.4: Linear approximation of Alanine's peak area

Concentration of every sample containing alanine can be determined by solving the calibration line's equation:

$$C_{sample} = \frac{Peak + 1723228.35}{13720251.56} \tag{3.1}$$

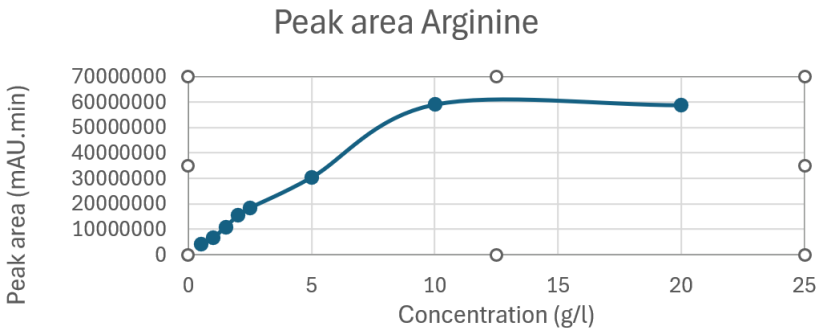

Figure 3.5: HPLC peak area of varying concentrations of arginine

For arginine we can observe from **Figure 3.5** that saturation occurs at a higher concentration. The linear part is considered between 0.5 and 10 g/L, which will be approximated:.

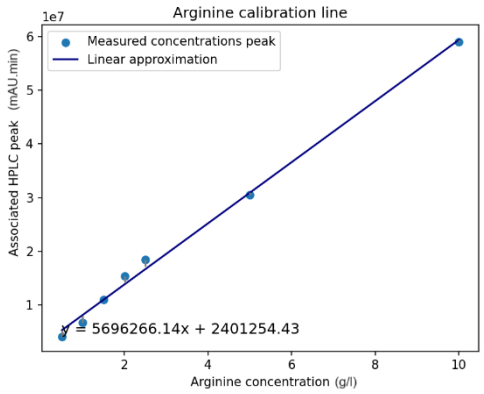

Figure 3.6: Linear approximation of Arginine's peak area

Concentration of every sample containing arginine can be determined by solving the calibration line's equation:

$$C_{sample} = \frac{Peak - 2401254.43}{5696266.14} \tag{3.2}$$

3.1.2 DES

Following the established methodology outlined in the methods section, DESs were prepared. Noteworthy among these DES mixtures are three compositions that formed solid mixtures, those being the mixtures with higher molar ratios of TOPO (**Figure 3.7**). These solidified blends displayed heterogeneous solidification patterns. Interestingly, mixtures with elevated thymol proportions, retained their liquid state due to the inherent self-association property of thymol molecules, thereby lowering the overall melting energy threshold. Based on these different states, some mixtures will yield better analysis results than others. All DES characterisation data can be retrieved in Appendix C.

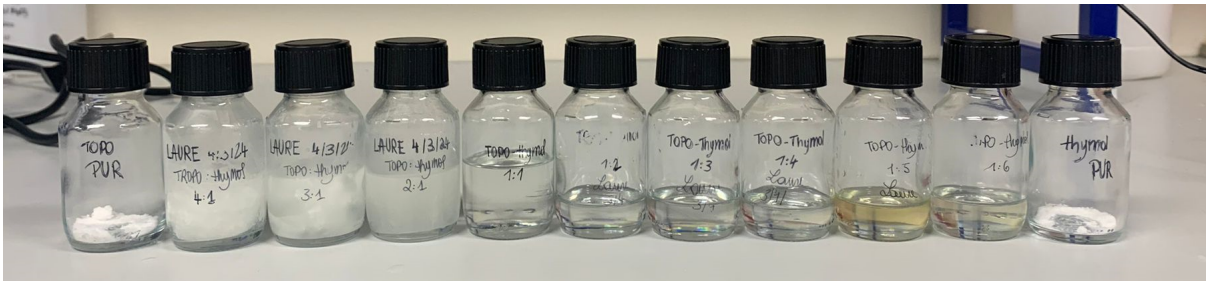

Figure 3.7: Prepared DES mixtures with TOPO and thymol varying molar ratios. Thymol molar ratio increasing from left to right.

The initial analysis conducted is the **DSC**. The primary interest is on the pure components, given their solid state at room temperature, with particular attention to the temperature range from 25°C to 80°C.

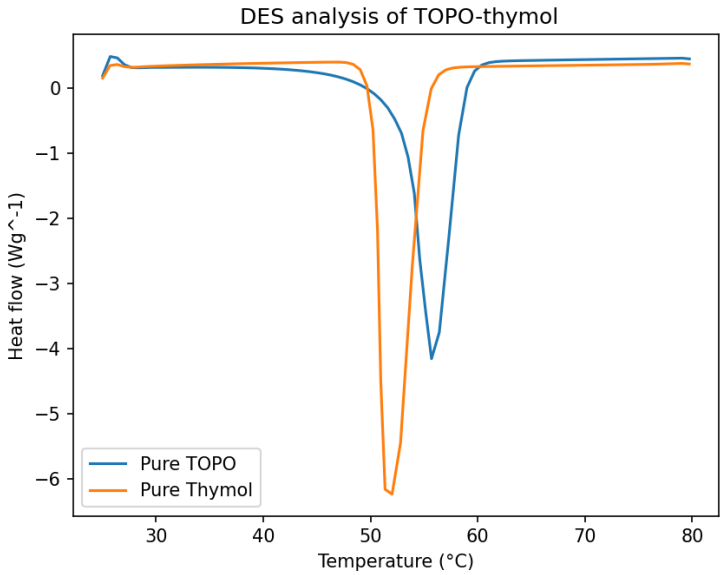

Figure 3.8: DSC analysis of pure TOPO and thymol

Figure 3.8 illustrates negative peaks corresponding to the melting temperatures of the analysed components. The initial slight variation signifies the disturbance at the onset of the heating phase, a common occurrence in DSC analyses. Based on this figure, it can be observed that Thymol exhibits a melting temperature of approximately 53°C, while TOPO around 57°C, this corresponds accurately to the numbers retrieved in Abranches and Coutinho [72]. As anticipated, the mixture of both components may result in distinct melting points, considering that DESs typically do not demonstrate a direct combination of constituent elements.

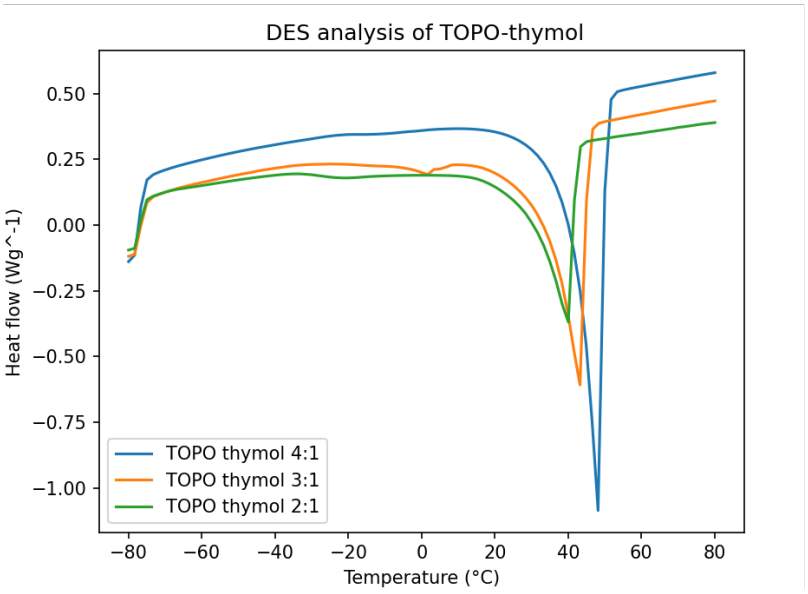

Figure 3.9: DSC analysis of TOPO-thymol 1:1

Begining with the solid mixtures in **Figure 3.9**, melting temperature can be easily identified. It's worth noting that as the molar fraction of TOPO increases, the melting temperature becomes closer to that of the pure TOPO. On the contrary, if the thymol ratio increases, melting temperature decreases, this phenomenon is due to the very intrinsic property of DES. The hydrogen bonding between the two components lowers the phase transition energy. It can also be observed that the values of the peaks are much smaller than those of the pure components. Based on results obtain we can conclude that these mixtures have require lower heat to transition than TOPO and thymol.

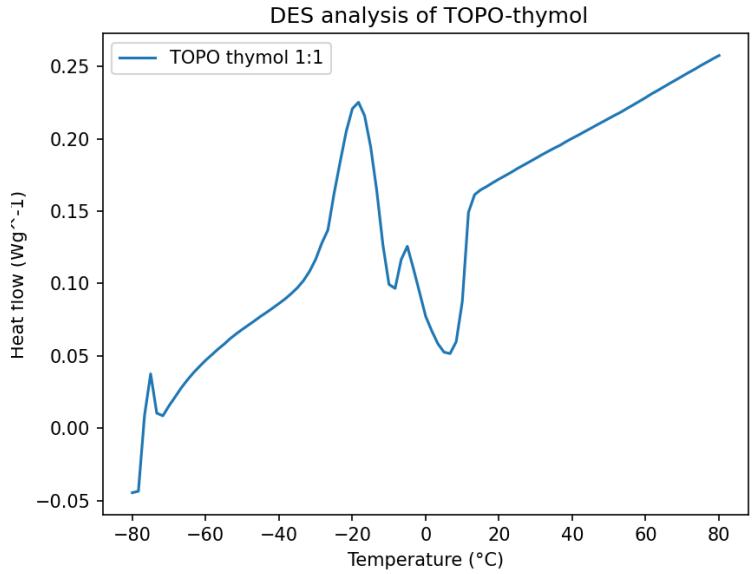

Figure 3.10: DSC analysis of TOPO-thymol 1:1

Figure 3.10 depicts the TOPO-thymol 1:1 behaviours towards temperature variations. Here, a clean DSC analysis is presented. The positive peak indicates the solidification temperature, while the negative peak suggests the melting temperature. This behaviour is typical in DSC analysis; indeed, melting and solidifying temperatures do not always align. This phenomenon, known as thermal hysteresis [73], shows the influence of kinetic properties of the sample. Under -20°C, this mixture is fully solid, the melting starts around 0°C.

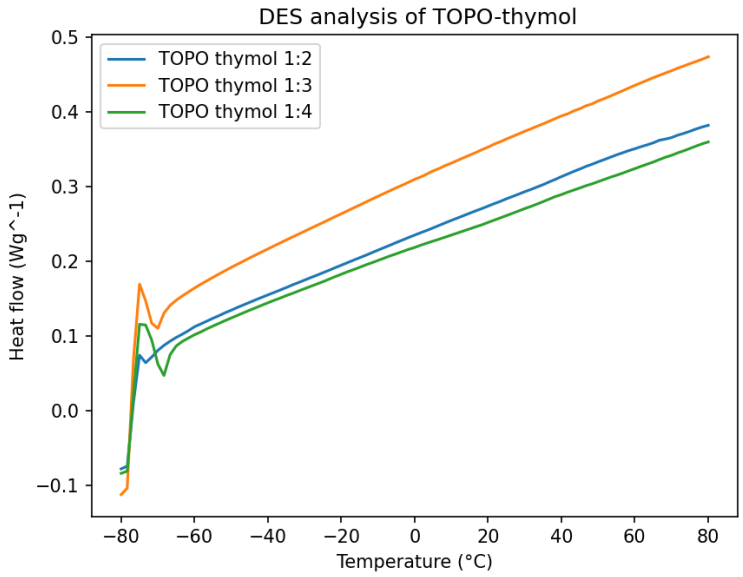

Figure 3.11: DSC analysis of TOPO-thymol 1:1

Focusing now on the liquid mixture, nothing can be observed on **Figure 3.11**. Such outcomes are very common in DES analyses. DSC instruments typically reach a minimum temperature of -80°C, which is sufficient to induce solidification for most materials. To validate the results, a subsequent examination was conducted on the three DES samples. They were cooled to -80°C and maintained at this temperature for 30 minutes to stimulate crystallisation. However, no crystallisation was observed in the second test. This indicates that these three liquid mixtures do not present discernible melting temperature within the range of the DSC instrument. The robust interactions between their components give them resistance to crystallisation even at such low temperatures. Unfortunately, the DSC analyses did not enable to identify the eutectic mixture. Mixtures 1:5 and 1:6 were actually synthesised at this point to find a solid mixture with high molar ratio of thymol, however these two were also liquid, did not undergo DSC.

TGA experiments were initially conducted only on DES 1:1 and DES 1:6 across a range of temperatures varying from ambient to 200°C. However, the TGA results did not clearly indicate the water content, as there was no abrupt weight loss near 100°C, which typically corresponds to water evaporation.

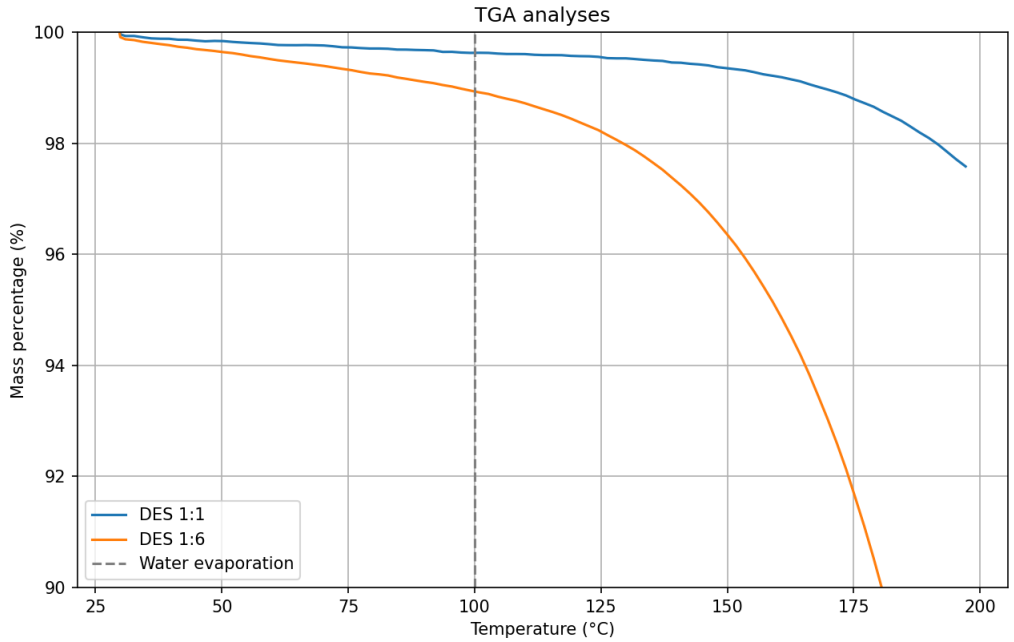

Figure 3.12: TGA results for DES 1:1 and 1:6

Illustrated in **Figure 3.12**, at 100°C, the DES 1:1 mixture exhibits a mass retention of 99.67%, while the DES 1:6 mixture shows a slightly lower retention at 98.95%. This slight difference between the two mixtures does not provide a significant enough indication of water content. Given the small percentage, it remains unclear whether this weight loss is due to water evaporation, the presence of other volatiles, or the initial stages of sample evaporation. The choice of solvents tested was based on the fact that these represent the two extreme mixtures. Intermediate mixtures behaviour can be determined by combination. As the proportion of TOPO increases, the overall water content in the mixture decreases due to TOPO's hydrophobic properties. Consequently, other combinations were not tested, as the maximum weight loss observed was around 1%, without any abrupt changes in the curve. This minimal weight loss cannot be accurately interpreted in terms of water content. Therefore, testing intermediate mixtures, which would exhibit even less than 1% weight loss, was considered unnecessary.

The final assessment of DES properties involves **FTIR analysis**. However, the preparation of samples posed limitations for certain mixtures. Given that FTIR examines interactions and specifically bonds within a sample, heterogeneous mixtures are unsuited for this analysis. The spectrum absorbed or transmitted by the sample depends on the location where the light hits it. Consequently, in heterogeneous samples, the precise composition at a given location cannot be determined accurately. Fortunately, the DES 2:1 mixture could be analysed as it solidifies slowly. Conversely, higher TOPO ratios exhibited immediate formation of nuclei under the microscope within a few seconds, resulting in unanalysable DES 3:1 and 4:1. To understand and compare accurately the samples using FTIR, it is necessary to first observe the spectrum of the pure components.

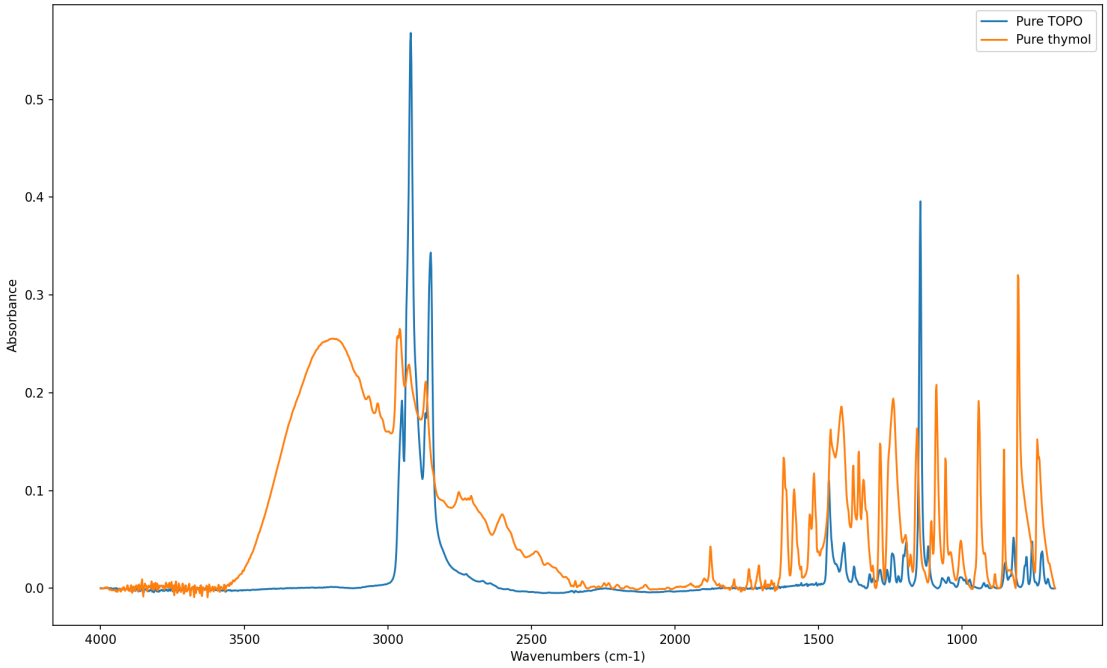

Figure 3.13: TOPO and thymol FTIR Absorbance spectrum

From **Figure 3.13**, distinct spectral ranges of interest can be distinguished. TOPO, being composed of three alkyl chains, typically exhibits absorption peaks in the 3000 to 2500 cm^{-1} region [74]. This characteristic absorption is expected across all mixtures containing TOPO. Conversely, thymol displays fewer C-H bonds and therefore a smaller peak in that region. Moreover, it shows a prominent peak between 3500 and 3000 cm^{-1}, attributable to O-H bonds. Also, TOPO lacks absorbance in this spectral range, as it lacks O-H bonds. To facilitate interpretation, it is necessary to fit spectra from the different mixtures for accurate comparison. Furthermore, an hypothesis is suggested: there is minimal alteration to the aromatic ring of thymol when mixed with TOPO. The zone of interest being the 1700 to 1500 cm^{-1} region, where aromatic ring peaks are typically observed. Each mixture's aromatic ring is adjusted to 0.1 absorbance, enhancing the clarity of the spectral data for comprehensive analysis. Moving forward, attention is directed towards the O-H region.

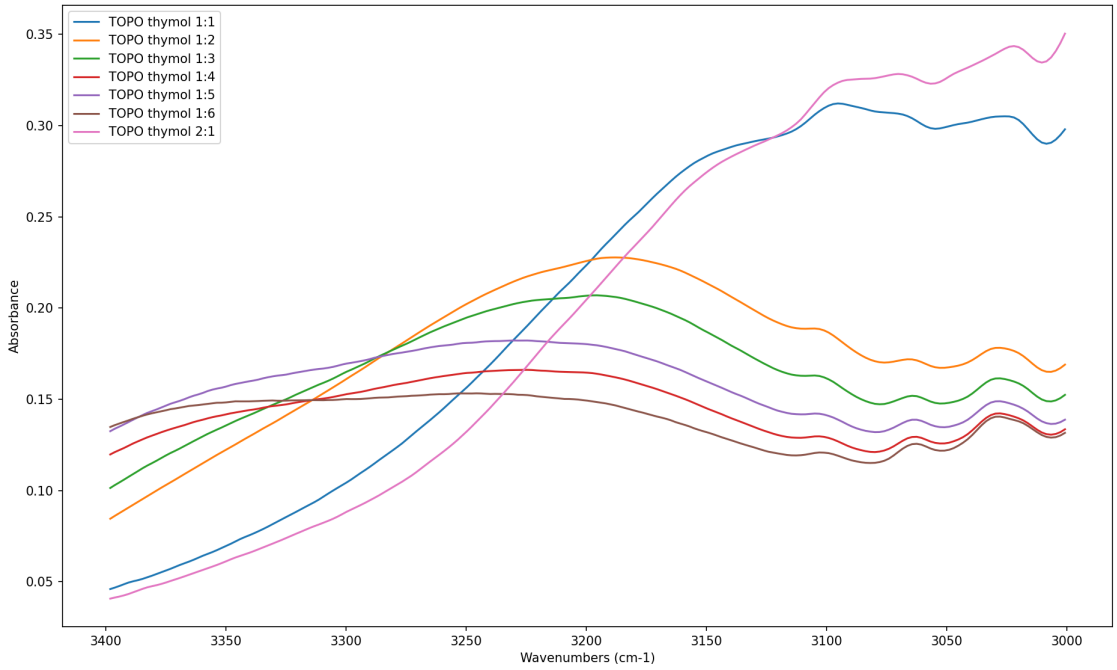

Figure 3.14: TOPO:thymol mixtures fitted curves, wavelenth range between 3400 and 3000 cm^{-1}

It is expected that with an increase in thymol fraction, the predominance of thymol-thymol bonds would rise at the expense of TOPO-thymol bonds. As depicted in **Figure 3.14**, two distinct regions can be discerned. The range from 3400 to 3250 cm^{-1} exhibits an augmentation in absorbance with increasing thymol concentration. Conversely, the zone spanning 3150 to 3000 cm^{-1} demonstrates a correlation between increasing TOPO content and increased absorbance. This suggests that the first region (3400-3250) reflects characteristics associated with thymol, while the second (3150-3000) to TOPO. Given the absence of O-H bonds in TOPO's structure, the observed absorbance likely corresponds hydrogen bonding between thymol and TOPO. As the fraction of TOPO decreases, thymol fraction increases, resulting in a proportional reduction in the number of bonds between TOPO and thymol. Consequently, the first region corresponds to thymol's self-bonding. In the 1:1 ratio, all thymol is assumed to be linked to TOPO, resulting in minimal absorbance. Similarly, in the 2:1 ratio (with residual TOPO), the absorbance remains low. It is worth pointing out that the 1:5 mixture deviates from the trends established earlier. This anomaly could be attributed to saturation of the phenomenon since mixtures 1:4 and 1:6 show minimal changes or perhaps, an analytical error.

To wrap up the characterisation, the investigation into the properties of TOPO:thymol has revealed insights into their behaviour, and potential limitations for the application to pursue. Preparing these DES mixtures, exposed notable variations among them. Particularly the solid formations observed in mixtures with higher molar ratios of TOPO, displaying heterogeneous solidification patterns. Conversely, mixtures with elevated thymol proportions remained in a liquid state, attributed to the self-association property of thymol molecules, reducing the overall melting energy threshold. This diversity in states impacted the subsequent analyses differently. The DSC analyses revealed that solid mixtures were unsuited for extraction purposes due to their too high melting temperatures. Despite expectations that higher thymol content would yield more active sites for extraction, FTIR

examinations indicated minimal differences among the various thymol mixtures, with occasional inconsistencies observed. Moreover, TGA analyses demonstrated that the liquid DES samples exhibited negligible water absorption, rendering them highly promising candidates for membrane technology applications involving aqueous phases.

3.2 Liquid-Liquid Extraction

Preliminary liquid-liquid extraction tests were conducted to refine the operational parameters of the system. Focusing on pH variations, acidic solutions displayed a total extraction.

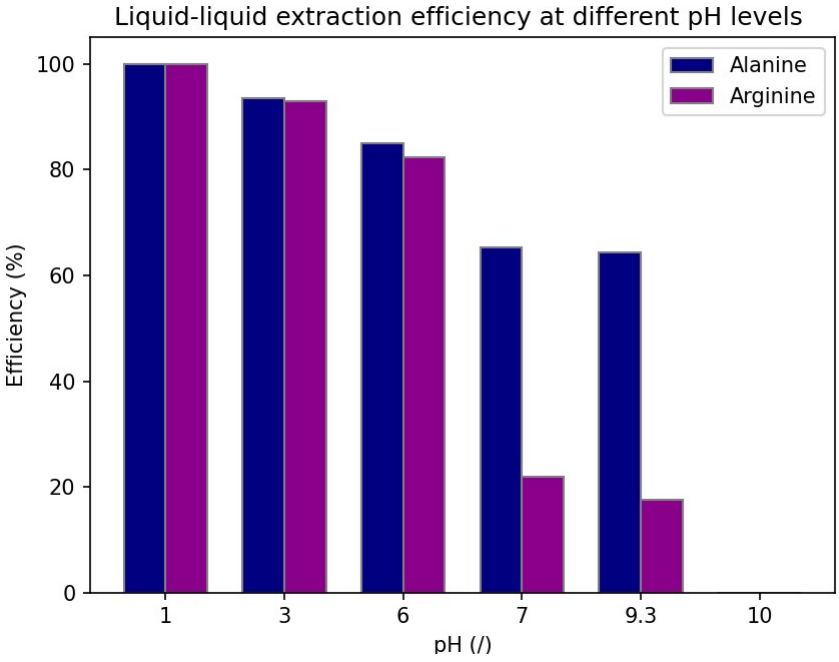

Figure 3.15: Liquid-liquid extraction efficiency of both amino acids depending on the pH level

It was expected that as pH levels gradually increase, extraction efficiency experiences a decline. However, some unexpected results (illustrated on **Figure 3.15**, data in Appendix D) emerge. Although alanine follows the expected trend, there is no significant variation in extraction efficiency of arginine between pH 7 and 9, but efficiency suddenly drops to zero above pH 10. This observation challenges the hypothesis of a gradual decline in efficiency, particularly noticeable in acidic buffers but less expected above pH 7. The efficiency of extraction is directly tied to the molecular forms of amino acids. In acidic solutions, amino acids progressively transition into their zwitterionic forms as their first pKa lies between 2 and 3, resulting in a gradual decrease in efficiency. Even if the zwitteronic form has an HBD sites, the presence of both HBA and HBD sites, reduces the interactions with the extractant. Surprisingly, beyond pH 7, further increases in pH do not significantly alter the situation; both alanine and arginine remain predominantly in their zwitterionic forms, despite arginine's second pKa being 9, it still has an HBD site beyond 9. Above pH 10, however, extraction efficiency drastically falls. This unexpected outcome challenges previous assumptions, suggesting that additional factors beyond pH may influence arginine's extraction, despite its guanidine groups remaining protonated until pH 12.1. Among possible explanations, the guanidine group is the only HBD group remaining,

it is much more complex than the amine group, which might not bond as effectively with the thymol. Another notable difference between the two amino acids is their solubility in water, as discussed in the litterature study. Although both amino acids are highly soluble, alanine is slightly less soluble in water compared to arginine. This reduced solubility might facilitate a greater tendency for alanine to migrate to the DES phase, potentially improving its extraction efficiency. This subtle difference in solubility could contribute (at basic pHs) to the observed variations in their behaviour during the extraction process.

Both subsequent experiments did not demonstrate any significant differences. First, variations in molar ratios of thymol had no impact on efficiency, with the results remaining consistent. This can be attributed to thymol's propensity to link to itself, which means that the number of active sites available for application does not vary significantly despite changes in molar ratios. As a result, adjusting the thymol ratio does not affect the efficiency.

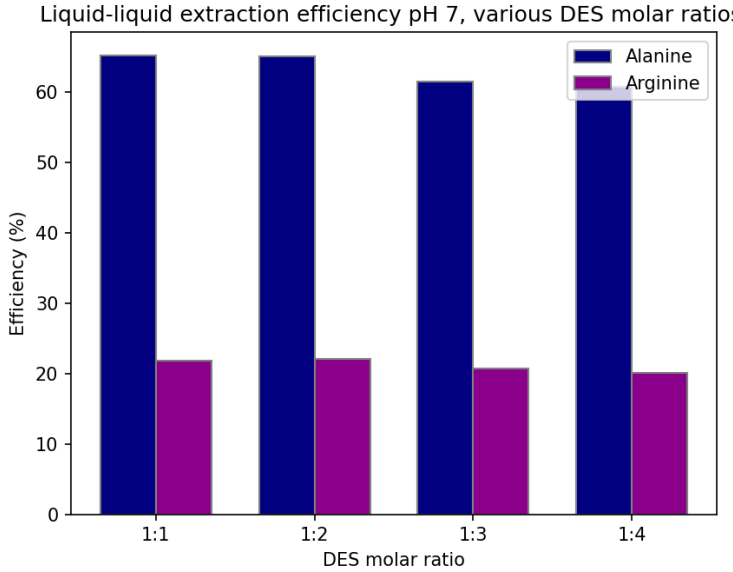

Figure 3.16: Liquid-liquid extraction efficiency for varying solvent

The second experiment examined was the effect of different concentrations on the efficiency. Similar to the previous findings, no notable differences were observed between using concentrations of 3 g/L and 5 g/L. This suggests that within this range, the concentration of the solution does not significantly influence the efficiency of the process.

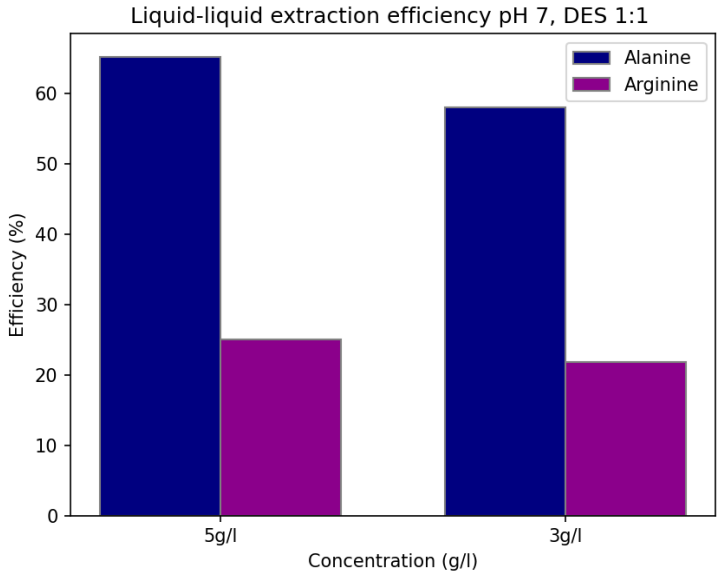

Figure 3.17: Liquid-Liquid extraction results for varying solute concentration

A concentration of 5g/L was chosen, despite the efficiency being somewhat reduced at 3g/L. The slight variations between the two concentrations, however, imply that concentration might not have a major impact on the outcomes.

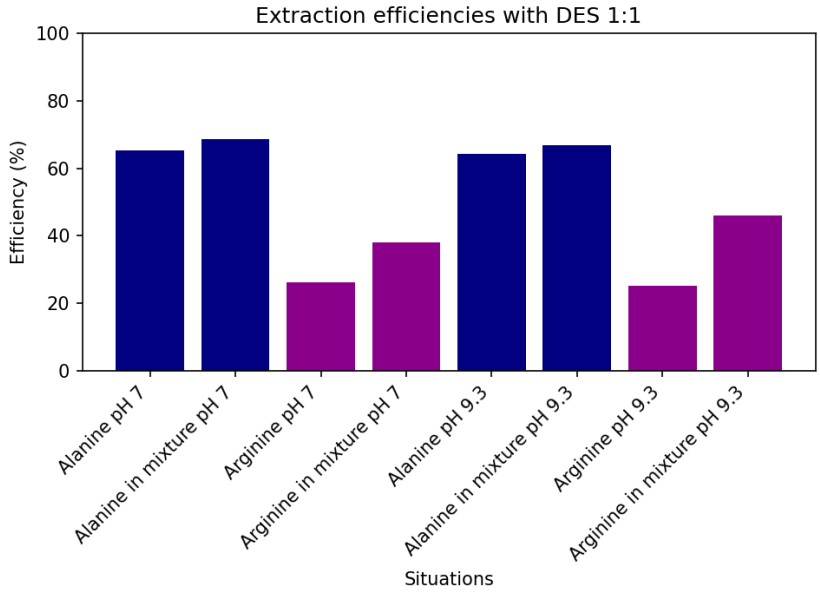

Figure 3.18: Liquid-liquid extraction efficiency of different scenarios, DES 1:1

Nonetheless, a difference in efficiency was observed for both pH 7 and pH 9.3 when alanine and arginine were mixed together (**Figure 3.18**). Alanine's extraction efficiency remained essentially the same, but arginine's efficiency significantly increased. Two hypothesis arise, primarily, the interactions between the amino acids might be modifying their charge and solubility, facilitating better extraction. Secondly, it could be a case of co-extraction, where the extraction of alanine simultaneously favours

the extraction of arginine.

It was then decided that the membrane system would be conducted at 5 g/l, pH 7 with the molar ratio 1:1 of TOPO-thymol. This choice was based on previous results. The concentration of the feed phase is simply chosen because it is the highest concentration at which the HPLC can analyse the amino acids in aqueous solutions. pH 7 was selected due to its demonstrated selectivity between alanine and arginine. Although pH 9.3 obtained very similar results, pH 7 was preferred as it is a more neutral level, thereby preserving the integrity of the equipment. Additionally, pH 7 is more distinct from pH 10, the pH of the stripping solution, which might be advantageous for extraction by having two distinct systems. The molar ratio of 1:1 for the DES was chosen as varying ratios showed no significant differences in results. However, the 1:1 ratio contains the most TOPO, making it the most viscous mixture (this was observed during manipulations). A higher viscosity solvent is preferred for membrane technology because it is less likely to mix with water and leak from the membrane. Therefore, using DES with a 1:1 ratio will help conserve the integrity of the membrane. For this scenario we can then derived the separation numbers, based on the results included in the appendix:

$$SF_{AL} = \frac{m_{AL_{DES}}}{m_{AL_{aq}}} = \frac{10.389}{14.94} = 0.69538 \tag{3.3}$$

$$SR_{AL} = \frac{SF_{AL}}{1 - SF_{AL}} = \frac{69.538}{30.462} = 2.283 \tag{3.4}$$

$$SF_{AG} = \frac{m_{AG_{DES}}}{m_{AG_{aq}}} = \frac{5.8125}{15.06} = 0.38596 \tag{3.5}$$

$$SR_{AG} = \frac{SF_{AG}}{1 - SF_{AG}} = \frac{38.596}{61.404} = 0.629 \tag{3.6}$$

$$SP_{AL,AG} = \frac{SR_{AL}}{SR_{AG}} = \frac{2.283}{0.629} = 3.630 \tag{3.7}$$

The liquid-liquid extraction method provides a satisfactory separation efficiency for the mixture of alanine and arginine.

3.3 Membrane experiments

3.3.1 Membrane Impregnation

The results of membrane impregnation are summarised in **Table 3.1**.

Table 3.1: Membrane imprinting

Membrane type	Pore size	Dry mass (mg)	Imprinted mass (mg)	Solvent mass (mg)
PVDF	0.1 µm	226	394.6	168.6
PVDF	0.1 µm	220	359.5	139.5
PVDF	0.2 µm	240	403.9	163.9
PVDF	0.2 µm	240.7	383.4	142.7
PTFE	0.1 µm	150.9	218.5	67.6
PTFE	0.1 µm	143.7	201.3	57.6

Despite having different pore diameters, the solvent absorption levels in both PVDF membranes were quite the same. On the other hand, because the PTFE membrane is thinner than the PVDF equivalents, it absorbed about half as much solvent. According to results, the DES interacts with PVDF and PTFE membranes in a comparable way. Due to high viscosity, the DES might not completely fill the pores, it can also form a superficial layer on the membrane surface.

3.3.2 SLM results

The subsequent flux and concentration results presented are averaged. Each successful experiment was repeated, and the results represented are the mean of both trials. Every calculations were based on experimental data retrieved in Appendix E.

PVDF 100 nm pore size experiment

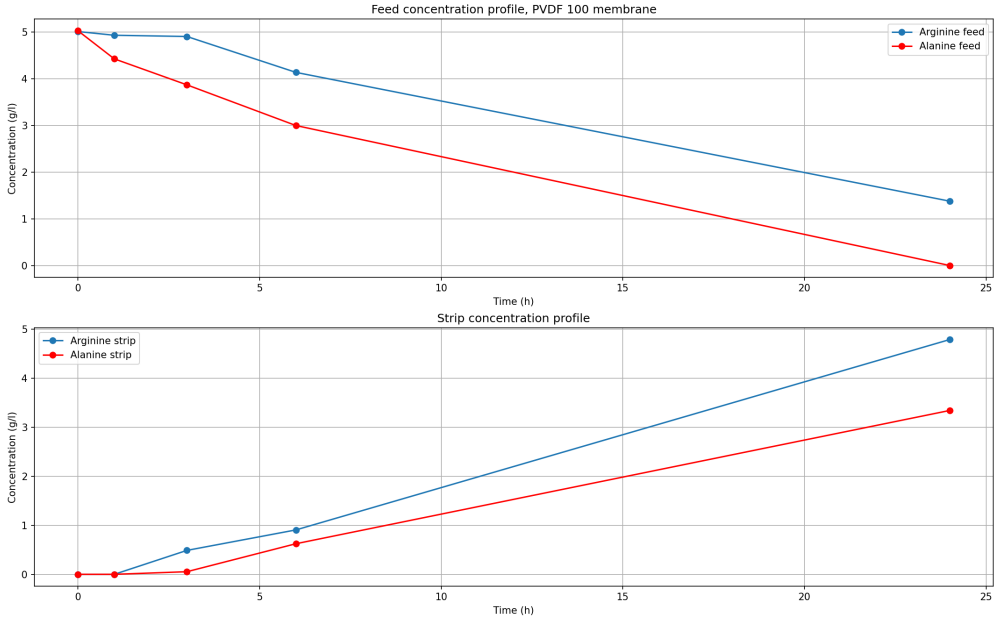

Figure 3.19: PVDF 100 nm: Concentration profiles

Given that the membrane radius is 2.3 cm and its effective area can be considered as : πr^2

Table 3.2: Selectivity calculations of membrane PVDF 100 nm

Time (h)	Alanine feed flux (g/m^2.h)	Arginine feed flux (g/m^2.h)	selectivity (/)
1	-90.6	-12.0	7.57
3	-41.9	-1.99	21.0
6	-43.7	-38.5	1.1
24	-25.1	-23.1	1.09

$$J_{AL}(24) = \frac{C_{f,AL}(0) - C_{f,AL}(24)}{24 - 0} \times \frac{250ml}{\pi \times 0.023^2} = -31.516 \ \frac{g}{h.m^2} \tag{3.8}$$

$$K_{AL} = \frac{J_{AL}(24)}{(C_{f,AL}(24) - C_{s,AL}(24))} = 6.584 \quad \frac{l}{m^2.h} \tag{3.9}$$

$$J_{AG}(24) = \frac{C_{f,AG}(0) - C_{f,AG}(24)}{24 - 0} \times \frac{0.25}{\pi \times 0.023^2} = -22.770 \quad \frac{g}{h.m^2} \tag{3.10}$$

$$K_{AG} = \frac{J_A G}{(C_{f,AG}(24) - C_{s,AG}(24))} = 4.756 \quad \frac{l}{m^2.h} \tag{3.11}$$

Table 3.3: PVDF 100 nm : mass transfer calculations

Amino Acid	Averaged membrane flux (g/m^2.h)	Transfer coeffcient (l/m^2.h)
Alanine	-31.516	6.584
Arginine	-22.770	4.756

The outcomes demonstrated that alanine was fully transmitted through the PVDF membranes. However, there was a noticeably large recovery of arginine. This high rate of recovery implies that, while to a lesser degree than alanine, arginine molecules were also able to cross the membrane. Remarkably, the maximum selectivity was noted around three hours, where arginine was almost not extracted from feed. However by this time, only very little alanine was recovered. Both arginine and alanine can diffuse at different speeds. Because it is smaller and less complicated than arginine, alanine may diffuse across the membrane more quickly. The observations are on experimental data presented in Appendix E.1, which illustrates the evolution of arginine and alanine concentration profiles.

PVDF 200 nm pore size experiment

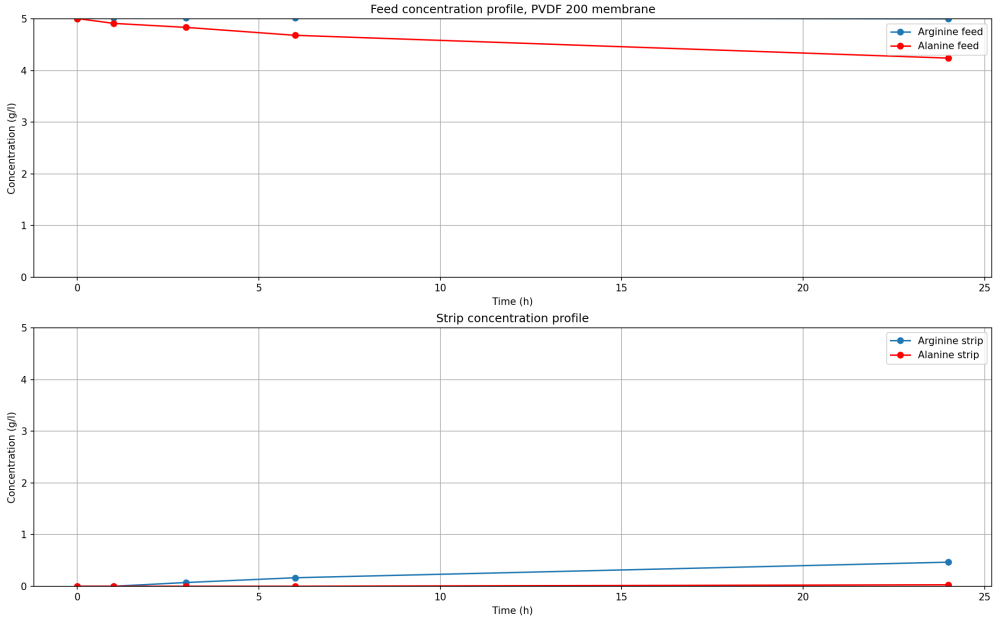

Figure 3.20: PVDF 200 nm: Concentration profiles

Table 3.4: Selectivity calculations of membrane PVDF 200 nm

Time (h)	Alanine feed flux (g/m^2.h)	Arginine feed flux (g/m^2.h)	selectivity (/)
1	- 14.1	2.27	-6.22
3	-5.84	0.298	-19.6
6	-7.68	0.055	140
24	-3.69	-0.174	21.2

$$J_{AL}(24) = \frac{C_{f,AL}(0) - C_{f,AL}(24)}{24 - 0} \times \frac{0.25}{\pi \times 0.023^2} = -4.801 \quad \frac{g}{h.m^2} \tag{3.12}$$

$$K_{AL} = \frac{J_{AL}}{(C_{f,AL}(24) - C_{s,AL}(24))} = -1.272 \quad \frac{l}{m^2.h} \tag{3.13}$$

$$J_{AG}(24) = \frac{C_{f,AG}(0) - C_{f,AG}(24)}{24 - 0} \times \frac{0.25}{\pi \times 0.023^2} = -0.018 \quad \frac{g}{h.m^2} \tag{3.14}$$

$$K_{AG} = \frac{J_A G}{(C_{f,AG}(24) - C_{s,AG}(24))} = -0.0036 \quad \frac{l}{m^2.h} \tag{3.15}$$

Table 3.5: PVDF 200 nm : mass transfer calculations

Amino Acid	Averaged membrane flux (g/m^2.h)	Transfer coeffcient (l/m^2.h)
Alanine	-4.801	-1.272
Arginine	-0.018	-0.0036

The absence of arginine extraction indicates that the membrane is very successful in stopping arginine from passing through, which is essential for attaining high selectivity. The potential for high-purity separation applications of the membrane is demonstrated by its ability to recover nearly pure alanine. However, very few molecules were retrieved from the stripping side, and those that were mostly contained pure alanine. Very low transfer coefficients are obtained, which translate a high membrane resistance to the transfer of both amino acids. Optimal performance was noted near six hours. For procedures that require the exact separation of amino acids or other substances, this membrane can be interesting. Data supporting these observations can be found in Appendix E.2.

PTFE 100 nm pore size experiment

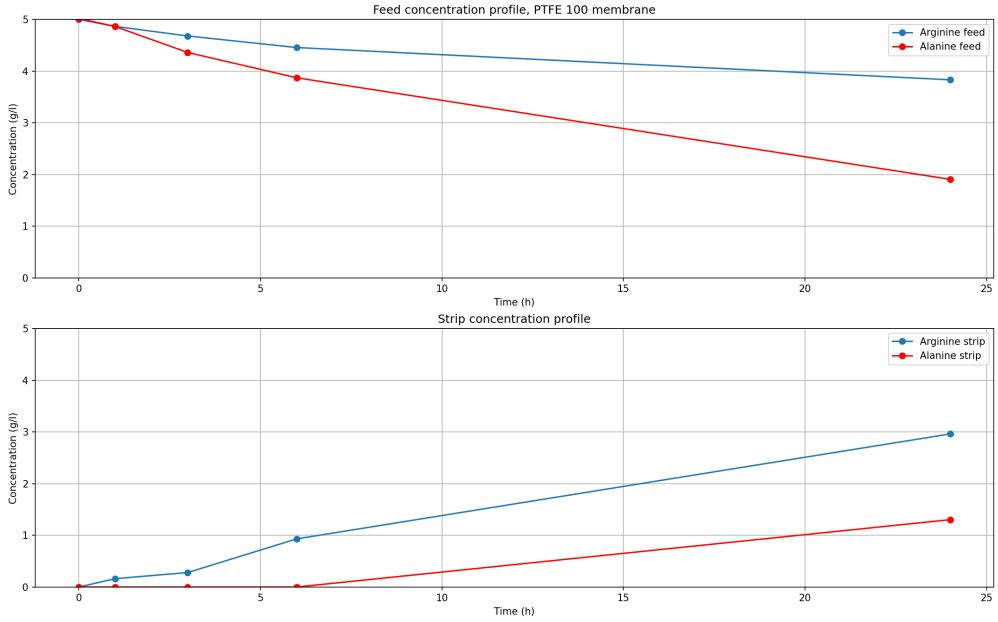

Figure 3.21: PTFE 100: Concentration profiles

Table 3.6: Selectivity calculations of membrane PTFE 100 nm

Time (h)	Alanine feed flux (g/m^2.h)	Arginine feed flux (g/m^2.h)	selectivity (/)
1	-23.7	-20.5	1.16
3	-37.8	-13.9	2.71
6	-24.6	-11.2	2.19
24	-16.4	-5.22	3.15

$$J_{AL}(24) = \frac{C_{f,AL}(0) - C_{f,AL}(24)}{24 - 0} \times \frac{0.25}{\pi \times 0.023^2} = -19.521.57708 \quad \frac{g}{h.m^2} \tag{3.16}$$

$$K_{AL} = \frac{J_{AL}}{(C_{f,AL}(24) - C_{s,AL}(24))} = 18.512 \quad \frac{l}{m^2.h} \tag{3.17}$$

$$J_{AG}(24) = \frac{C_{f,AG}(0) - C_{f,AG}(24)}{24 - 0} \times \frac{0.25}{\pi \times 0.023^2} = -7.329 \quad \frac{g}{h.m^2} \tag{3.18}$$

$$K_{AG} = \frac{J_AG}{(C_{f,AG}(24) - C_{s,AG}(24))} = -2.897 \quad \frac{l}{m^2.h} \tag{3.19}$$

Table 3.7: PTFE 100 nm : mass transfer calculations

Amino Acid	Averaged membrane flux (g/m^2.h)	Transfer coefficient (l/m^2.h)
Alanine	-19.521	18.512
Arginine	- 7.329	-2.897

While relatively little arginine was recovered, alanine was recovered from the PTFE membranes at a significant rate. This suggests that arginine is mainly blocked by the PTFE membranes, which

are quite good at letting alanine pass through. The PTFE membranes show the greatest transfer coefficient among the investigated membranes. Lower resistance to flow through the membrane is indicated by a high transfer coefficient, which raises the separation total efficiency. By the time the process was finished, the highest selectivity was noted. This indicates that as the process went on, the ability to transfer alanine selectively while blocking the passage of arginine increased. Data supporting these observations are retrieved in the Appendix E.3. Unfortunately, two experiments failed, since PTFE is quite brittle and the membranes were very thin. At the locations where the aqueous phases were pumped out, the membranes ruptured. The same solution with an intermediate pH were obtained in the first few hours, on both sides.

3.4 Membrane Comparison

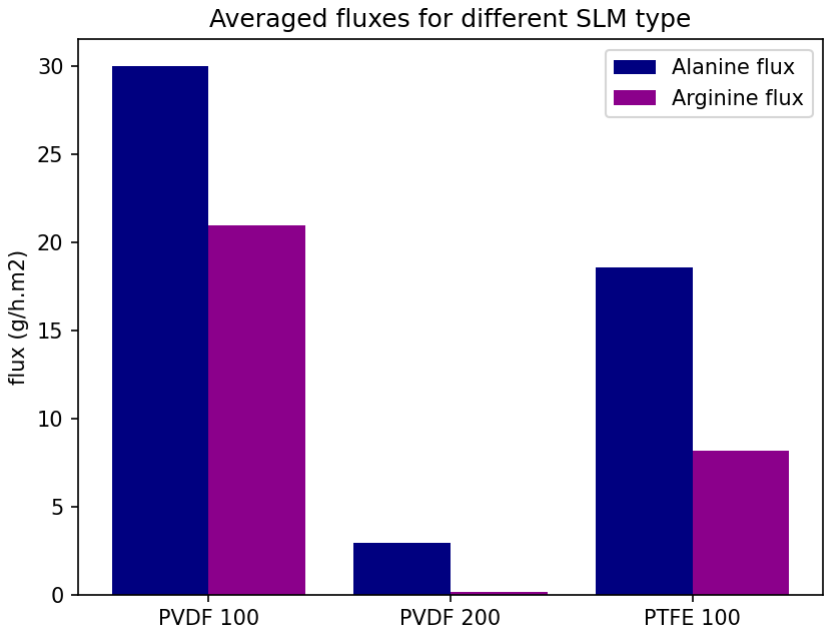

Figure 3.22: Amino acids flux through membrane comparison

The PVDF membranes with pore size of 100 nm are the most efficient in terms of mass transfer, as shown in **Figure 3.22**. Their high transfer coefficients allow for the largest fluxes of both solutes. The performance of PTFE membranes with pore sizes of 100 nm is intermediate. On the other hand, because of their strong resistance to mass transfer, PVDF membranes with pore sizes of 200 nm show nearly negligible solute transport. These results demonstrate that PVDF 200 nm can only be interesting in cases when very strong alanine selectivity is required, regardless of recovery yield (illustrated in **Figure 3.23**).

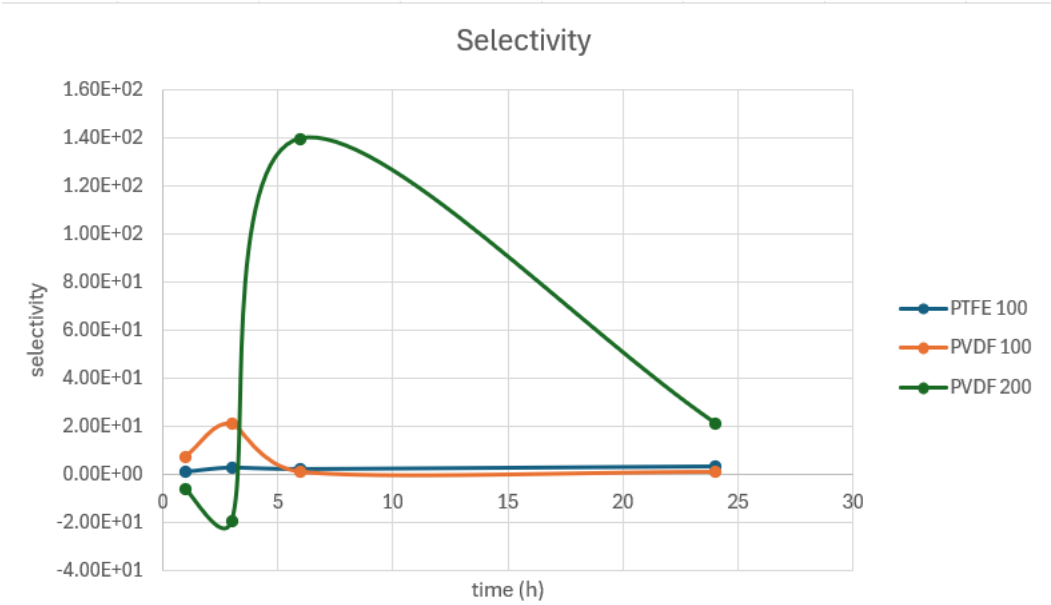

Figure 3.23: Selectivity comparison of all SLM tested

The results obtained with PVDF membranes with 200 nm pores offer an interesting case study. The absence of recovered arginine is noteworthy. In spite of this, a very low yield of alanine was observed therefore with a very high selectivity (**Figure 3.23**). Notably, these results were associated with the lowest transfer coefficients, suggesting a strong resistance in the system. This resistance therefore probably played a part in the difficulties in obtaining acceptable yields. Consequently, even though the selectivity component seemed promising, the poor alanine yield indicates the existence of underlying issues affecting the overall efficacy. Extremely low yields may artificially inflate the selectivity results. Based on obtained results and limited time, a possible hypothesis can be that the effects of higher pore diameters include multiple factors, such as increased wetting phenomena [75]. Wetting refers to a liquid spreading and sticking to a solid surface. Effective exchanges may be restricted if the aqueous phases stick to the membrane polymeric support inside the pores. Such adhesion could cause a stagnant layer to accumulate inside the pores, preventing the pumping mechanism from regenerating. This can be due to the increased contact area (within the pores) and decreased contact angle, which represent the angle created at the aqueous-DES interface. Larger pore diameters tend to reduce the desired greater contact angles, which are meant to prevent the aqueous phase from penetrating the pores. Additionally, greater capillary activities are facilitated by bigger pores. As a result, aqueous wetness increases, which causes flow through the membrane to drop.

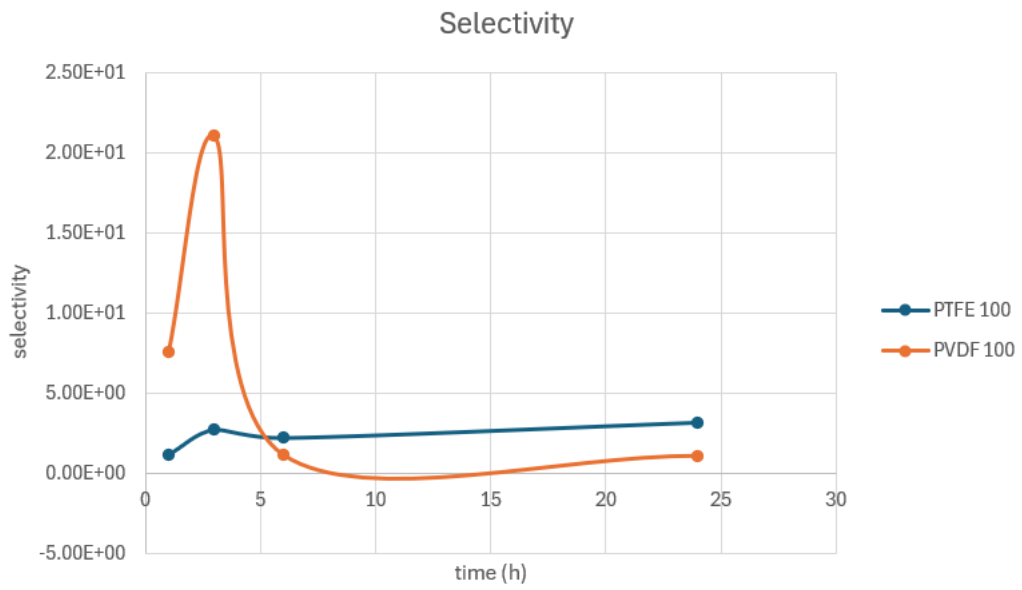

Figure 3.24: Selectivity comparison of PVDF 100 nm and PTFE 100 nm

Focusing on PVDF 100 nm and PTFE 100 nm membranes, a few findings are worth highlighting. Depicted in **Figure 3.24**, the most selective PVDF 100 nm yields almost pure 10% alanine recovery after around three hours. This effect could be explained by the reduced size of alanine in the DES, which causes it to diffuse faster. Reversely, PTFE shows a better final selectivity (about three times greater). PTFE shows a higher transfer coefficient than PVDF, even though solutes move through it more efficiently. This could be because of variations in pore architectures and surface qualities. Compared to PVDF, PTFE exhibits greater solvent selectivity because of its intrinsic hydrophobicity, which also improves the purity of the solutes that are obtained [16]. PTFE is a highly fluorinated chemical made up of repeating tetrafluoroethylene units. Due to their electronegative nature and strong electron affinity, fluorine atoms form a very stable, non-polar configuration. As a result, PTFE is very hydrophobic, having a low surface energy and a high resistance to wetting by aqueous solutions. This membrane polymer exhibits then, higher selectivity and a considerable recovery of alanine coupled with few arginine. On the other hand, PVDF, less hydrophobic, produces greater solute yields, but it also lets more contaminants through, which lowers purity. It is noteworthy that PVDF 100 nm exhibits potential for specific separations, since after 24 hours, roughly 30 % of arginine in feed is still regarded as pure.

Because the mechanisms governing PVDF 200 nm membranes are not fully understood, using PVDF 100 nm could be interesting if great selectivity at the expense of low yield is needed; nevertheless, depending on the desired purity levels, operation should be stopped after around three hours. On the other hand, PTFE, as illustrated in **Figure 3.24**, provides a more balanced process in terms of selectivity and yield. Higher recovery rates are possible with this membrane, at the expense of purity.

3.5 Quality of results

During the course of the whole experimental process, numerous elements might have contributed to possible errors in the outcomes. First, irregularities were noted in the pumping performance. Two membrane tests failed as a result of random halts caused by previous damages on the system. Tubes were positioned at the surface of the liquid, this allowed air bubbles to enter the tubes and push the aqueous phase, guaranteeing the flow. As such, there were variations in the fluid fluxes during the experiment. These differences might lead to unequal reagent mixing or delivery, which could affect the reliability of the experiment. Furthermore, fluctuation in the weighing machine's readings have been observed, which could introduce mistakes in the sample mass measurements. Moreover, another possible source of inaccuracy is the sensitivity of the HPLC technology. Chromatographic results can alter significantly depending on even small changes in sample composition or instrument settings, which might compromise the precision of analyte quantification. Similarly, inaccurate pH readings could affect how experimental data is interpreted due to the pH meter's sensitivity to variations in temperature, humidity, or electrode condition. Finally, the lack of technical sheets of the PVDF membranes made it difficult to evaluate the findings. Notably, one important aspect to take into account is the membrane thickness; if the PVDF 200 nm membranes were to be thicker, this could explain the noticeably lower flow rates. Since the solute must travel a greater distance, increased membrane thickness would result in increased barrier to transfer.

3.6 Future perspectives

To assess the PVDF 200 nm issue, testing membranes with pore sizes ranging from less than 0.1 µm to between 100 and 200 nm can be benefic. The goal of this comprehensive study is to clarify the complex effects of pore size on the effectiveness of solute separation, wetting behaviour, and membrane performance as a whole. It is possible to obtain understanding of how differences in pore proportions impact solute transport kinetics and membrane selectivity by methodically investigating the impact of various pore sizes.

To improve membrane selectivity, techniques for surface modification present a way to improve the ability of membranes to separate arginine and alanine. It is possible to modify the membrane's affinity for particular solutes by investigating techniques to increase the hydrophobicity of the membrane surface. Techniques such as chemical treatments, coatings, or functionalisation strategies [76]. Selectivity can be improved by reducing wetting phenomena, which occurs when the aqueous phase sticks to the membrane surface. Membranes can demonstrate increased resistance to fouling and improved separation efficiency by reducing wetness.

Flow rates can be tuned to maximise the separation of arginine and alanine. Reduced flow rate allows for more time for the feed solution to be in contact with the membrane, as alanine diffuses faster, more retention time might promote alanine to permeate while quantity of arginine passing through is not increased. On the other hand, investigating considerably higher flow rates can aid in assessing how separation efficiency is affected by changes in flow rate, offering information about the best operating circumstances for membrane-based separation procedures. Flow rates can be intresting to test on PTFE membrane to enhance the transfer of alanine and obtain higher yields. Testing it on PVDF 100 will not be necessary as alanine already diffuses completely.

Conclusion

This studey investigated the use of deep eutectic solvents (DESs) in conjunction with supported liquid membranes (SLMs) to separate amino acids from aqueous phases. The requirement for hydrophobic solvents drove the choice of DES. Thymol was selected as the hydrogen bond donor (HBD) and trioctylphosphine oxide (TOPO) as the hydrogen bond acceptor (HBA), this couple showed prior successful use in supported liquid membranes. Testing different molar ratios allowed for the adaption of properties due to the adjustable nature of DESs. Arginine and alanine were identified and chosen as a result of close examination using High-Performance Liquid Chromatography (HPLC).

As the research progressed, it examined liquid-liquid extraction techniques in greater detail and disclosed the interactions between DESs and amino acids. It was decided rapidly to extract alanine preferentially after observing that it reacted more strongly with the solvent. This comprehensive understanding facilitated the optimisation of parameters for more membrane-based research, allowing for the fine-tuning of elements such as pH variations and TOPO-thymol molar ratio. To maximise alanine selectivity, these working conditions were chosen.

The key objective of the study was membrane research, which involved looking into support polymers, polyvinylidene fluoride (PVDF) and polytetrafluoroethylene (PTFE), with varying pore sizes were investigated. Positive outcomes were obtained, especially with PTFE, which demonstrated its capacity to enable high alanine recovery while preserving levels of acceptable purity. This demonstrated how important material selection is in membrane technology, where polymers structure will strongly affect different aspects of the membrane and its efficiency.

In summary, whereas this work advances understanding of amino acid extraction and separation methods, it also opens up new pathways for future investigation. Through the use of the knowledge gained from this investigation, refining separation processes in membrane technology by investigating new methods and increasing efficiency can be accounted. Subsequent studies might explore pore geometry in greater detail, surface treatments for polymer support, and other flow rates.

Bibliography

[1] M. Akram, H. M. Asif, M. Uzair, *et al.*, "Amino acids: A review article," *Journal of Medicinal Plants Research*, 2011. DOI: https://doi.org/10.5897/JMPR.9000061.

[2] J. Batista, F. McGarvey, and A. Vieira, "The removal of perchlorate from waters using ion-exchange resins," in *Perchlorate in the Environment*, 2000. DOI: https://doi.org/10.1007/978-1-4615-4303-9_13.

[3] Z. Li, Y. Cui, Y. Shen, and C. L, "Extraction process of amino acids with deep eutectic solvents based supported liquid membranes," *Industrial Engineering Chemistry Research*, 2018. DOI: https://doi.org/10.1021/acs.iecr.7b05221.

[4] R. Bischoff and H. Schlüter, "Amino acids: Chemistry, functionality and selected non-enzymatic post-translational modifications," *Journal of Proteomics*, 2012. DOI: https://doi.org/10.1016/j.jprot.2012.01.041.

[5] *Molview*. [Online]. Available: https://molview.org.

[6] "Amino acid: Structure and function." Consulted [January 14th 2024]. (2022), [Online]. Available: https://www.easybiologyclass.com/amino-acid-structure-and-functions-biochemistry-short-notes/.

[7] BD Editors. "Peptide bond." Reviewed by: BD Editors. Last Updated: January 28, 2020, Biology Dictionary. (2020), [Online]. Available: https://www.biologydictionary.net/peptide-bond/.

[8] S. Verbych, N. Hilal, G. Sorokin, and M. Leaper, "Ion exchange extraction of heavy metal ions from wastewater," *Separation Science and Technology*, 2005. DOI: 10.1081/SS-120039317.

[9] M. A. Malik, M. A. Hashim, and F. Nabi, "Ionic liquids in supported liquid membrane technology," *Chemical Engineering Journal*, 2011. DOI: https://doi.org/10.1016/j.cej.2011.03.041.

[10] K. Chakrabarty, K. V. Krishna, P. Saha, and A. K. Ghoshal, "Extraction and recovery of lignosulfonate from its aqueous solution using bulk liquid membrane," *Journal of Membrane Science*, 2009. DOI: https://doi.org/10.1016/j.memsci.2008.12.069.

[11] L. Yang, J. Xiao, Y. Shen, X. Liu, W. L. W. Wang, and Y. Yang, "The efficient removal of thallium from sintering flue gas desulfurization wastewater in ferrous metallurgy using emulsion liquid membrane," *Environmental Science and Pollution Research*, 2017. DOI: https://doi.org/10.1007/s11356-017-0040-0.

[12] N. Kocherginsky, Q. Yang, and L. Seelam, "Recent advances in supported liquid membrane technology," *Separation and Purification Technology*, 2007. DOI: https://doi.org/10.1016/j.seppur.2006.06.022.

[13] Y. Mikhak, M. M. A. Torabi, and A. Fouladitajar, "Chapter 3 - refinery and petrochemical wastewater treatment," *Sustainable Water and Wastewater Processing*, 2019. DOI: https://doi.org/10.1016/B978-0-12-816170-8.00003-X.

[14] T. Eljaddi, L. Lebrun, and M. Hlaibi, "Review on mechanism of facilitated transport on liquid membranes," *Journal of Membrane Science Research*, 2017. DOI: https://doi.org/10.22079/JMSR.2017.50137.1110.

[15] Microsoft Corporation, *Microsoft paint*, https://www.microsoft.com/en-us/p/microsoft-paint/9pcfs5b6t72h, Software used for generating schemas, 2023.

[16] S. Feng, Z. Zhong, Y. Wang, W. Xing, and E. Drioli, "Progress and perspectives in ptfe membrane: Preparation, modification, and applications," *Journal of Membrane Science*, 2020. DOI: https://doi.org/10.1016/j.memsci.2017.12.032.

[17] S. Biswas and K. Vijayan, "Friction and wear of ptfe — a review," *Wear*, 1992. DOI: https://doi.org/10.1016/0043-1648(92)90039-B.

[18] F. Liu, N. A. Hashim, Y. Liu, M. Moghareh Abed, and K. Li, "Progress in the production and modification of pvdf membranes," *Journal of Membrane Science*, 2011. DOI: https://doi.org/10.1016/j.memsci.2011.03.014.

[19] W. contributors, *Polytetrafluoroethylene — wikipedia, the free encyclopedia*, Accessed: 2024-05-25, 2024. [Online]. Available: https://en.wikipedia.org/wiki/Polytetrafluoroethylene.

[20] W. contributors, *Polyvinylidene fluoride — wikipedia, the free encyclopedia*, Accessed: 2024-05-25, 2024. [Online]. Available: https://en.wikipedia.org/wiki/Polyvinylidene_fluoride.

[21] P. R. Danesi, "Separation of metal species by supported liquid membranes," *Separation Science and Technology*, 2006. DOI: https://doi.org/10.1080/01496398408068598.

[22] F. Zha, A. Fane, and C. Fell, "Instability mechanisms of supported liquid membranes in phenol transport process," *Journal of Membrane Science*, 1995. DOI: https://doi.org/10.1016/0376-7388(95)00104-K.

[23] T. Köddermann, D. Paschek, and R. Ludwig, "Molecular dynamic simulations of ionic liquids: A reliable description of structure, thermodynamics and dynamics," *Chemphyschem*, 2007. DOI: https://doi.org/10.1002/cphc.200700552.

[24] S. Zhang, N. S. X. He, X. Lu, and X. Zhang, "Physical properties of ionic liquids: Database and evaluation," *Journal of Physical and Chemical Reference Data*, 2006. DOI: https://doi.org/10.1063/1.2204959.

[25] P. Kubisa, "Application of ionic liquids as solvents for polymerization processes," *Progress in Polymer Science*, 2004. DOI: https://doi.org/10.1016/j.progpolymsci.2003.10.002.

[26] H. Liu and H. Yu, "Ionic liquids for electrochemical energy storage devices applications," *Journal of Materials Science Technology*, 2019. DOI: https://doi.org/10.1016/j.jmst.2018.10.007.

[27] V. I. Pârvulescu and C. Hardacre, "Catalysis in ionic liquids," *Chemical Reviews*, 2007. DOI: https://doi.org/10.1021/cr050948h.

[28] D. R. MacFarlane and K. R. Seddon, "Ionic liquids—progress on the fundamental issues," *Australian Journal of Chemistry*, 2007. DOI: https://doi.org/10.1071/CH06478.

[29] D. Zhao, Y. Liao, and Z. Zhang, "Toxicity of ionic liquids," *Clean soil air water*, 2007. DOI: https://doi.org/10.1002/clen.200600015.

[30] E. L. Smith, A. P. Abbott, and K. S. Ryder, "Deep eutectic solvents (dess) and their applications," *Chemical Reviews*, 2014. DOI: https://pubs.acs.org/doi/epdf/10.1021/cr300162p.

[31] L. B. Santos, R. S. Assis, J. A. Barreto, M. A. Bezerra, C. G. Novaes, and V. A. Lemos, "Deep eutectic solvents in liquid-phase microextraction: Contribution to green chemistry," *Trends in Analytical Chemistry*, 2022. DOI: https://doi.org/10.1016/j.trac.2021.116478.

[32] F. M. Perna, P. Vitale, and V. Capriati, "Deep eutectic solvents and their applications as green solvents," *Current Opinion in Green and Sustainable Chemistry*, 2020. DOI: https://doi.org/10.1016/j.cogsc.2019.09.004.

[33] A. P. Santana, J. A. Mora-Vargas, T. G. Guimarães, C. D. Amaral, A. Oliveira, and M. H. Gonzalez, "Sustainable synthesis of natural deep eutectic solvents (nades) by different methods," *Journal of Molecular Liquis*, 2019. DOI: https://doi.org/10.1016/j.molliq.2019.111452.

[34] E. Durand, J. Lecomte, and P. Villeneuve, "Deep eutectic solvents: Synthesis, application, and focus on lipase-catalyzed reactions," *European Journal of Lipid Science and Technology*, 2013. DOI: https://doi.org/10.1002/ejlt.201200416.

[35] T. El Achkar, G.-G. H., and F. S., "Basics and properties of deep eutectic solvents: A review," *Environmental Chemistry Letters*, 2021. DOI: https://doi.org/10.1007/s10311-021-01225-8.

[36] B. Tang and K. Row, "Recent developments in deep eutectic solvents in chemical sciences," *Monatsh Chem*, 2013. DOI: https://doi.org/10.1007/s00706-013-1050-3.

[37] A. P. A. Prof., G. C. Dr., and S. Gray, "Design of improved deep eutectic solvents using hole theory," *ChemPhysChem*, 2006. DOI: https://doi.org/10.1002/cphc.200500489.

[38] G. García, S. Aparicio, R. Ullah, and M. Atilhan, "Deep eutectic solvents: Physicochemical properties and gas separation applications," *Energy Fuels*, 2015. DOI: https://doi.org/10.1021/ef5028873.

[39] T. E. Achkar, S. Fourmentin, and H. Greige-Gerges, "Deep eutectic solvents: An overview on their interactions with water and biochemical compounds," *Journal of Molecular Liquids*, 2019. DOI: https://doi.org/10.1016/j.molliq.2019.111028.

[40] W. Abdussalam-Mohammed, A. Q. Ali, and A. O. Errayes, "Green chemistry: Principles, applications, and disadvantages," *Chemical Methodologies*, 2020. DOI: https://www.chemmethod.com/article_101213.html.

[41] P. T. Anastas and J. C. Warner, "Green chemistry: Theory and practice," *Green Chemistry: Theory and Practice*, 2000. DOI: https://doi.org/10.1093/oso/9780198506980.001.0001.

[42] J. Płotka-Wasylka, M. de la Guardia, V. Andruch, and M. Vilkova, "Deep eutectic solvents vs ionic liquids: Similarities and differences," *Microchemical Journal*, 2020. DOI: https://doi.org/10.1016/j.microc.2020.105539.

[43] H. J. S. Jnr and R. E. Marsh, "The crystal structure of l-alanine," *Acta Crystallographica*, 1966. DOI: https://doi.org/10.1107/S0365110X66001221.

[44] P. J. Roberts and D. R. Webster, "Turbulent diffusion," in *Engineering and Environmental Science*, 2002. DOI: https://doi.org/10.1016/B0-12-227090-8/00441-3.

[45] M. Swartz, "Hplc detectors: A brief review," *Journal of Liquid Chromatography Related Technologies*, 2010. DOI: https://doi.org/10.1080/10826076.2010.484356.

[46] V. David, S. C. Moldoveanu, and T. Galaon, "Derivatization procedures and their analytical performances for hplc determination in bioanalysis," *Biomedical Chromatography*, 2020. DOI: https://doi.org/10.1002/bmc.5008.

[47] Carl Roth, *L-alanine*. [Online]. Available: https://www.carlroth.com/fr/fr/alanine/l-alanine/p/3076.2.

[48] P. Felig, "The glucose-alanine cycle," *Metabolism*, 1973. DOI: https://doi.org/10.1016/0026-0495(73)90269-2.

[49] H. J. J. Simpson and R. E. Marsh, "The crystal structure of l-alanine," *Acta Crystallographica*, 1966. DOI: https://doi.org/10.1107/S0365110X66001221.

[50] M. Chalamaiah, B. D. Kumar, R. Hemalatha, and T. Jyothirmayi, "Fish protein hydrolysates: Proximate composition, amino acid composition, antioxidant activities and applications: A review," *Food Chemistry*, 2023. DOI: https://doi.org/10.1016/j.foodchem.2012.06.100.

[51] H. Tapiero, G. Mathé, P. Couvreur, and K. D. Tew, "I. arginine," *Biomedicine & Pharmacotherapy*, 2002. DOI: https://doi.org/10.1016/S0753-3322(02)00284-6.

[52] D. Coman, J. Yaplito-Lee, and A. Boneh, "New indications and controversies in arginine therapy," *Clinical Nutrition*, 2008. DOI: https://doi.org/10.1016/j.clnu.2008.05.007.

[53] Carl Roth, *L-arginine*. [Online]. Available: https://www.carlroth.com/fr/fr/arginine/l-arginine/p/3144.3.

[54] Y. Hasegawa, T. Shimada, and M. Niitsu, "Solvent extraction of 3b group metal ions from hydrochloric acid with trioctylphosphine oxide," *Journal of Inorganic and Nuclear Chemistry*, 1980. DOI: https://doi.org/10.1016/0022-1902(80)80176-5.

[55] NIH National Library of Medicine NCBI, *Compound summary for cid 65577, trioctylphosphine oxide*, PubChem, Available online: https://pubchem.ncbi.nlm.nih.gov/compound/65577, 2024. [Online]. Available: https://pubchem.ncbi.nlm.nih.gov/compound/65577.

[56] M. Gilmore, É. N. McCourt, F. Connolly, P. Nockemann, M. Swadźba-Kwaśny, and J. D. Holbrey, "Hydrophobic deep eutectic solvents incorporating trioctylphosphine oxide: Advanced liquid extractants," *ACS Sustainable Chemistry & Engineering*, 2018. DOI: https://doi.org/10.1021/acssuschemeng.8b04843.

[57] A. Marchese, I. E. Orhan, M. Daglia, *et al.*, "Antibacterial and antifungal activities of thymol: A brief review of the literature," *Food Chemistry*, 2016. DOI: https://doi.org/10.1016/j.foodchem.2016.04.111.

[58] NIH National Library of Medicine NCBI, *Compound summary for cid 6989, thymol*, PubChem, Available online: https://pubchem.ncbi.nlm.nih.gov/compound/6989, 2024. [Online]. Available: https://pubchem.ncbi.nlm.nih.gov/compound/6989.

[59] B. Salehi, A. P. Mishra, I. Shukla, *et al.*, "Thymol, thyme, and other plant sources: Health and potential uses," *Phytotherapy Research*, 2018. DOI: https://doi.org/10.1002/ptr.6109.

[60] M. Tiecco, A. Grillo, E. Mosconi, W. Kaiser, T. D. Giacco, and R. Germani, "Advances in the development of novel green liquids: Thymol/water, thymol/urea and thymol/phenylacetic acid as innovative hydrophobic natural deep eutectic solvents," *Journal of Molecular Liquids*, 2022. DOI: https://doi.org/10.1016/j.molliq.2022.120043.

[61] C. G. Biliaderis, "Differential scanning calorimetry in food research—a review," *Food Chemistry*, 1983. DOI: https://doi.org/10.1016/0308-8146(83)90081-X.

[62] J. D. Menczel and R. B. Prime, *Thermal Analysis of Polymers: Fundamentals and Applications*. 2009. DOI: https://doi.org/10.1002/9780470423837.

[63] N. R. Rodriguez, L. Machiels, and K. Binnemans, "P-toluenesulfonic acid-based deep-eutectic solvents for solubilizing metal oxides," *ACS Sustainable Chemistry & Engineering*, DOI: https://doi.org/10.1021/acssuschemeng.8b05072.

[64] C. Berthomieu and R. Hienerwadel, "Fourier transform infrared (ftir) spectroscopy," *Photosynthesis Research*, 2009. DOI: https://doi.org/10.1007/s11120-009-9439-x.

[65] C. Chen, J. Gao, and Y. Yan, "Observation of the type of hydrogen bonds in coal by ftir," *Energy & Fuels*, 1998. DOI: https://doi.org/10.1021/ef970100z.

[66] Y. Amini, A. Hassanvand, V. Ghazanfari, M. M. Shadman, M. Heydari, and Z. S. Alborzi, "Optimization of liquid-liquid extraction of calcium with a serpentine microfluidic device," *International Communications in Heat and Mass Transfer*, 2023. DOI: https://doi.org/10.1016/j.icheatmasstransfer.2022.106551.

[67] E. Abe, S. G. Delyle, and J. C. Alvarez, "Liquid-liquid extraction: Theory, applications and difficulties," *Annales de Toxicologie Analytique*, 2010. DOI: https://doi.org/10.1051/ata/2010018.

[68] J. D. Enderle, *Compartmental Modeling*, J. D. Enderle, Ed. Elsevier, 2012. DOI: https://doi.org/10.1016/B978-0-12-374979-6.00007-1.

[69] L. A. Patricia and M. Denis, *Fluid-fluid separations*, English, French-friendly, Louvain-la-Neuve. 5.00 credits, 30.0 h + 22.5 h Q2, 2024-2025. [Online]. Available: https://www.uclouvain.be/cours-2024-LMAPR2118.

[70] M. Cai and T. Kagawa, "Design and application of air power meter in compressed air systems," 2001. DOI: https://doi.org/10.1109/ECODIM.2001.992347.

[71] G. Van Eygen, B. Van der Bruggen, A. Buekenhoudt, and P. Luis Alconero, "Efficient membrane-based affinity separations for chemical applications: A review," *Chemical Engineering and Processing - Process Intensification*, 2021. DOI: https://doi.org/10.1016/j.cep.2021.108613.

[72] D. O. Abranches and J. A. Coutinho, "Type v deep eutectic solvents: Design and applications," *Current Opinion in Green and Sustainable Chemistry*, 2022. DOI: https://doi.org/10.1016/j.cogsc.2022.100612.

[73] G. Errandonéa, J. Tolédano, A. Litzler, H. Savary, J. Schneck, and J. Aubrée, "Kinetic characteristics of the thermal hysteresis in an incommensurate system," *J. Physique Lett.*, 1984. DOI: https://doi.org/10.1051%2Fjphyslet%3A01984004507032900.

[74] F. C. Wang, M. Feve, T. M. Lam, and J.-P. Pascault, "Ftir analysis of hydrogen bonding in amorphous linear aromatic polyurethanes. i. influence of temperature," *Journal of Polymer Science*, 1994. DOI: hhttps://doi.org/10.1002/polb.1994.090320801.

[75] H. Chamani, J. Woloszyn, T. Matsuura, D. Rana, and C. Q. Lan, "Pore wetting in membrane distillation: A comprehensive review," *Progress in Materials Science*, 2021. DOI: https://doi.org/10.1016/j.pmatsci.2021.100843.

[76] D. J. Miller, D. R. Dreyer, C. W. Bielawski, D. R. Paul, and B. D. Freeman, "Surface modification of water purification membranes," *Angewandte Chemie International Edition*, pp. 11 237–11 245, 2016. DOI: https://doi.org/10.1002/anie.201601509.

Appendices

A HPLC solutions

Solvent Agents

- Mobile phase A :
    1. 2.04 g potassium dihydrogenphosphate
    2. 0.87 g dipotassium hydrogenphosphate
    3. 1L ultrapure water
- Mobile phase B :
    1. 450 mL acetonitrile
    2. 400 mL methanol
    3. 150 mL ultrapure water
- Rinse R0 :
    1. 800 mL methanol
    2. 200 mL ultrapure water
- Rinse R3 :
    1. 200 mL acetonitrile
    2. 800 mL ultrapure water
- Column cleaning :
    1. 500 mL ultrapure water
    2. 500 mL methanol
    3. 1 mL formic acid

Derivatisation Agents

- Borate buffer :
    1. 1 L ultrapure water
    2. 6.18 g boric acid

3. 2 g NaOH

- MPA :
  1. 10 mL Borate buffer
  2. 10 µL 3-Mercapto propionic acid
- OPA :
  1. 10 mg O-phtalaldehyde
  2. 0.3 mL pure ethanol
  3. 0.7 mL borate buffer
  4. 4 mL ultrapure water
- FMOC replaced with water, not required for these solutions
- Acidic phosphate buffer :
  1. 1 L ultrapure water
  2. 3.4 mL phosphoric acid 85%
  3. 6.8 g potassium dihydrogenphosphate

B HPLC Calibration of Amino Acids

Different amino acid rentention times within the HPLC device

Amino Acid	Averaged HPLC retention time (min)
L-Glutamine	5.5
L-Valine	5.7
L-Methionine	Noise
L-Arginine	6.5
L-Proline	Noise
L-Leucine	2.4
L-Phenylalanine	2.5
L-Alanine	13
L-Glycine	7.5
L-Serine	5.5

Calibration values of Alanine

Concentration (g/L)	Peak Area
0.5	6062260
1	10824424
1.5	18663903
2	26548489
2.5	32714920
5	45917510
10	48603456
20	48204999

Calibration values of Arginine

Concentration (g/L)	Peak Area
0.5	4139837
1	6696735
1.5	10951971
2	15433070
2.5	18492516
5	30470264
10	59041012
20	58792622

C DES calibration

C.1 DSC experiments

DSC experiments and sample mass

DES	Sample mass (mg)
4:1	5.000
3:1	5.400
2:1	6.000
1:1	6.100
1:2	6.300
1:3	6.200
1:4	6.200
1:0	5.200
0:1	5.400

C.2 TGA experiments

TGA experiments and sample mass

DES	Sample mass (mg)
1:1	5.080
1:6	6.040

C.3 FTIR spectra

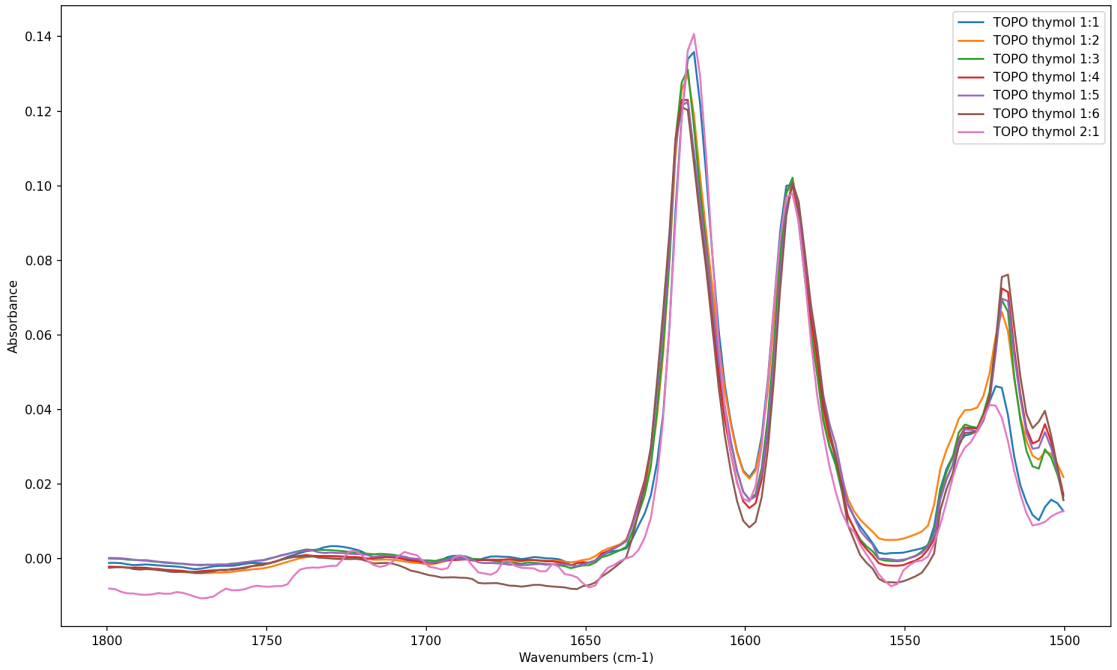

*

TOPO:thymol mixtures aromatic ring fitting

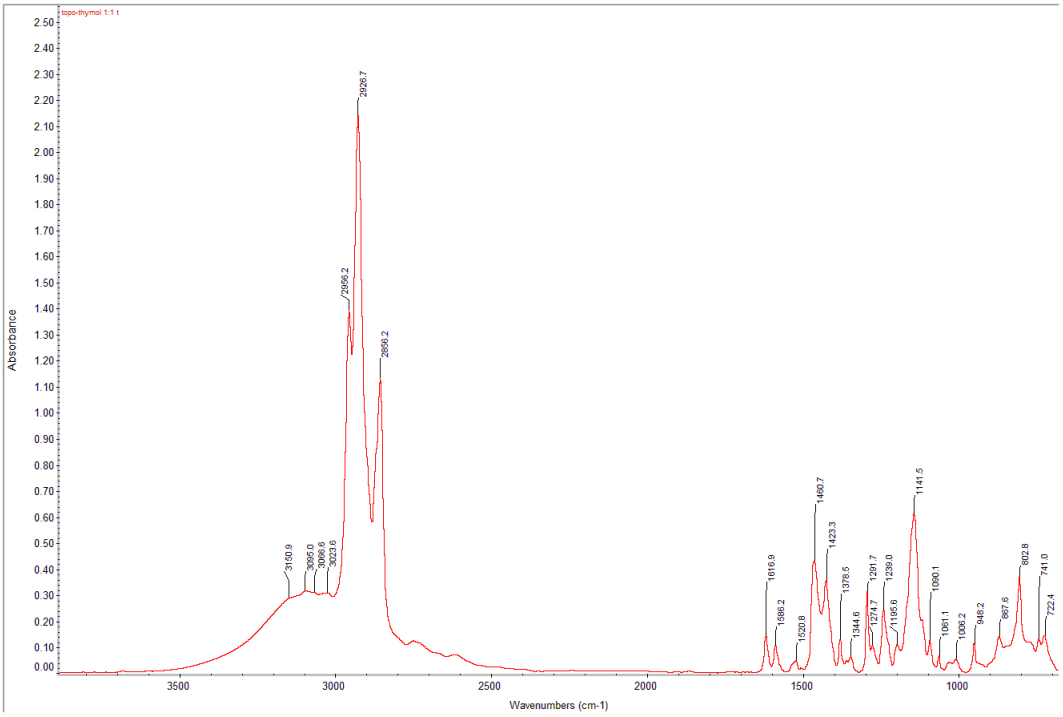

TOPO:thymol 1:1 FTIR absorbance sepctrum

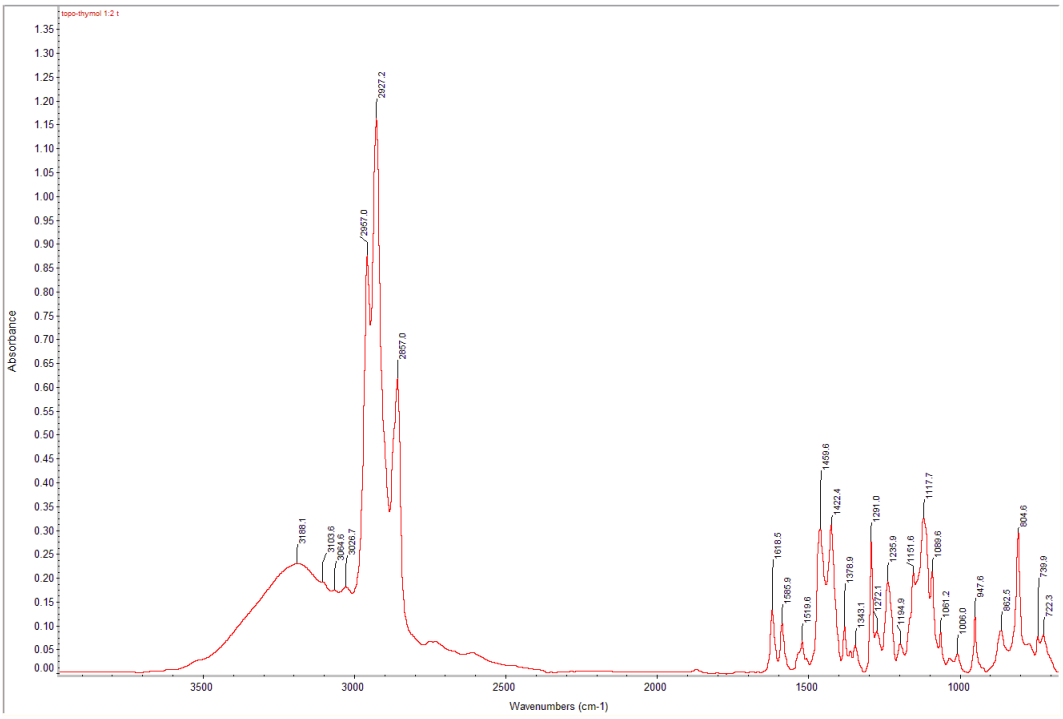

TOPO:thymol 1:2 FTIR absorbance sepctrum

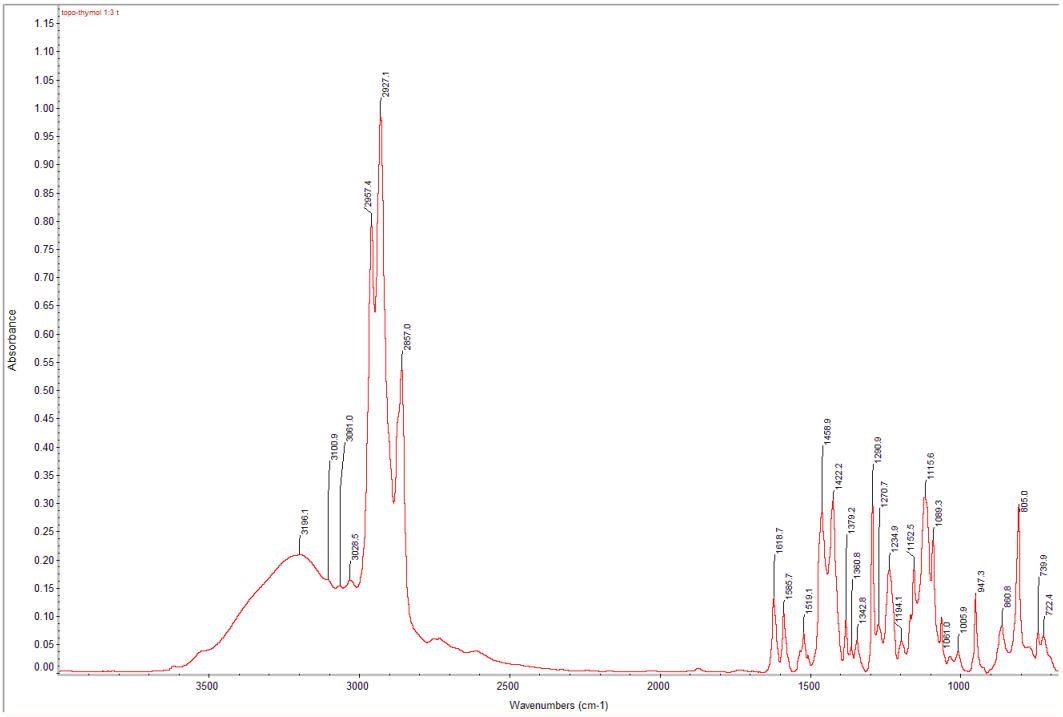

TOPO:thymol 1:3 FTIR absorbance sepctrum

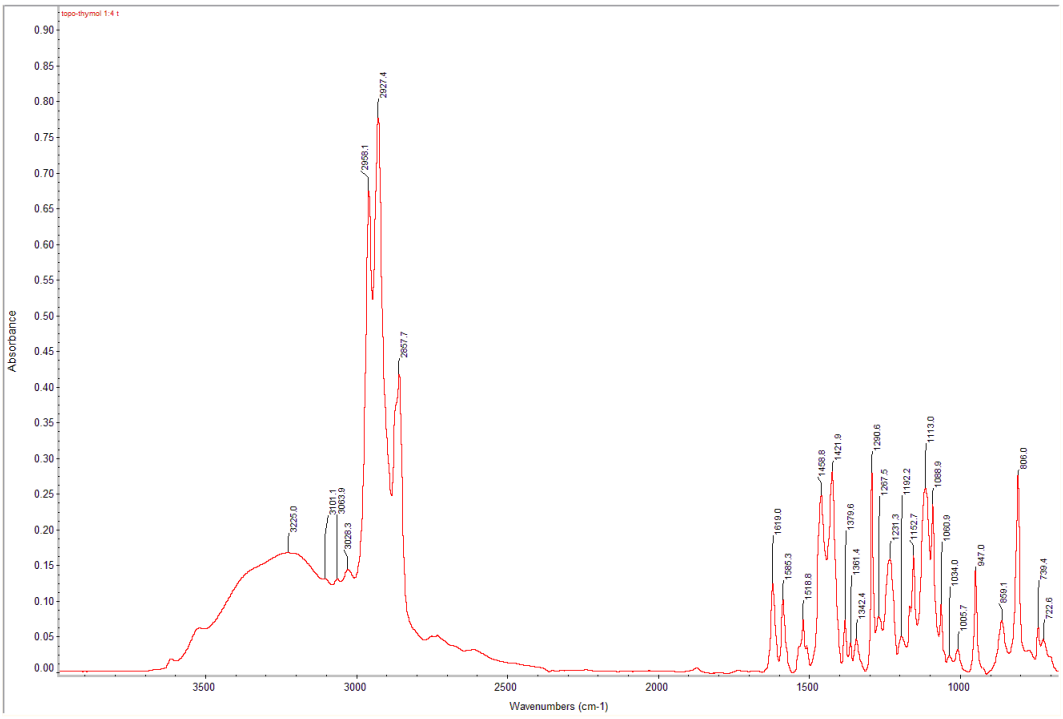

TOPO:thymol 1:4 FTIR absorbance sepctrum

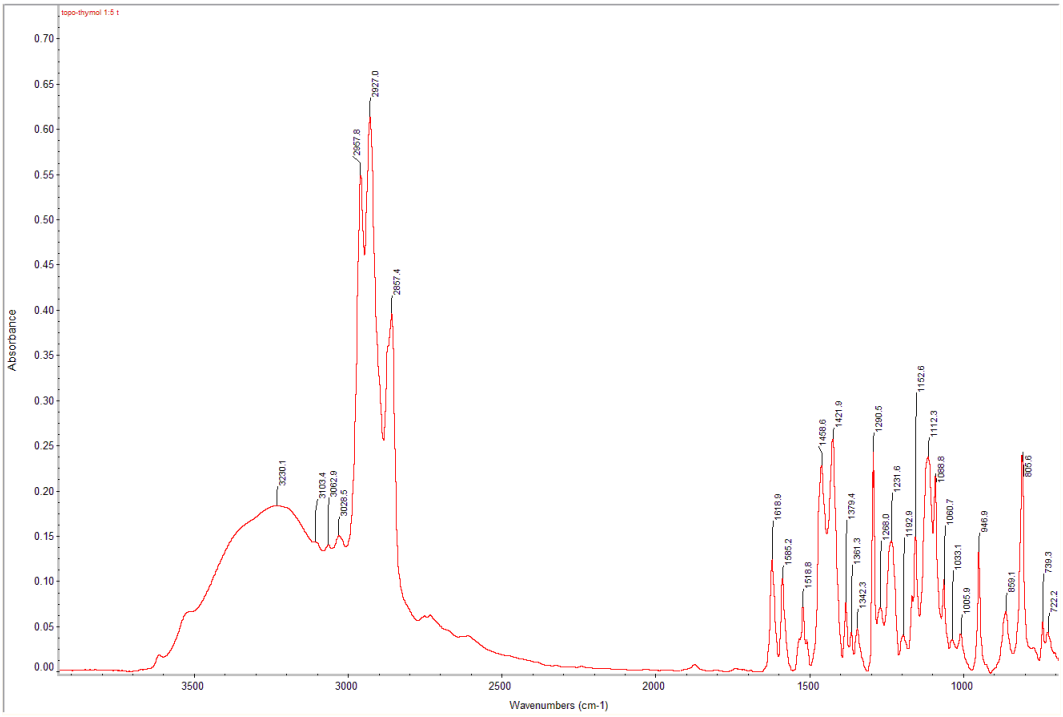

TOPO:thymol 1:5 FTIR absorbance sepctrum

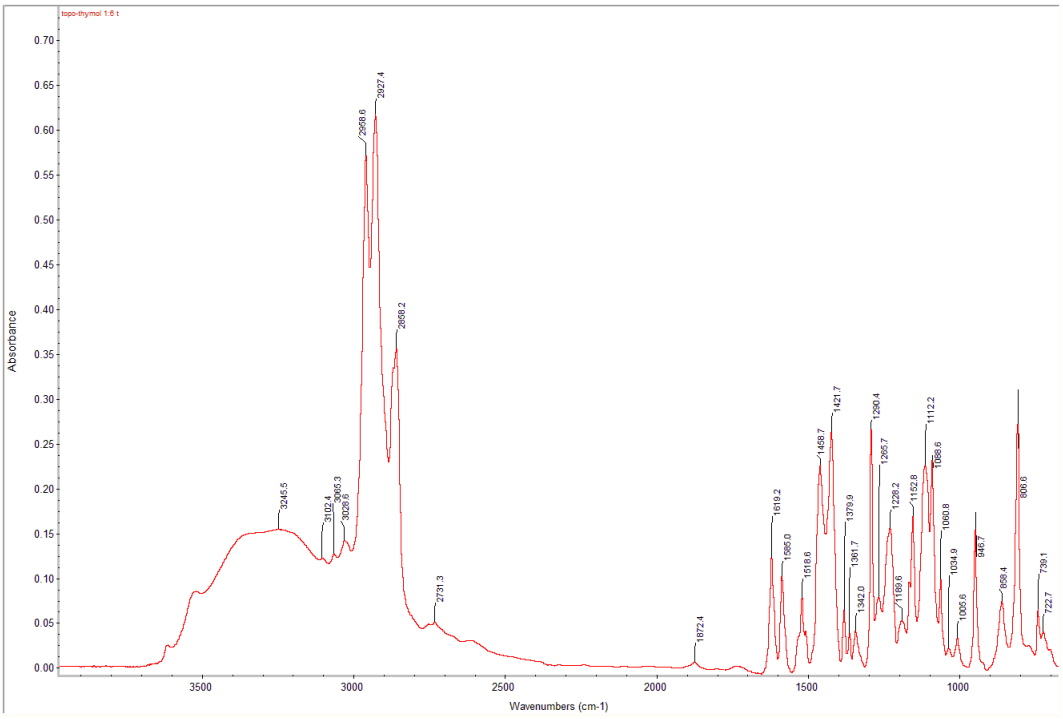

TOPO:thymol 1:6 FTIR absorbance sepctrum

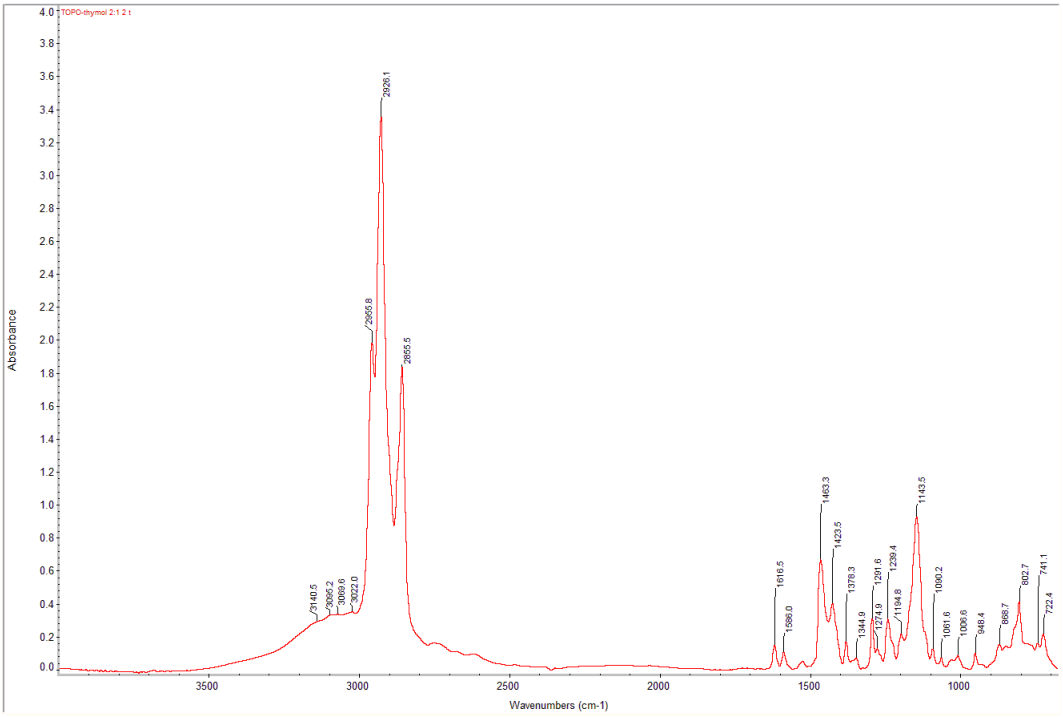

TOPO:thymol 2:1 FTIR absorbance sepctrum

D LLE experiments

Results 15/04: Acidic solutions wih initial concentrations 3 g/L, TOPO-thymol 1:1 as extractant

Amino Acid	pH	Peak	Concentration	Mass left (g)	Initial mass (g)	Extracted mass (g)
Alanine	1	No peak	0	0	9.214285714	9.214285714
	1	No peak	0	0	9.214285714	9.214285714
	3	1102941	0.21	0.63	9.3	8.67
	3	918433	0.19	0.57	9.3	8.73
	6	5172101	0.5	1.5	9.257142857	7.757142857
	6	4182985	0.43	1.29	9.257142857	7.967142857
Arginine	1	No peak	0	0	9.214285714	9.214285714
	1	No peak	0	0	9.214285714	9.214285714
	3	3537979	0.199	0.597	9.128571429	8.531571429
	3	3720576	0.23	0.69	9.128571429	8.438571429
	6	5054800	0.465	1.395	8.957142857	7.562142857
	6	5783062	0.593	1.779	8.957142857	7.178142857

Results 15/04: Acidic solutions with initial concentration of 3 g/L, TOPO-thymol 1:1 as extractant

Amino Acid	pH	Averaged efficiency %
Alanine	1	100
	3	93.5483871
	6	84.93055556
Arginine	1	100
	3	92.95070423
	6	82.28229665

Results 19/04: Basic solutions wih initial concentrations 5 g/L, TOPO-thymol 1:1 as extractant

Amino Acid	pH	Peak	Concentration	Mass left (g)	Initial mass (g)	Extracted mass (g)
Alanine	7	22170607	1.742771477	5.22831443	15.012	9.78368557
	7'	22747104	1.785	5.355	15.012	9.657
	7	21309695	1.679978172	5.039934516	15.012	9.972065484
	7'	22334582	1.755	5.265	15.012	9.747
	9.3	22364317	1.75690032	5.27070096	15.0	9.72929904
	9.3'	23554114	1.844	5.532	15.0	9.468
	9.3	22309109	1.752873552	5.258620657	15.0	9.741379343
	9.3'	22703562	1.782	5.346	15.0	9.654
Arginine	7	23245433	3.659270483	10.97781145	15.024	4.046188551
	7'	22991810	3.615	10.845	15.024	4.179
	7	23461210	3.697150911	11.09145273	15.024	3.932547267
	7'	24138933	3.816	11.454	15.024	3.576
	9.3	23279714	3.665288636	10.99586591	15.0	4.004134093
	9.3'	24186312	3,824	11.472	15.0	3,528
	9.3	23838950	3.763464526	11.29039358	15.0	3.709606422
	9.3'	23649680	3.73	11.19	15.0	3.81

': stands for second HPLC analysis of same sample

Results 19/04: Basic solutions wih initial concentrations 5 g/L, TOPO-thymol 1:1 as extractant

Amino Acid	pH	Averaged efficiency %
Alanine	7	65.21408049
	9.3	64.32113064
Arginine	7	26.18100342
	9.3	25,08623419

Results 24/04: DES test at intresting pH, initial concentration 5 g/L

AA	DES	pH	Peak	Concentration	Mass left (g)	Initial mass (g)	Extracted mass (g)
Alanine	01:02	7	20182544	1.597	4.791	15.1	10.309
	01:02	7	24544937	1.915	5.745	15.1	9.355
	01:02	9.3	25660833	1.997	5.991	15.08	9.089
	01:02	9.3	28775291	2.221	6.663	15.08	8.417
Arginine	01:02	7	23328270	3.673	11.019	15.024	4.005
	01:02	7	23463738	3.698	11.094	15.024	3.93
	01:02	9.3	21855004	3.415	10.245	15	4.755
	01:02	9.3	24771815	3.927	11.781	15	3.219

Results 24/04: Basic solutions wih initial concentrations 5 g/L, TOPO-thymol 1:2 as extractant

Amino Acid	pH	Averaged efficiency %
Alanine	7	65.113
	9.3	58.044
Arginine	7	26.408
	9.3	26.580

Results 23/04: DES test at intresting pH, initial concentration 5 g/L

AA	DES	pH	Peak	Concentration	Mass left (g)	Initial mass (g)	Extracted mass (g)
Alanine	01:03	7	25413728	1.979	5.937	15.012	9.075
	01:03	7	23936553	1.872	5.616	15.012	9.396
	01:03	9.3	21762245	1.713	5.139	15	9.861
	01:03	9.3	23062056	1.808	5.424	15	9.576
Arginine	01:03	7	24900515	3.95	11.85	15.024	3.174
	01:03	7	25446542	4.046	12.138	15.024	2.886
	01:03	9.3	22807439	3.582	10.746	15	4.254
	01:03	9.3	24407167	3.863	11.589	15	3.411

Results 23/04: Basic solutions wih initial concentrations 5 g/L, TOPO-thymol 1:3 as extractant

Amino Acid	pH	Averaged efficiency %
Alanine	7	61.52078337
	9.3	64.79
Arginine	7	20.16773163
	9.3	25.55

Results 25/04: DES test at interesting pH, initial concentration 5 g/L

AA	DES	pH	Peak	Concentration	Mass left (g)	Initial mass (g)	Extracted mass (g)
Alanine	01:04	7	25727194	2.002	6.006	15.1	9.094
	01:04	7	24958885	1.946	5.838	15.1	9.262
	01:04	9.3	25613380	1.994	5.982	15.08	9.098
	01:04	9.3	23100928	1.818	5.454	15.08	9.626
Arginine	01:04	7	39454040	6.504	Above	15.024	0
	01:04	7	22437643	3.517	10.551	15.024	4.473
	01:04	9.3	22644809	3.554	10.662	15	4.338
	01:04	9.3	24288146	3.842	11.526	15	3.474

Results 25/04: Basic solutions wih initial concentrations 5 g/L, TOPO-thymol 1:4 as extractant

Amino Acid	pH	Averaged efficiency %
Alanine	7	60.78145695
	9.3	58.04376658
Arginine	7	14.88618211
	9.3	26.04

Results 26/04: Mixture of alanine and arginine at interesting pH, initial concentration 5 g/L - Part 1

Amino	pH	DES	AL peak	AG peak	AL concent	AG concent	AL initial (g)	AG initial (g)
AL & AG	7	01:01	17565919	19651659	1.409	3.029	14.94	15.06
AL & AG	7	01:01	20559469	20264298	1.625	3.136	14.94	15.06
AL & AG	9	01:01	21364396	17328330	1.684	2.62	15.16	15.14
AL & AG	9	01:01	21379220	18474974	1.685	2.821	15.16	15.14

Results 26/04: Mixture of alanine and arginine at interesting pH, initial concentration 5 g/L - Part 2

Amino	AL extracted	AG extracted	AL eff%	AG eff%
AL & AG	10.713	5.973	71.13545817	39.66135458
AL & AG	10.065	5.652	66.83266932	37.52988048
AL & AG	10.108	7.28	66.76354029	48.08454425
AL & AG	10.105	6.677	66.74372523	44.10171731

Results 23.04: Variation in concentration test, initial concentration 3g/L, with TOPO-thymol 1:1 as extractant

AA	DES	pH	Peak	Concentration	Mass left (g)	Initial mass (g)	Extracted mass (g)
Alanine	01:01	7	16841529	1.354	4.062	9.171428571	5.109428571
Alanine	01:01	9.3	29275636	2.261	6.783	9.214285714	2.431285714
Alanine	01:01	9.3	23050158	1.807	5.421	9.214285714	3.793285714
Arginine	01:01	7	16252883	2.431	7.293	9.257142857	1.964142857
Arginine	01:01	7	15668666	2.392	7.176	9.257142857	2.081142857
Arginine	01:01	9.3	16106494	2.408	7.224	9.171428571	1.947428571
Arginine	01:01	9.3	17402487	2.634	7.902	9.171428571	1.269428571

E Membrane experiments

E.1 PVDF 100 nm experiments

Results 15/05: Alanine transfer through PVDF 0.1 µm

Solution	Peak	Concentration (mg/mL)	Mass (mg)	Efficiency (%)
0 h strip	0	0	0	0
1 h strip	0	0	0	0
3 h strip	5037771	0.4931	122.2974	9.7760
6 h strip	10501813	0.8917	220.2429	17.6053
24 h strip	63530133	4.7590	1170.7140	93.5823
0 h feed	66882870	5.0040	1251.0000	0
1 h feed	59102426	4.4370	1104.8130	11.6856
3 h feed	51445300	3.8780	961.7440	23.1220
6 h feed	39220085	2.9863	737.6231	41.0373
24 h feed	0	0	0	100

Results 15/05: Arginine transfer through PVDF 100 nm

Solution	Peak	Concentration (mg/mL)	Mass (mg)	Efficiency (%)
0 h strip	0	0	0	0
1 h strip	0	0	0	0
3 h strip	2677591	0.0485	12.0309	0.9628
6 h strip	5964106	0.6255	154.4914	12.3633
24 h strip	21087546	3.2804	806.9896	64.5798
0 h feed	30873471	4.9984	1249.6000	0
1 h feed	30540171	4.9399	1230.0321	1.5659
3 h feed	30263834	4.8914	1213.0613	2.9240
6 h feed	26700982	4.2659	1053.6785	15.6787
24 h feed	10814639	1.4770	363.3420	70.9233

Results 16/05: Alanine transfer through PVDF 100 nm

Solution	Peak	Concentration (mg/mL)	Mass (mg)	Efficiency (%)
0 h strip	0	0	0	0
1 h strip	0	0	0	0
3 h strip	4896521	0.4828	119.7424	9.4902
6 h strip	10876200	0.9190	226.9877	17.9899
24 h strip	64283124	4.8144	1184.3373	93.8647
0 h feed	67472411	5.0470	1261.7500	0
1 h feed	58745120	4.4104	1098.2015	12.9620
3 h feed	51147800	3.8563	956.3658	24.2032
6 h feed	39500000	3.0067	742.6660	41.1400
24 h feed	0	0	0	100

Results 16/05: Arginine transfer through PVDF 100 nm

Solution	Peak	Concentration (mg/mL)	Mass (mg)	Efficiency (%)
0 h strip	0	0	0	0
1 h strip	0	0	0	0
3 h strip	2734567	0.0585	14.5115	1.1501
6 h strip	5943182	0.6218	153.5841	12.1723
24 h strip	21776890	3.4015	836.7598	66.3174
0 h feed	30985117	5.0180	1254.5000	0.5746
1 h feed	30412875	4.9175	1224.4676	2.9548
3 h feed	30387500	4.9131	1218.4453	3.4321
6 h feed	25201963	4.0027	988.6784	21.6423
24 h feed	9679500	1.2777	314.3197	75.0886

Results 21/05: Alanine transfer through PVDF 200 nm

Solution	Peak	Concentration (mg/mL)	Mass (mg)	Efficiency (%)
0 h strip	0	0	0	0
1 h strip	0	0	0	0
3 h strip	0	0	0	0
6 h strip	290462	0.1469	36.2781	2.8984
24 h strip	526965	0.1641	40.3747	3.2257
0 h feed	66919431	5.0067	1251.6667	0
1 h feed	65780275	4.9236	1225.9711	2.0529
3 h feed	65160133	4.8783	1209.8300	3.3425
6 h feed	63259698	4.7397	1170.7140	6.4676
24 h feed	61419712	4.6055	1132.9598	9.4839

E.2 PVDF 200 nm experiments

Results 21/05: Arginine transfer through PVDF 200 nm

Solution	Peak	Concentration (mg/mL)	Mass (mg)	Efficiency (%)
0 h strip	0	0	0	0
1 h strip	0	0	0	0
3 h strip	0	0	0	0
6 h strip	0	0	0	0
24 h strip	2459000	0.0101	2.4938	0.1993
0 h feed	30916762	5.0060	1251.5000	0
1 h feed	30974091	5.0161	1249.0000	0.1998
3 h feed	30997429	5.0202	1245.0000	0.5194
6 h feed	30997274	5.0201	1240.0000	0.9210
24 h feed	30911942	5.0052	1231.2678	1.6166

Results 14/05: Alanine transfer through PVDF 200 nm

Solution	Peak	Concentration (mg/mL)	Mass (mg)	Efficiency (%)
0 h strip	0	0	0	0
1 h strip	0	0	0	0
3 h strip	251011	0.1440	35.7113	2.8546
6 h strip	771966	0.1820	44.9527	3.5933
24 h strip	8794569	0.7671	188.7185	15.0854
0 h feed	66882870	5.0040	1251.0000	0
1 h feed	65449906	4.8995	1219.9711	2.4803
3 h feed	63943901	4.7896	1187.8300	5.0496
6 h feed	61648979	4.6222	1141.6957	8.7374
24 h feed	51387120	3.8738	952.9472	23.8252

Results 14/05: Arginine transfer through PVDF 200 nm

Solution	Peak	Concentration (mg/mL)	Mass (mg)	Efficiency (%)
0 h strip	0	0	0	0
1 h strip	0	0	0	0
3 h strip	0	0	0	0
6 h strip	416528	0	0	0
24 h strip	2662386	0.0458	11.2773	0.9015
0 h feed	30873471	4.9984	1249.6000	0
1 h feed	33292404	5.0185	1249.6000	0
3 h feed	31009602	5.0223	1245.5300	0.3257
6 h feed	31566283	5.0201	1239.9731	0.7704
24 h feed	30845422	4.9935	1228.3951	1.6969

E.3 PTFE 100 nm experiments

Results 22/05: Alanine transfer through PTFE 100 nm

Solution	Peak	Concentration (mg/mL)	Mass (mg)	Efficiency (%)
0 h strip	0	0	0	0
1 h strip	636546	0.1721	42.8573	3.4151
3 h strip	2910098	0.3379	83.8106	6.6786
6 h strip	11031539	0.9303	229.7863	18.3109
24 h strip	36609499	2.7959	687.7956	54.8081
0 h feed	67097664	5.0197	1254.9167	0
1 h feed	64401820	4.8230	1200.9362	4.3015
3 h feed	58191318	4.3701	1083.7735	13.6378
6 h feed	52840887	3.9798	983.0116	21.6672
24 h feed	27106991	2.1028	517.2942	58.7786

Results 22/05: Arginine transfer through PTFE 100 nm

Solution	Peak	Concentration (mg/mL)	Mass (mg)	Efficiency (%)
0 h strip	0	0	0	0
1 h strip	0	0	0	0
3 h strip	817215	0	0	0
6 h strip	1527077	0	0	0
24 h strip	9800388	1.2989	319.5403	25.5598
0 h feed	30886382	5.0007	1250.1667	0
1 h feed	29500852	4.7574	1189.3579	4.8640
3 h feed	28554403	4.5913	1147.8198	8.1867
6 h feed	27912403	4.4786	1119.6435	10.4405
24 h feed	23764011	3.7503	922.5759	26.2038

Results 23/05: Alanine transfer through PTFE 100 nm

Solution	Peak	Concentration (mg/mL)	Mass (mg)	Efficiency (%)
0 h strip	0	0	0	0
1 h strip	341239	0.1506	37.4940	2.9878
3 h strip	1333273	0.2229	55.2880	4.4057
6 h strip	11050080	0.9317	230.1203	18.3375
24 h strip	41145761	3.1268	769.1888	61.2940
0 h feed	67543219	5.0197	1254.9167	0
1 h feed	65480927	4.9017	1220.5345	2.7398
3 h feed	57936377	4.3515	1079.1620	14.0053
6 h feed	49867702	3.7629	929.4476	25.9355
24 h feed	21732901	1.7108	420.8681	66.4625

Results 23/05: Arginine transfer through PTFE 100 nm

Solution	Peak	Concentration (mg/mL)	Mass (mg)	Efficiency (%)
0 h strip	0	0	0	0
1 h strip	0	0	0	0
3 h strip	1165995	0	0	0
6 h strip	1538921	0	0	0
24 h strip	9843756	1.3066	321.4132	25.7096
0 h feed	30783241	5.0007	1250.1667	0
1 h feed	30723289	4.9720	1238.0367	0.9703
3 h feed	29560817	4.7680	1182.4538	5.4163
6 h feed	27658312	4.4340	1090.7559	12.7512
24 h feed	24694271	3.9136	962.7503	22.9902

E.4 Fluxes Calculations

PVDF 100 nm, Alanine flux calculations in (g/h.m^2) using transfer coefficient $K_{AL} = 6.584$, σ standart deviation

Time (h)	Averaged flux	15 May flux	16 May flux	Alanine σ
0	33.0889065	32.94734616	33.23046684	0.14156034
1	29.12669107	29.2141037	29.0392784	0.087412634
3	22.24915993	22.28663713	22.21168273	0.0374772
6	13.768959	13.79164379	13.74627422	0.022684784
24	-31.5165312	-31.3342167	-31.6988457	0.1823145

PVDF 100 nm, Arginine flux calculations in (g/h.m^2) using transfer coefficient $K_{AG} = 4.756$, σ standart deviation

Time (h)	Averaged flux	15 May flux	16 May flux	Alanine σ
0	-23.82388101	-23.77726266	-23.87049936	0.046618353
1	-23.44576968	-23.49892238	-23.39261697	0.053152701
3	-23.065229	-23.03738246	-23.09307555	0.027846544
6	-16.70026736	-17.31744926	-16.08308546	0.617181901
24	9.34076249	8.578945945	10.10257903	0.761816545

PVDF 200 nm, Alanine flux calculations in (g/h.m^2) using transfer coefficient K_{AL} = -1.272 , σ standart deviation

Time (h)	Averaged flux	21 May flux	14 May flux	Standard deviation σ
0	-6.366784	-6.36848	-6.365088	0.001696
1	-6.247466812	-6.262792182	-6.232141441	0.01532537
3	-6.057255443	-6.205257087	-5.909253798	0.148001644
6	-5.745059749	-5.84211514	-5.648004358	0.097055391
24	-4.80054281	-5.649464116	-3.951621504	0.848921306

PVDF 200 nm, Arginine flux calculations in (g/h.m^2) using transfer coefficient $K_{AG} = -0.0036$, σ standart deviation

Time (h)	Averaged flux	21 May flux	14 May flux	Standard deviation σ
0	-0.01800792	-0.0180216	-0.01799424	1.368E-05
1	-0.018062169	-0.018057831	-0.018066506	4.33749E-06
3	-0.018076427	-0.01807258	-0.018080274	3.84663E-06
6	-0.018072483	-0.018072483	-0.018072483	0
24	-0.017896769	-0.017982059	-0.01781148	8.52893E-05

PTFE 100 nm, Alanine flux calculations in (g/h.m^2) using transfer coefficient $K_{AL} = 18.512352$, σ standart deviation

Time (h)	Averaged flux	22 May flux	23 May flux	Standard deviation σ
0	92.92583564	92.92583626	92.92583502	6.17078E-07
1	87.02736129	86.09945579	87.9552668	0.927905504
3	75.5362504	74.64380938	76.42869143	0.892441025
6	54.43353258	56.45333085	52.4137343	2.019798272
24	-19.52157728	-12.83082023	-26.21233434	6.690757056

PTFE 100 nm, Alanine flux calculations in (g/h.m^2) using transfer coefficient K_{AG} = - 2.897, σ standart deviation

Time (h)	Averaged flux	22 May flux	23 May flux	Standard deviation σ
0	-14.49123191	-14.49123191	-14.49123191	1.93191E-10
1	-14.09731628	-13.78637125	-14.40826131	0.310945029
3	-13.56088086	-13.30488449	-13.81687723	0.255996367
6	-12.91364818	-12.97828	-12.84901635	0.064631824
24	-7.32930448	-7.103710311	-7.554898649	0.225594169

UNIVERSITÉ CATHOLIQUE DE LOUVAIN
École polytechnique de Louvain
Rue Archimède, 1 bte L6.11.01, 1348 Louvain-la-Neuve, Belgique | **www.uclouvain.be/epl**